Université de Sherbrooke

Influence of transcription elongation rate on gene expression in the fission yeast *Schizosaccharomyces pombe*

Par
Yann Vanrobaeys
Programmes de Biochimie

Mémoire présenté à la Faculté de médecine et des sciences de la santé
en vue de l'obtention du grade de maitre ès sciences (M. Sc.)
en biochimie

Sherbrooke, Québec, Canada
[Septembre, 2019]

Membres du jury d'évaluation
François Bachand, Biochimie
Pierre-Étienne Jacques, Biologie, Faculté des sciences, Université de Sherbrooke
Michelle Scott, Biochimie
Antonio Conconi, Microbiologie et Infectiologie

Intelligence is the ability to adapt to change.

-Stephen Hawking

Résumé

Influence de l'élongation de la transcription sur l'expression génique chez la levure fission *Schizosaccharomyces pombe*

Par
Yann Vanrobaeys
Programmes de Biochimie

Mémoire présenté à la Faculté de médecine et des sciences de la santé en vue de l'obtention du diplôme de maitre ès sciences (M.Sc.) en Biochimie, Faculté de médecine et des sciences de la santé, Université de Sherbrooke, Sherbrooke, Québec, Canada, J1H 5N4

Bien qu'il soit évident que l'étape de transcription régule directement l'expression des gènes, comment l'élongation de la transcription régule cette dernière reste encore méconnue. Des évidences montrent en effet que certains facteurs de transcription mutés influent sur l'élongation de la transcription et mènent à la surexpression de certains gènes, et dans un cas extrême, d'oncogènes dans un contexte de cancer. Mais que se passe-t-il si le problème est pris à l'envers ? C'est-à-dire, si la cinétique d'élongation de la transcription est ralentie, quelles sont les conséquences sur l'expression génique ?

Pour ce faire, nous utilisons l'édition génomique CRISPR-cas9 chez *Schizosaccharomyces pombe* afin de générer un mutant Rpb1 qui produit un complexe ARN polymerase II dont la cinétique d'élongation de la transcription est plus lente qu'une souche sauvage.

L'analyse de gènes différentiellement exprimés par RNA-seq nous a permis l'identification de gènes significativement sur-exprimés en réponse à différents stress et de gènes significativement sous-exprimés en lien avec les ARN non-codants. De plus, en combinant ces données avec une cartographie publiée des sites de polyadénylation alternatifs, il a été possible d'observer un usage accentué et significatif des sites de polyadénylation proximaux dans le mutant « slow ». Ensemble, ces résultats suggèrent l'étude du gène *tgp1* codant pour un transporteur transmembranaire de phosphate et qui est régulé en *cis* par un ARN non-codant long. Des expériences de ChIP-qPCR ont permis de rassembler des indices mécanistiques sur le lien entre une vitesse d'élongation lente et la sur-expression de *tgp1*.

Mots clés : *Schizosaccharomyces pombe*, expression génique, cinétique d'élongation transcriptionnelle, Rpb1, *nc-tgp1*, *tgp1,* polyadénylation alternative, terminaison transcriptionnelle.

iv

Summary

Influence of transcription elongation rate on gene expression in the fission yeast *Schizosaccharomyces pombe*

By
Yann Vanrobaeys
Biochemistry Program

Thesis presented at the Faculty of medicine and health sciences for the obtention of Master degree diploma maitre ès sciences (M.Sc.) in Biochemistry, Faculty of medicine and health sciences, Université de Sherbrooke, Sherbrooke, Québec, Canada, J1H 5N4

Although it has become clear that transcription is intimately coupled to gene expression, how transcription elongation influences the transcriptome remains poorly understood. Some studies have shown that mutations in particular transcription factors impact transcription elongation leading to the potential overexpression of some genes, and in extreme situations, oncogenes which are associated with cancer. However, what if we approached this problem another way? How would gene expression be affected if transcription elongation rate was slowing down?

To examine those consequences, we used genome editing in the fission yeast *Schizosaccharomyces pombe* to generate *rpb1* mutants that produce a RNA polymerase II complex that transcribes slower than the wild type RNAPII.

Using RNA-seq, differential gene expression analysis revealed a list of genes significantly up-regulated in conjunction with stress responses and a list of genes significantly down-regulated in conjunction with non-coding RNAs. Moreover, after merging those data with published genome-wide alternative polyadenylation sites, we discovered a more efficient function of the proximal polyadenylation sites in the slow mutant. Together, these results suggest a focus on *tgp1* whose protein product is a phosphate transmembrane transporter, and which is known to be regulated by a *cis* long non-coding RNA. Several ChIP-qPCR assays have allowed us to gather mechanistic evidence about the link between a slow transcription elongation rate and *tgp1* overexpression.

Keywords: *Schizosaccharomyces pombe*, gene expression, transcription elongation rate, Rpb1, *nc-tgp1*, *tgp1,* alternative polyadenylation, transcription termination

Acknowledgments

I would like first to thank my supervisor Dr François Bachand of the Biochemistry department at the University of Sherbrooke. The door to Prof. Bachand's office was always open whenever I ran into a trouble spot or had a question about my research. He consistently allowed this project to be my own work but steered me in the right direction whenever he thought I needed it.

Secondly but nevertheless, I would like to thank my co-supervisor Dr Pierre-Etienne Jacques of the biology department at the University of Sherbrooke who was involved in the development of my bioinformatics skills as well as his student Marc-Antoine Robert who helped me with great professionalism and attentiveness through all my dry analyses. Without their passionate participation and input, the data analyses could not have been successfully conducted.

A very special gratitude goes out to our research assistant Dr Marc Larochelle who brought all the technical assistance I needed along my wet experiments, I am gratefully indebted for his very valuable inputs on this project.

I am grateful to my parents Marie-Hélène and Christophe, who have provided me through moral and emotional support in my life. I am also grateful to my fiancée Lindsey who has supported and challenged me along the way.

Finally, I must express my gratitude to the other members of the lab, Danny, Anne-Marie, Lauren and Carlo, for providing me with unfailing support.

Table of contents

List of figures

List of tables

List of abbreviation

5'/3' UTR(s)	5' or 3' untranslated region(s)
BAM	Binary alignment map
BSA	Bovine serum albumin
ChIP	Chromatin immunoprecipitation
CPM	Counts per million
C_T	Threshold cycle
CTD	Carboxy-Terminal Domain
CUTs	Cryptic unstable transcripts
DNA	Deoxyribonucleic acid
DSR	Determinant of selective removal
EMM	Edinburgh minimal media
Kb	Kilobases
kDa	KiloDalton
lncRNAs	Long non-coding RNAs
miRNA	Micro ribonucleic acid
ncRNA	Non-coding ribonucleic acid
NTP	Nucleoside triphosphate
p(A)/PAS	Polyadenylation site or Polyadenylation signals
PBS	Phosphate buffered saline
RNA	Ribonucleic acid
RNAPI/II/III	RNA polymerase I/II/III
RNA-seq	Next-generation sequencing of RNA
rRNA	Ribosomal RNA
RT	Room temperature
RT-qPCR	Reverse transcription followed by polymerase chain reaction
S. cerevisiae	*Saccharomyces cerevisiae*
S. pombe	*Schizosaccharomyces pombe*
Ser2-P/ Ser5-P	Phosphorylated serine 2/5 of the RNAPII CTD
TE	Tris-EDTA
TL	Trigger Loop

tRNA	Transfer RNA
TSS	Transcription start site
WCE	Whole-cell extract

Introduction

1. *Schizosaccharomyces pombe*: A Key Model Organism

The fission yeast *Schizosaccharomyces pombe* is an important model organism for the study of eukaryotic molecular and cellular biology. On one hand it is a unicellular organism, sharing many useful features with the first and well-known model organism for molecular biology, *Escherichia coli*. Since both are microorganisms, it is easy to reach extremely large numbers of cells allowing quick and substantial coverage in a single experiment. They can also maintain autonomous plasmids that reversibly introduce genetic material to modify the behavior of a strain, and pairing that with their highly active homologous recombination mechanisms makes *S. pombe* a user-friendly tool for genetic manipulation for the discovery of genes involved in a given biological process (Orr-Weaver *et al*., 1981). On the other hand, it is a eukaryotic organism. In that way it provides important insights of conserved processes in humans which directly helps experiments in more complicated cell types (Hoffman *et al*., 2015).

Most people are familiar with brewer's or baker's yeast, *Saccharomyces cerevisiae*, which is a popular laboratory yeast model system, as well as the "Yeast infections" from *Candida albicans*. However, the fission yeast *S. pombe* is a very different organism because it has diverged from the ascomycete lineage before *S. cerevisiae* (Heckman *et al*., 2001). In other words, *S. pombe* has undergone fewer evolutionary changes since divergence from the common ancestor, leading to the retention of more characteristics with the common ancient yeast ancestor and, by association, more features with humans (Aravind *et al*., 2000; Wood, 2006). For example, *S. cerevisiae* has lost 300 more genes than *S. pombe* compared to the common ancestor (Aravind *et al*., 2000) resulting in an increased number of homologous genes between the fission yeast and human. Furthermore, the genome of *S. pombe* has 43% of genes with introns (Wood *et al*., 2002) which, according to this feature, puts the fission yeast equidistant between *S. cerevisiae* with around 4% of genes with introns (Lopez and Séraphin, 1999) and human with 97% of genes with introns (Grzybowska, 2012). Briefly, *S.*

pombe has become one of the two major yeast model systems, together with *S. cerevisiae*, providing important insights regarding cell cycle, chromosome dynamics and gene expression (Hoffman *et al*., 2015). The outcome of its rise in popularity as a research organism was the creation of a comprehensive database for the fission yeast called Pombase (Wood *et al*., 2012) providing structural and functional annotation, literature curation and access to large-scale data sets, as well as the website PombeNet offering more practical advices for working with fission yeast.

2. Gene expression (coding versus noncoding transcription units)

The information database of a cell is encoded in DNA subunits called genes. Gene expression refers to a complex series of processes in which the information encoded in a gene is used to produce a functional biochemical product. There are two categories of genes in every organism: the coding genes where the final product is a protein, and the non-coding genes, which do not provide instructions for making proteins.

Gene regulation is a multilayer process by which, depending on the needs of the cell, a gene can be tuned at each step from DNA to RNA to protein providing the cell checkpoints for self-regulating its functions to adjust the amount and type of proteins it manufactures. Both coding and non-coding genes must undergo the very first step of gene expression called transcription. Even though the final product is completely different for a coding or non-coding gene, and is obtained from potentially three different enzymes, they still share common mechanism of transcription termination in the fission yeast (Larochelle *et al*., 2018).

2.1. The transcription process (initiation, elongation, and termination)

In order to read the information encoded in genes, every living organism has to deal with the transcription step. The DNA-directed enzyme, RNA polymerase, is the main component of this process. It is subject to regulatory control at all stages of the transcription cycle, including initiation, elongation and termination.

During the first stage of initiation, the polymerase is recruited to a gene promoter, sometimes with the help of a transcriptional activator binding upstream from the promoter

(Blackwood and Kadonaga, 1998) or sometimes because of the absence of a transcription repressor and its steric hindrance (Hanna-Rose and Hansen, 1996). The DNA double helix is unwound to expose the template single strand, the first few nucleotides of RNA are synthesized and then the polymerase pauses in early transcriptional elongation, between 30 and 60 nucleotides downstream of the transcription start site (Kwak and Lis, 2013). The paused polymerase remains stably associated with the nascent RNA and is fully capable of resuming elongation, however further signals are required to elicit the transition to a productive elongation complex (Adelman and Lis, 2012). Once this maturation is reached, the enzyme escapes from the promoter to enter a phase of productive elongation (Juven-Gershon and Kadonaga, 2010).

The elongation step involves the complimentary copy of a single strand template of DNA into RNA composed of ribonucleotides including uracil where thymine occurred in the DNA sequence. Interestingly, promoter clearance is more complex than initially thought (Sims *et al*., 2004). Multiple factors can modulate elongation rates between genes or within the same gene from ∼1 to 6 kilobases (kb) per minute (Jonkers and Lis, 2015). Those factors include histone marks and gene features such as the number of exons. It suggests that elongation rate plays an important role in co-transcriptional processes such as splicing and transcription termination (Alexander *et al*., 2010; Jonkers *et al*., 2014; Veloso *et al*., 2014).

Finally, the end of the transcription unit is delimited by transcription termination when the polymerase and the nascent RNA are released from the DNA template (Richard and Manley, 2009). In that way, it prevents the polymerase from interfering with downstream DNA elements, such as promoters, and promotes polymerase recycling (Rosonina *et al*., 2006).

2.1.1. RNA polymerases

The ribonucleic acid polymerase (RNAP) is one of the most essential enzymes for life because it is implicated in the polymerization of ribonucleotides chains, the basic building blocks of DNA and RNA. Eukaryotes have 3 types of RNAP, each of which responsible for the synthesis of specific subsets of RNA. In yeast, RNA polymerase I

(RNAPI) and III (RNAPIII) transcribe ribosomal RNAs (rRNAs), which represents 80% of the total RNAs. A single unit of rDNA contains two transcribed genes, the 35S rRNA gene which is transcribed by RNAPI and will mature into the 5.8S, 18S and 25S (Russell and Zomerdijk, 2005), and the 5S rRNA gene transcribed by RNAPIII as well as transfer RNAs (tRNAs) and few small non-coding RNAs (ncRNAs) (Dieci *et al*., 2013, 2007).

Even though its contribution in terms of RNA abundance is smaller, the transcriptional activity of the RNA polymerase II (RNAPII) is the widest and the most extensively studied. It synthesizes messenger RNAs (mRNA) that are translated into proteins. RNAPII also transcribes a variety of ncRNAs, that are not translated because of their importance in gene regulation.

2.1.2. RNAPII Rbp1 subunit and its role in the transcription elongation rate

The RNAPII is a multiprotein complex composed of 12 subunits (Rpb1 to Rpb12), 10 of them forming the core of the enzyme to which a subcomplex Rpb4/7 is fixed (Cramer *et al*., 2008). The largest subunit of this complex is Rpb1 (194.16 kilodaltons (kDa)) encoded in *S. pombe* by the *rpb1* gene. It is the catalytic component of the enzyme and physically represents the bottom clamp that moves to grab the incoming DNA template and move forward during the transcription elongation step.

Another component of Rpb1 is a highly conserved subdomain known as the trigger loop (TL), critical for rapid catalysis and selection of correct substrates (Wang *et al*., 2006). During elongation, the translocation state of the RNAPII determines whether this active site is available for incorporation of the next nucleoside triphosphate (NTP) into the nascent RNA (Kaplan, 2013). This active site of Rpb1 undergoes conformational changes to preferential catalysis substrate interactions to correctly matched substrates over mismatched substrates (Kaplan *et al*., 2008). One of the steps that ensure faithful addition of correct substrates is the interaction between residue N494 (N479 in *S. cerevisiae* (Wang *et al*., 2006)) and 2′ and 3′ hydroxyl groups on the NTP ribose. The assumption made so far is that NTP interactions with N479 (**Figure 1A**, black circle), very close to the RNA-DNA hybrids, may stabilize or begin to promote TL-folding which could explain why a N479S mutant shows an *in vitro*

elongation rate ten times slower than a wild-type (**Figure 1B**, Kaplan *et al*., 2012). Finally, during the same year in *S. cerevisiae*, Francisco Malagon has demonstrated that another residue in the trigger loop plays an important role for the transcription elongation rate *in vitro*. Indeed, he showed in his paper that N488D mutation causes a change in the intrinsic elongation properties of the enzyme, resulting in an RNAPII that is slower than the wild-type polymerase (Malagon *et al*., 2006).

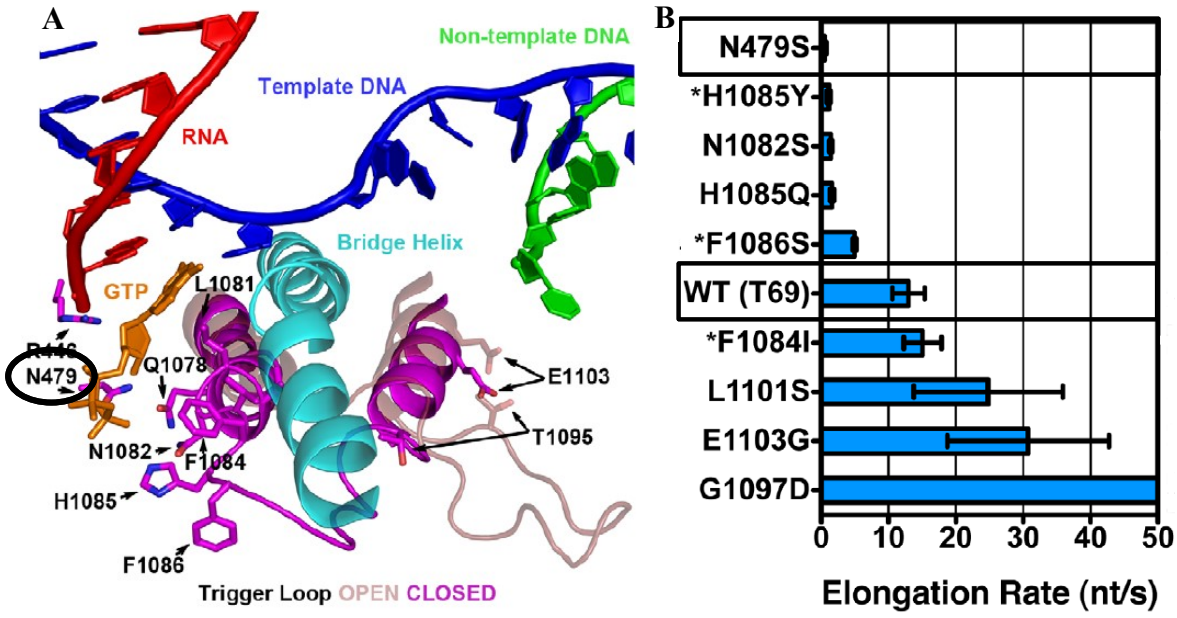

Figure 1. RNAPII N479 TL substitution mutants show a slower elongation rate *in vitro*.
Adapted from (Kaplan *et al*., 2012).
A. Diagram of ‘‘closed’’ RNAPII TL in Rpb1 in relation to nucleic acids. The black circle shows the mutated residue that induces a slow transcription elongation rate *in vitro*.
B. RNAPII TL single substitution elongation rates as determined *in vitro* using reconstituted RNAPII elongation complexes with synthetic oligonucleotides and an RNA primer.

2.1.3. RNA 3’ end processing and transcription termination

In order for a gene to be correctly expressed, the transcription step must be terminated effectively and release the newly synthesized RNA (Proudfoot, 2016). Polyadenylation signals (PAS or p(A)) at the 3’ end of the genes, typically a variation of the AAUAAA hexamer, and a uridine-rich downstream element, are the signals required for the assembly

of the pre-RNA 3' processing complex (Shi and Manley, 2015). In response to those elements, the cleavage and polyadenylation specificity factor and the cleavage stimulatory factor co-transcriptionally trigger an endonucleolytic cleavage of the pre-RNA, generating a free hydroxyl group at the 3′end to which adenosine monophosphate are successively added by poly(A) polymerases in order to protect the pre-RNA from degradation by 3'-5' exonucleases (Casañal *et al*., 2017). However, this association makes RNAPII pausing (Gromak *et al*., 2006) which correlates with maximal recruitment of cleavage and polyadenylation factors (Glover-Cutter *et al*., 2008).

Nevertheless, the RNAPII is still transcribing the unit. To fully complete the transcription termination, according to the kinetic model (also known as "torpedo" model), this new transcript will be a substrate of Dhp1, a processive 5'-3' exoribonuclease that catches up with the RNAPII and disassembles the transcription elongation complex, allowing the polymerase to be released and recycled for another transcription cycle (Baejen *et al*., 2017).

Moreover, it was reported that a gene can give rise to transcripts with multiple PASs and that differential usage of these sites can lead to the formation of distinct mRNA isoforms, a phenomenon termed as alternative polyadenylation (APA) (Barabino and Keller, 1999; Edwalds-Gilbert *et al*., 1997). More recent analyses using high-throughput sequencing have shown that APA is very common and occurs most frequently in the 3′ untranslated region (3′ UTR) of mRNAs, as expected from a transcription termination feature. Even though the expression levels of the growing number of APA-regulatory factors can alter PAS choice in different ways, the mechanism underlying this is still unknown.

2.1.4. Carboxy-Terminal Domain (CTD) of RNAPII

While all three RNAP possess Rpb1 subunits, RNAPII distinguishes itself by a flexible carboxy-terminal domain (CTD) from Rpb1 subunit near the newly synthesized RNA, which plays a central role in transcription regulation. The CTD domain is found among a very large scope of organisms (Buratowski, 2009). It is comprised of tandemly repetitive heptapeptides with the consensus sequence Tyr_1-Ser_2-Pro_3-Thr_4-Ser_5-Pro_6-Ser_7 ($Y^1S^2P^3T^4S^5P^6S^7$) which can vary from 26 repetitions in *S. cerevisiae* (Allison *et al*., 1985)

to 29 repetitions in *S. pombe* (Azuma *et al*., 1991) and 52 repetitions in mammals (Corden *et al*., 1985), underlying the scaling of CTD length with developmental complexity (Yang and Stiller, 2014).

In budding yeast, cells are viable with a CTD as short as 13 heptad repeats but further deletion down to ten repeats is lethal, indicating that the heptad repeats are partially redundant for the essential role of the CTD (Nonet *et al*., 1987).

In addition, work in *Drosophila melanogaster* showed that a truncated CTD composed exclusively of consensus repeats (YSPTSPS) supports Drosophila viability, but that a CTD with enough YSPTSPS repeats to match the length of the wildtype Drosophila CTD is defective (Lu *et al*., 2019).

Altogether, these studies suggest that sequence complexity and length of the CTD are important in development and viability, highlighting the essential role of the CTD domain, but it does not seem to be required for RNAPII transcription *per se*. Instead, it appears that the CTD operates as a recruitment platform for multiple factors involved in all steps of the transcription process. The specificity of the recruitment of those factors depends on different configurations adopted by the CTD due to the combination of post-translational modifications and conformational changes within the CTD defined as the "CTD code" (Buratowski, 2003).

2.1.5. Post-translational modification (PTM) of RNAPII CTD during transcription and its consequences

CTD is potentially modified on each of the seven residues of the consensus heptads. Five of them can be phosphorylated (Y^1, S^2, T^4, S^5 and S^7) whereas the two prolines (P^3 and P^6) can be subject to isomerization in either a *cis* or *trans* conformation (Heidemann *et al*., 2013). Other PTM include S^2, S^5 and T^4 glycosylation (Lu *et al*., 2016) and methylation, acetylation and ubiquitination of arginine residues in the non-consensus repeats (Schröder *et al*., 2013; Voss *et al*., 2015).

Nevertheless, the "CTD code" appears less complex than expected. Mass spectrometry shows that the phosphorylation of the serines in second (Ser2-P) and fifth (Ser5-P) position were 100 times more abundant than other PTM. While the absolute abundance of a modification is not a measure of its biological relevance, we will, for the sake of brevity, mainly focus on the role of the major modification Ser2-P, which became the most studied phosphorylation in correlation with the presence of a transcription termination site.

2.1.5.1. The chromatin immunoprecipitation assay: a powerful and versatile technique for protein-DNA interactions

The chromatin immunoprecipitation (ChIP) is a technique that determines whether a protein of interest interacts directly or indirectly with DNA sequences. It provides information about the association of a protein of interest like a transcription factor or the abundance of a PTM like the Ser2-P of the RNAPII CTD. The overall process is represented with the **Figure 2** bellow.

First, the usage of formaldehyde allows covalent bonds *in vivo* between protein and DNA as well as between protein and protein (Wells and Farnham, 2002). Indeed, many protein–DNA interactions are transient, and involve multi-protein complexes to orchestrate biological function.

Then, the chromatin is extracted using chemical and/or mechanical lysis and fragmented through either sonication (shear) or enzymatic digestion in order to have smaller and workable pieces of DNA (Bortz and Wamhoff, 2011). The chromatin fragments usually range between 300 and 500 bp.

Afterwards, the protein of interest is immunoprecipitated using a specific antibody against the protein (or against a PTM). This step selectively enriches for the protein–DNA complex of interest and eliminates all other unrelated cellular material.

Finally, the DNA is purified and reverse crosslinked to further be analyzed by either quantitative polymerase chain reaction (ChIP-qPCR) for a specific locus (Carey *et al*., 2009) or high throughput sequencing (ChIP-seq) for a genome-wide study (Robertson *et al*., 2007;

Schmidt *et al*., 2009). In a word, the amplified DNA will represent indirectly the abundance of the target along the DNA template.

However, because DNA fragmentation by sonication is not a truly random process (Grokhovsky, 2006; Grokhovsky *et al*., 2011), one must include a control called input. An input DNA sample must be generated for each strain included in the experiment and undergoes the cross-linking and sonication steps but not the immunoprecipitation. The main purpose in the end is to normalize the signal from the ChIP experiment by the appropriate input for each strain.

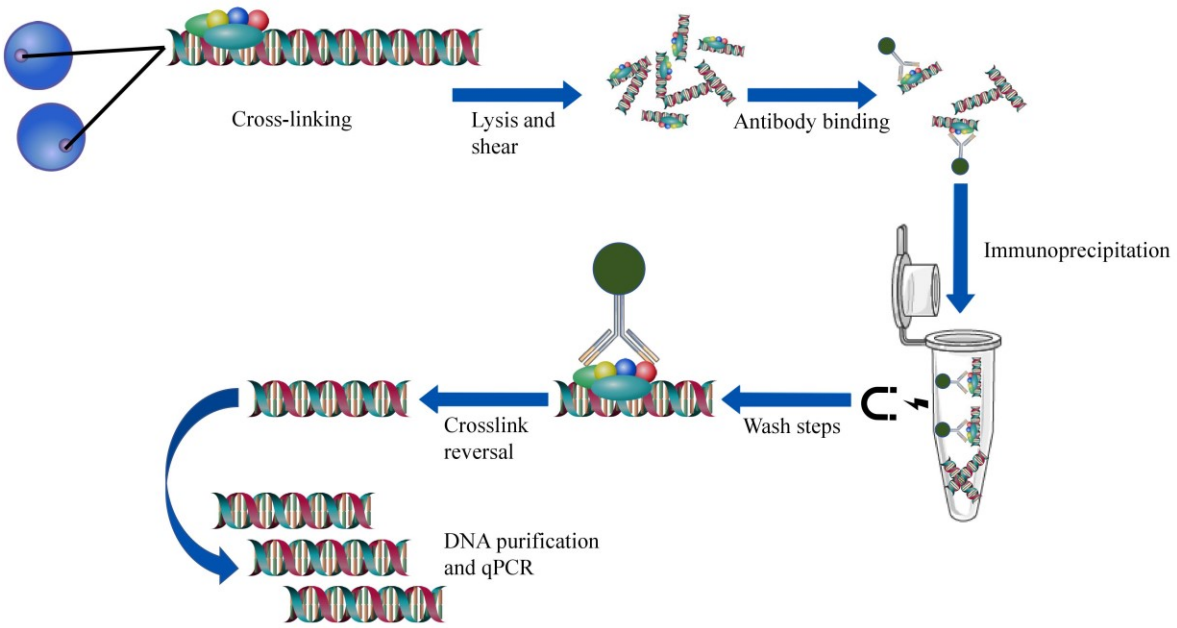

Figure 2. Chromatin immunoprecipitation overview.
Proteins associated with the chromatin in living cells or tissues are covalently bonded using formaldehyde, the DNA–protein complexes are then sheared into ~300-500 bp DNA fragments using either enzymatic digestion or physical shearing by sonication. Cross-linked DNA fragments associated with the protein(s) of interest are selectively immunoprecipitated from the cell debris using specific antibody coupled here to magnetic beads. After the crosslinks are reversed, the DNA fragments are purified, and their sequence is determined. These DNA sequences are reflecting the position and abundancy of the protein of interest *in vivo*. The DNA undergoes PCR amplification using primers targeting any genomic locus of interest. These DNA sequences can be subjected to several downstream analysis techniques.

2.1.5.2. Pattern of phosphorylated CTD Ser2 across transcription units

ChIP experiments using antibodies specific to Ser2-P revealed that this modification has a specific spatio-temporal framework in correlation with transcription cycle.

In fission yeast, Ser2 is phosphorylated during transcriptional elongation by its major kinase Lsk1 (Coudreuse *et al*., 2010). Previous ChIP-seq experiments in fission yeast from Bachand's lab (Larochelle *et al*., 2018) revealed a CTD phosphorylation pattern across transcription units where Ser2-P steadily increased along the gene body during transcription elongation and sharply peaked to its maximum level toward the 3' end of the coding genes (**Figure 3A**) as well as the non-coding genes (**Figure 3B**, in this example snoRNAs are used as a representation of non-coding gene transcription termination), downstream of the polyadenylation site (p(A)). It is then removed by the Fcp1 phosphatase (Cho *et al*., 2001).

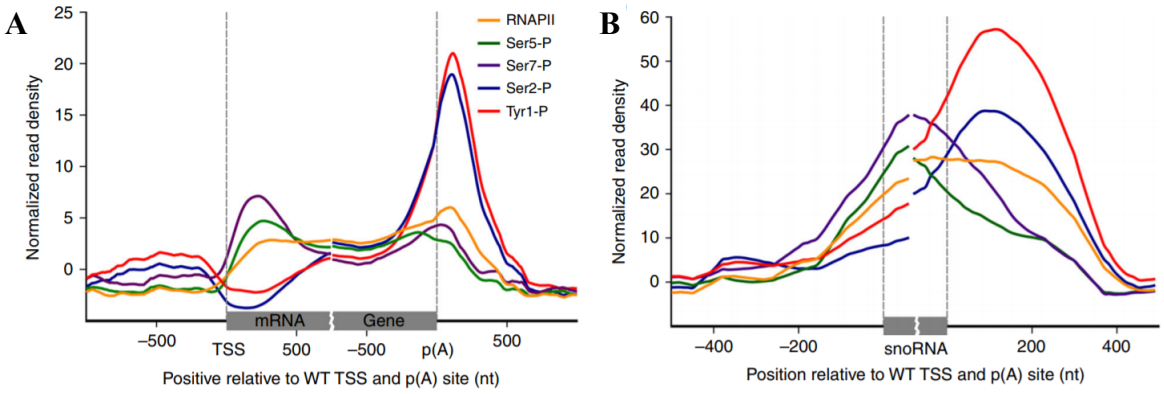

Figure 3. Genome-wide occupancy of the RNAPII and CTD modification in fission yeast.
Adapted from (Larochelle *et al*., 2018).
Average ChIP-seq profile of total RNAPII (Rpb1) and the indicated CTD modifications in a wildtype (WT) strain across 4755 mRNAs (**A**) and 24 monocistronic snoRNAs (**B**) with a mapped poly(A) site in minimal medium.

2.1.5.3. Coordination between Ser2-P and transcription termination

Several subunits of the 3' processing complex, such as Rna14, Pcf11 or Seb1, show a genome-wide binding profile at the 3' end of the coding genes (**Figure 4A**) as well as the non-coding genes (**Figure 4B**, in this example snoRNAs are used as a representation of non-coding gene transcription termination) (Larochelle *et al*., 2018). Therefore, an easy correlation has been made between the genome-wide profiles of Ser2P and 3' processing factors which both peak right after the poly(A) site. Indeed, many of those factors directly interact with the CTD of RNAPII via their conserved CTD-interacting domain (CID), including Pcf11 and Seb1, which preferentially interact with Ser2P (Lunde *et al*., 2010; Wittmann *et al*., 2017).

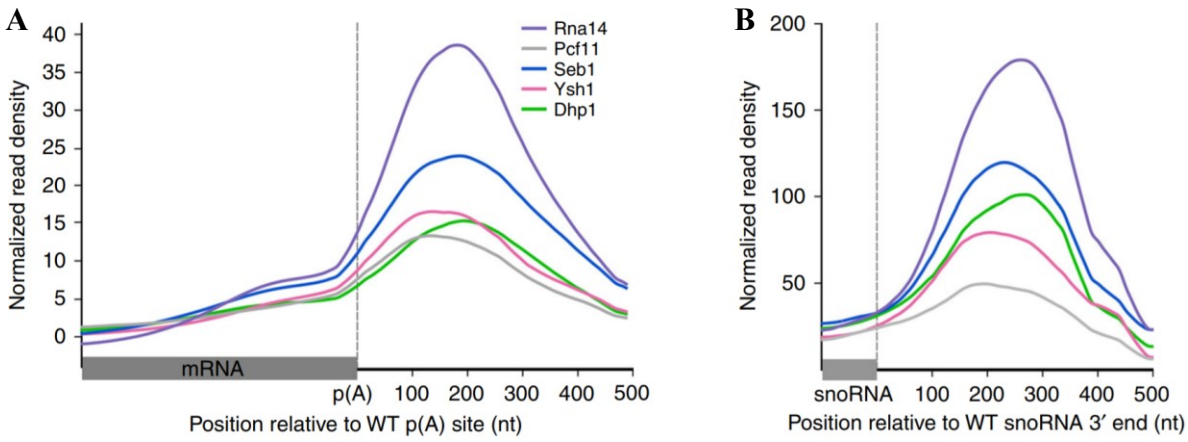

Figure 4. *S. pombe* mRNA 3′ end processing and transcription termination factors are recruited at the 3′ end of coding and non-coding genes.
Adapted from (Larochelle *et al*., 2018).
Average ChIP-seq profile of the indicated mRNA 3′ end processing factors modifications in a WT strain across 4755 mRNAs (**A**) and 24 monocistronic snoRNAs (**B**) with a mapped poly(A) site in minimal medium.

2.1.6. An example of gene regulation via non-coding RNA

Phosphate homeostasis in *S. pombe* is achieved by the regulation of the transcription of genes encoding three proteins involved in extracellular phosphate mobilization: a cell surface acid phosphatase Pho1, an inorganic phosphate transporter Pho84, and a glycerophosphate transporter Tgp1, with all three genes dependent on transcription factor Pho7 binding at their promoters (Carter-O'Connell *et al*., 2012). These genes are repressed during growth in phosphate-rich medium and induced during phosphate starvation.

Recent studies have unveiled a role for long non-coding RNAs (lncRNAs) in phosphate-regulated expression of the *pho1* and *tgp1* genes. In the case of *tgp1*, the lncRNA *nc-tgp1*, initiating 1865 nucleotides (nt) upstream of the *tgp1* AUG start codon, represses *tgp1* in *cis* during phosphate-replete growth. Indeed, *tgp1* is de-repressed when the *nc-tgp1* locus is disrupted by deleting the *nc-tgp*1 transcription start site (Ard *et al*., 2014). Moreover, the transcription factor Pho7 binds 187 nt upstream of the *tgp1* start codon (Schwer *et al*., 2017) exactly where the polyadenylation signal of *nc-tgp1* is (**Figure 5**, PAS2). The assumption made so far is that transcription of the upstream *nc-tgp1* lncRNA in *cis* interferes with expression of the downstream gene *tgp1* in phosphate-replete cells, likely by displacing the Pho7 transcription factor from *tgp1* promoter because of transcription termination of *nc-tgp1*.

It has been shown more recently that the same long non-coding RNA has another PAS (**Figure 5**, PAS1) more upstream from PAS2, leading to the discovery of a shorter RNA derived from *nc-tgp1* locus (Sanchez *et al*., 2018). Mutating PAS1 abolishes de-repression of the *tgp1* downstream, but how alternative polyadenylation of *nc-tgp1* regulates *tgp1* expression is still unknown.

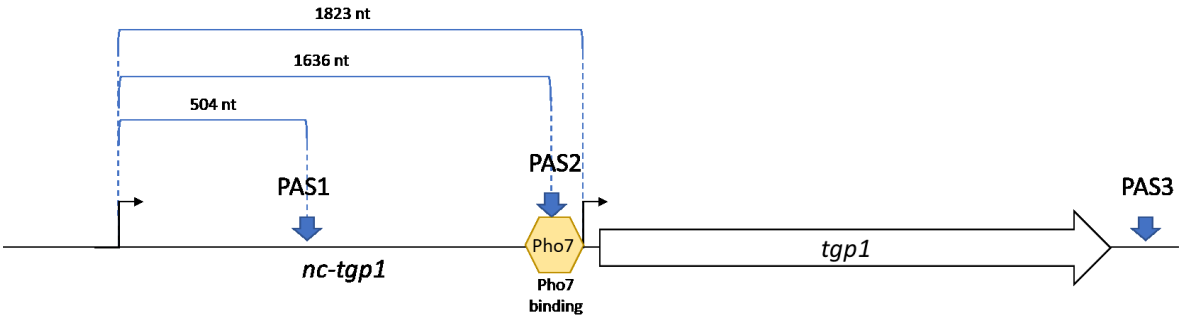

Figure 5. Schematic representation of *nc-tgp1* and *tgp1* loci.
The tandem *nc-tgp1–tgp1* locus is shown with the *nc-tgp1* and *tgp1* transcription start site indicated by the black arrows and the *tgp1* ORF depicted as a white bar with arrowhead indicating the direction of transcription. The *nc-tgp1* transcript has a two polyadenylation sites, a proximal one (PAS1) from 504 nucleotides to the transcription start site and a distal one (PAS2) from 1636 nucleotides to the same transcription start site. The transcription factor Pho7 binds the chromatin upstream of *tgp1* promoter. The *tgp1* transcript has a polyadenylation site (PAS3) from 2101 nucleotides to its transcription start site.

2.1.7. Transcriptome analysis by RNA-sequencing (RNA-seq)

Quantification of RNA transcripts is a critical step to understand the mechanism of gene regulation. The recent development of RNA amplification coupled to next generation sequencing revolutionized transcriptome analysis by providing the tools necessary to study the total cellular content of RNA using RNA-seq pipelines (**Figure 6**). Different library preparation protocols are available allowing the focus on different classes of RNA through different enrichment steps. Such strategies include polyA enrichment, rRNA depletion (or ribo-depletion) and small RNA enrichment (Conesa *et al*., 2016; Hrdlickova *et al*., 2017; O'Neil *et al*., 2013). Then RNAs are fragmented and reverse transcribed into complementary DNAs with appropriate ligated adapters for sequencing because DNA is more stable and suitable for amplification (use of DNA polymerase).

Furthermore, the sequencer produces millions of raw reads that need to be trimmed in order to remove the adapters sequences as well as some low quality bases associated with a low Phred score (Ewing et al., 1998). The remaining good quality reads are aligned to a reference genome (if available) using alignment tools that consider splicing events, otherwise reads overlapping exon-exon junctions could not be aligned.

Finally, the aligned reads are quantified for each gene and, at least, normalized by sequencing depth. If different strains or conditions are used in the experiment, differential

gene expression analyses are typically carried out to assess the genes that are significantly differently expressed.

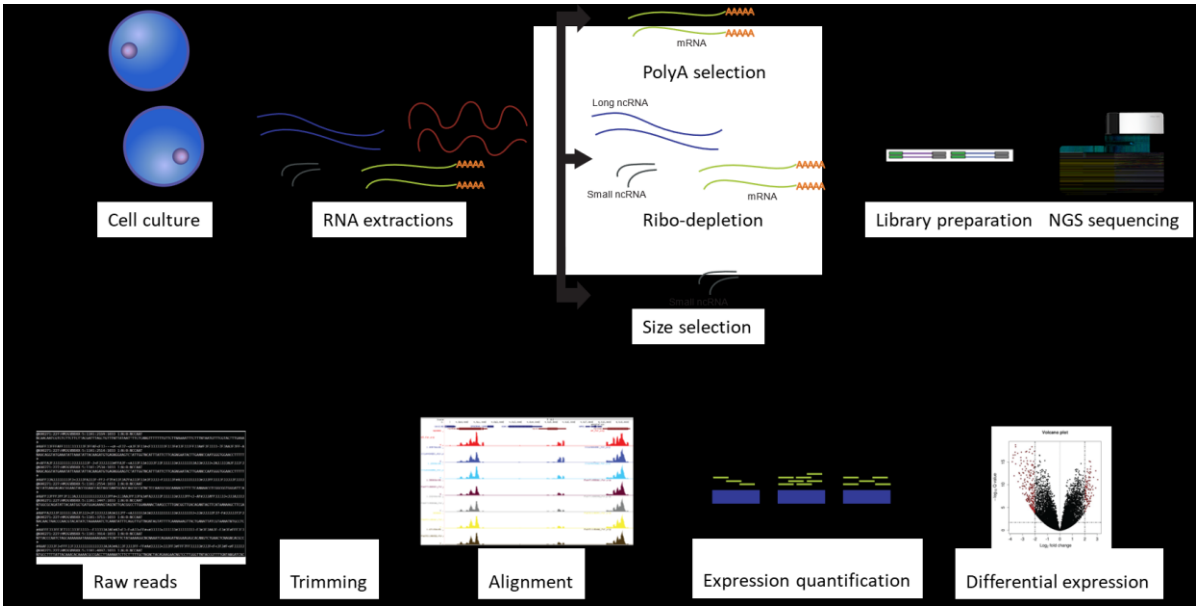

Figure 6. Overview of a typical RNA-Seq experimental workflow.

3. Problem statement, objectives and assumptions

Throughout the progression of transcription elongation, the RNAPII recruits different proteins in order to process the pre-mRNA that is co-synthesized. It is easy to imagine that changes in elongation rate could influence the co-transcriptional processing of RNAs that occurs during the elongation step, but how the transcription elongation rate influences the transcriptome remains poorly understood.

Some studies have started to answer this question and characterized mutations in RNAPII Rpb1 subunit in the budding yeast that slowed down the transcription elongation rate *in vitro* (Kaplan *et al*., 2012b; Malagon *et al*., 2006). Those mutations have been used in mammalian cells (Fong *et al*., 2015; Hazelbaker *et al*., 2013) and in the budding yeast (Aslanzadeh *et al*., 2018) to show an effect of elongation rate on different features of RNA maturation and gene expression. But it has never been done in fission yeast *S. pombe*. Here, we used a genome edited mutant of RNAPII that possesses a homologous mutation (N494D)

previously described in *S. cerevisiae* by Francisco Malagon in 2006 that decreases transcription elongation rate.

In this work, we investigate the transcriptome-wide effect of a slow transcription elongation rate on global gene expression. The first objective is to validate that transcription elongation rate influences gene expression in fission yeast, and if there are some genes that are more affected than others. In addition, I consider genes that use alternative polyadenylation, especially the use of the proximal PAS compared to the distal one. Indeed, we can simply imagine a train going very slowly and making two or more stops (represented here by two or more PAS). It is most likely that passengers will stop the trip at the first stop instead of the second one because they are bored of this slow trip and want to get out of the train (represented here by transcription termination at the proximal PAS because the RNAPII slowing transcribes).

Finally, if gene expression is indeed affected, then a focus will be made on the most significantly affected gene in order to have some mechanistic insights about how the transcription elongation rate influences gene expression.

Materials and Methods

Yeast strains and media

A list of all *S. pombe* strains used in this study is provided in **Supplementary Table 1**. Cells were routinely grown at 30 °C in YES media (3% glucose, 0.5% yeast extract, supplemented with adenine, histidine, leucine and uracil) or Edinburgh minimal media (EMM). Cells were collected at OD_{600nm} of ~0.5-0.7. Gene disruptions and C-terminal tagging of proteins were performed by PCR-mediated gene targeting (Bähler *et al*., 1998) using lithium acetate method for yeast transformation. Expression of tagged proteins was confirmed by western blotting and knockouts strains by the absence of RNA by RT-PCR.

Growth assays

For spotting assays, exponential cultures of *S. pombe* cells were adjusted to an OD_{600nm} of 1.0, and serially diluted tenfold using water. Each dilution was spotted (3 µL per

spot) on YES plates with or without hydroxyurea or KCl. Plates were incubated at 30 °C for 2–7 days. For liquid growth assays, cells were grown in either EMM or YES media and 50 µl of appropriated early-log-phase cell suspensions (OD_{600nm} of 0.02) were added to 50 µl of either EMM or YES. Samples were prepared in triplicate in Costar 96-well noncoated polystyrene microplates, and cell growth was monitored with a PowerWave microplate spectrophotometer reader (BioTek Instruments) with the following software settings: the optical density was measured at 660 nm, incubation was kept at 30 ± 0.1 °C, the microplates were subjected to continuous shaking at intensity 2, during 595 s. Readings were done every 10 min during a 48h period. The spotting and liquid growth assay experiments was repeated twice.

RNA preparation and analyses

Total RNA was extracted from one WT strain and two biological replicates of the slow mutant using the hot-acid phenol method. For Reverse Transcription Quantitative PCR (RT-qPCR) RNA samples (1 µg of total RNA) were treated with Promega DNase RQ1 and reverse transcribed using Qiagen Omniscript RT. cDNA was diluted 100-fold and analyzed on a LightCycler® 96 Instrument using perfecta SYBR supermix in the presence of a 150 nM concentration (each) of gene-specific primers in 15 µl reaction mixtures. For the calculation of RNA abundancy, the threshold cycle (C_T) of each average from three technical replicates was subtracted to the C_T of the housekeeping gene *nda2* (coding for tubulin alpha 1). The resulting difference in threshold cycles (ΔC_T) was used to calculate the relative change in RNA levels between the WT and the mutant by calculating the $2\Delta C_T$ value. The RNA abundancy was graphically presented as the relative abundance in the mutant, normalized to *nda2* and relative to the WT.

Library preparation and Illumina sequencing

Library preparation was performed at the Plateforme de l'Université de Sherbrooke. Briefly 10 µg of total RNA was used to perform a DNase treatment on a RNeasy Mini Kit column (Qiagen). DNase treatment on the column and RNA recovery were performed as per manufacturer's protocol. RNA integrity was assessed with Agilent 2100 Bioanalyzer (Agilent Technologies).

Ribo-depleted RNA was isolated from 1.25 µg of total RNA using Illumina Ribo-Zero (yeast), as per manufacturer's protocol, the RNA cleanup was performed by ethanol precipitation, and depleted RNA was resuspended in 10 µl of water. Quality and quantity assessments were performed on Agilent pico Chip. The RNA-seq library was then built using the Epicentre SSV21106 kit from 9 µl isolated ribo-depleted RNA with 13 cycles of amplification. Library quality was assessed using the Agilent DNA HS Chip. Library quantification was performed by Qubit quantification. Pooled libraries were sequenced at 100 bp paired-end reads using Illumina HiSeq 4000 PE100 at McGill University and Génome Québec Innovation Centre Sequencing Service. A summary of the output from the sequencer is listed in the **Table 1** bellow.

Table 1. Statistics of the samples after the sequencing run

Name	Number of reads sequenced	Number of bases sequenced	Average quality (Phred)	% duplicata
WT	40 853 659	8 170 731 800	38	55.3
Slow1	53 496 159	10 699 231 800	39	64.7
Slow2	39 265 137	7 853 027 400	39	65.3

RNA-seq data analysis: MUGQIC RNA-Seq pipeline

Read processing, alignment and differential expression analysis were done using the MUGQIC 1.10.4 pipeline (https://bitbucket.org/mugqic). Briefly, reads were trimmed from the 3' end to have a Phred score of at least 30 per nucleotide. Illumina sequencing adapters were removed from the reads, and all reads were required to have a length of at least 32 bp. Trimming and clipping was performed using Trimmomatic 0.36 software (with THREADS: 30, MINLEN: 32 and TRAILING: 30) (Bolger *et al*., 2014). The filtered reads were aligned to a reference genome. The genome used in this analysis was *S. pombe* assembly ASM294v2.

Each readset was aligned using STAR 2.5.1 with --runThreadN 46 and all other parameters by default (Dobin *et al*., 2013) which created a Binary Alignment Map file (.bam). Then, all readset BAM files from the same sample were merged into a single global BAM file using Picard 2.0.1. Raw read counts were obtained from EnsemblGenomes23 (.gtf) using HTSeq 0.11.0 (Anders *et al*., 2015) with -m intersection-nonempty and all other parameters by default. Even though the multimappers are kept in the BAM file, HTSeq does not count them. The results of the differential gene expression analysis were generated using R Bioconductor 3.1.2 with the package DESeq 1.36.0 (Anders and Huber, 2010) and default parameters. Screenshots of processed data at different loci were taken from the IGV-web browser (Robinson *et al*., 2011).

AnGeLi: Analysis of Gene Lists

Functional enrichment of gene lists was performed using the AnGeLi tool, which applies a two-tailed Fisher's exact test (Bitton *et al*., 2015). The inputs were the genes significantly (p-value < 0.05) and differentially expressed (|Log2_FC| > 0.5). No pre-defined background was selected ("all genes") and the results with a p-value smaller than 0.01 were displayed.

Protein analysis

Total cell extracts were prepared by harvesting mid-log cells in ice-cold lysis buffer (50 mM Tris (pH 7.5), 5 mM MgCl2, 150 mM NaCl and 0.1 % NP-40) containing a cocktail of protease inhibitors (1x PMSF and 1x PLAAC) with half of a phosphor STOP tablet, prior to lysis with glass beads using a FastPrep instrument (MP Biomedicals). Clarified lysates were normalized for total protein concentration using the Bradford protein assay. 30 µg of proteins were separated by SDS–PAGE, transferred to nitrocellulose membranes, and analyzed by immunoblotting using either, a mouse monoclonal antibody specific to α-tubulin (Sigma-Aldrich, T5168; 1:1,000 (v/v) dilution), or a rabbit polyclonal antibody against protein A (Sigma-Aldrich, P3775; 1:10,000 (v/v) dilution) in the case of HTP-tagged Seb1 or TAP-tagged proteins. Membranes were then probed with goat anti-rabbit or anti-mouse secondary antibodies conjugated to IRDye 800CW (LI-COR, 926-32213; 1:15,000 (v/v)

dilution) and AlexaFluor 680 (Life Technologies, A21057; 1:15,000 (v/v) dilution), respectively. Detection of the proteins was performed using an Odyssey infrared imaging system (LI-COR).

Chromatin immunoprecipitation (ChIP) assays

For each IP, 50 mL of cells were grown at OD_{600nm} of ~0.5-0.7 at 30 °C in EMM. Formaldehyde was added to a final concentration of 1% with diluent solution (0.143 M NaCl, 1.43 mM EDTA and 71.34 mM HEPES-KOH pH 7.5), cells were incubated at room temperature (RT) for 20 min and manually agitated every 5 min. After quenching the reaction with glycine (final concentration of 360 mM) for 5 min at RT, cells were washed twice with cold Tris-buffered saline (20 mM Tris–HCl pH 7.5, 150 mM NaCl). Cell pellets from 50 ml cultures were resuspended in 500 µL of lysis buffer (50 mM HEPES-KOH pH 7.5, 140 mM NaCl, 1 mM EDTA pH 8.0, 1% Triton X-100, 0,1% Na-deoxycholate) containing protease inhibitors (1 mM phenylmethylsulfonyl fluoride, 1 mM benzamidine, 10 µg of aprotinin/µL, 1 µg of leupeptin/µL, and 1 µg of pepstatin/µL) and disrupted vigorously with glass beads three times for 30 s using a FastPrep instrument. Samples were then sonicated 10 times for 10 s at 20% using a Branson digital sonifier. Whole-cell extracts (WCE, 500 µL) were incubated with a mix of 30 µL of beads coupled to 2 µg of antibodies. The magnetic beads coupled to the antibodies of interest used in this study are listed in the **Table 2** below.

Table 2. List of antibodies and beads used in this study for ChIP analyses.

Target	Antibody	Beads
RNAPII Rpb1 non-phosphorylated CTD (total RNAPII)	8WG16 (ENZ-ABS132A-0100)	Dynabeads Pan Mouse IgG #110.41 (Invitrogen)
RNAPII Rpb1 phosphorylated CTD Ser2	Clone 3E10 (04-1571)	Dynabeads Protein G #10003D (Invitrogen)
RNAPII Rpb1 phosphorylated CTD Ser5	Clone 3E8 (04-1572)	Dynabeads Protein G #10003D (Invitrogen)
RNAPII Rpb1 phosphorylated CTD Ser7	Clone 4E12 (04-1570)	Dynabeads Protein G #10003D (Invitrogen)
TAP/HTP tag		Dynabeads Pan Mouse IgG #110.41 (Invitrogen)

Beads were washed twice with 1 mL of lysis buffer, twice with 1 mL of lysis buffer plus 500 mM NaCl, twice with 1 mL of wash buffer (10 mM Tris-HCl pH 8.0, 250 mM LiCl, 0.5% NP-40, 0.5% sodium deoxycholate, and 1 mM EDTA) and once with 1 ml of Tris-EDTA (TE; 10 mM Tris-HCl pH 8.0, 1 mM EDTA). Bound material was eluted by

resuspending beads in 50 µL of elution buffer (50 mM Tris-HCl pH 8.0, 10 mM EDTA, and 1% SDS) and incubated in a Thermomixer Eppendorf for 15 min at 65 °C at 1200 rpm with additional slow vortex every 5 min. Samples were centrifuged briefly and the cross-linking was reversed by incubating 50 µL of supernatant with 120 µL of TE plus 1% SDS or 5 µL of WCE with 95 µL of TE plus 1% SDS during overnight at 65 °C. Samples were treated with proteinase K, extracted twice with phenol chloroform isoamyl alcohol pH 8.0 (Invitrogen), extracted once with chloroform (Bioshop), precipitated with ethanol, and resuspended in 30 µL of TE. DNA was then treated with 10 µg of RNase A at 37 °C for 60 min and purified using a PCR purification kit from Qiagen. DNA from the inputs were diluted 100-fold and DNA from the IPs were diluted 20-fold and analyzed on a LightCycler® 96 Instrument using perfecta SYBR supermix in the presence of a 150 nM concentration (each) of gene-specific primers in 15 µL reaction mixtures. Protein density was calculated by subtracting the CT of each average from three technical replicates of the IP from the CT of the average from three technical replicates of the input. The resulting difference in threshold cycles was used to calculate the relative abundance of the immunoprecipitated target by calculating the $2\Delta C_T$ value. The protein binding abundancy in the mutant was graphically represented normalized to the input and relative to the WT. Some targets, like the phosphorylated CTD or 3'end processing factors, needed to be normalized to total RNAPII because they were dependent of the abundancy of RNAPII at a given locus.

Results

1. Genome-wide consequences of a slow transcription elongation rate

To gain further insight into the coupling between transcription elongation rate and gene expression, we examined the genome-wide gene expression profile between a wild-type (WT) strain and two biological replicates containing the same slow *rpb1* allele (**Supplementary Table 1**). A total average of 44,538,318 reads were obtained from paired-end next generation RNA sequencing (RNA-seq) on total ribo-depleted RNA. On average, only 8,328 reads did not meet the quality requirements (Phred score per nucleotide > 30 amd minimum length of 32 nucleotides) and were removed from the analysis. After aligning the good quality reads (with an average read length of 197 nt) to the *S. pombe* ASM294v2 reference genome, we obtained, on average, 39,768,507 uniquely mapped split reads, 4.79% reads mapped to less or equal than 10 loci, 0.42% reads mapped to more than 10 loci and 5.27% reads unmapped (too short).

1.1. Slow *rpb1* allele significantly affects gene expression

As a classic purpose of an RNA-seq experiment, we wanted to know how many genes were up or down-regulated in the slow mutants compared to the WT. To investigate this, raw reads were quantified for 7,005 genes by HTSeq-count using EnsemblGenomes23.gtf file, producing a number of reads for each gene in Counts Per Million (CPM) normalized to the size of the library. Since here we iteratively compare each gene expression between different strains, there is no need to normalize to the size of the gene because it will be the expression of the same gene studied in the WT and the slow mutants.

Raw read counts generated by HTSeq were used as input for the differential gene expression analysis with DESeq. To do so, 6,633 filtered genes (CPM > 3) were statistically compared between the WT and two biological replicates of the slow mutant (**Figure 7A**). The difference in expression level in the slow mutant compared to the WT was significantly (adjusted p-value<0.05) greater than 0.5-fold for 382 genes (**Supplemental Table 2**) and

significantly lower than 0.5-fold for 494 genes (**Supplemental Table 3**). As a side note, *tgp1* appears to be the most significant up-regulated gene in the slow mutant (**Figure 7A**).

Unfortunately, this result alone does not allow us to conclude anything besides how many genes are up and down-regulated in the context of a slow *rpb1* allele. However, such gene lists often contain valuable, hidden biological information which can be uncovered by submitting those lists to AnGeLi (Analysis of Gene Lists), an online tool specifically designed for the fission yeast (Bitton *et al*., 2015). It takes as an input a list of systematic gene identifiers, and searches for any enrichment of common features using different sources such as specific GO categories, phenotypes, or published gene lists. Consequently, the up-regulated genes in the slow mutant present significantly enriched categories related to different stress responses (**Figure 7B**), which correlates with the slow growth observed in minimal media (**Supplemental Figure 1**), and the increased sensitivity to DNA damage and osmotic stress (**Supplemental Figure 2)**. Furthermore, the down-regulated genes in the slow mutant present some significantly enriched categories related to ribosomal RNAs, which can be explained by the state of stress of the slow mutants. But, interestingly, some categories related to the non-coding RNAs were also identified (**Figure 7C**). In other words, there is an enrichment of down-regulated ncRNAs as well as genes involved in their processing.

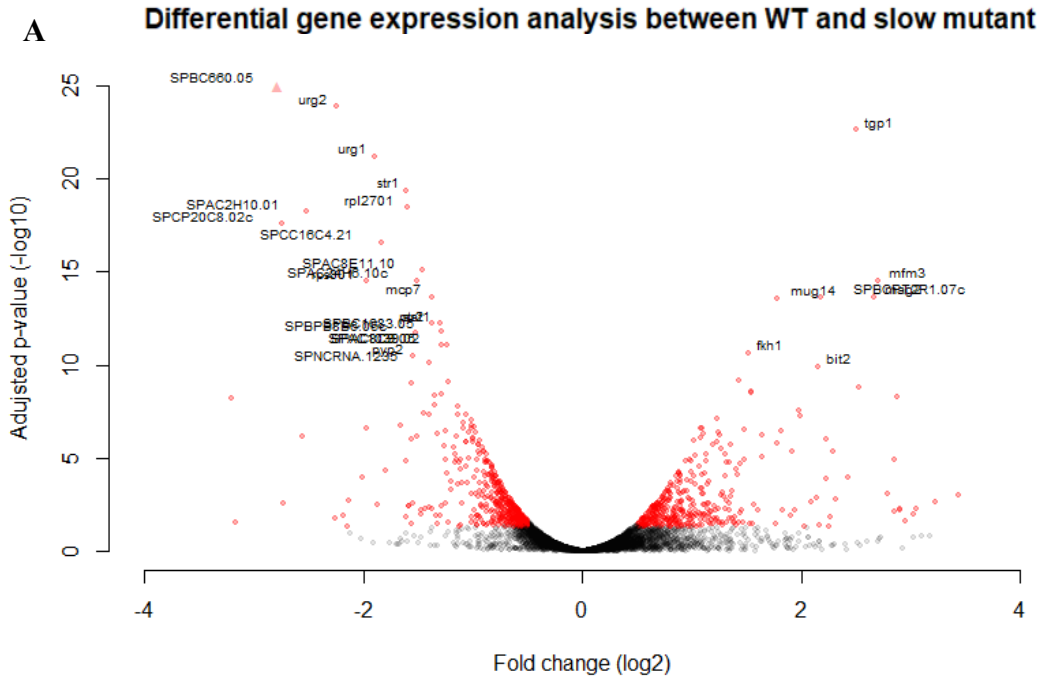

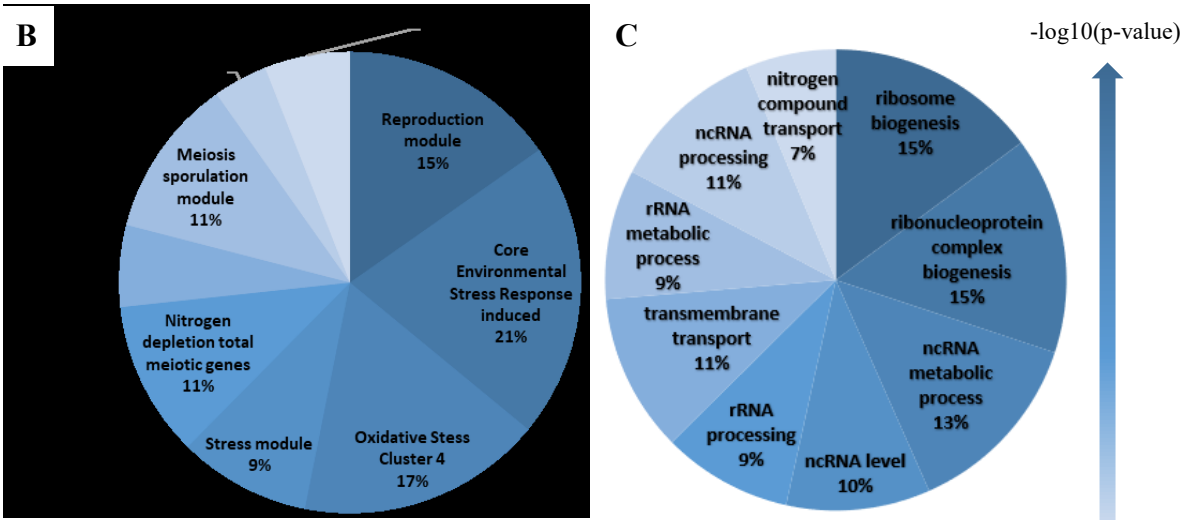

Figure 7. Transcriptome-wide analysis of gene expression changes in *S. pombe* Rpb1 slow mutant.

(**A**) Volcano plot showing differentially expressed genes between the Rpb1 slow mutant and the WT. The x-axis is log2 ratio of gene expression levels between the WT and the slow mutant; the y-axis is adjusted p-value based on -log10. Data for genes that were not classified as differentially expressed are plotted in black. The red dots represent the differentially expressed genes in the slow mutant compared to the WT based on p-value.adj<0.05 and an absolute log2 fold change greater than 0.5. Only the top hits of the significantly differentially expressed genes are labelled (p-value.adj<5E-10) (complete list in supplementary tables). SPBC660.05 has an arrow because the p-value is highly significant. (**B**)-(**C**) Enrichment analysis of functional categories of respectively 382 genes significantly up-regulated and 494 genes significantly down-regulated using AnGeli (FDR<0.01). The percentage represents the frequency of genes significantly up or down-regulated in each category. Only significant enrichments at a corrected p-value<1.3E-06 are plotted (complete results in supplementary tables). A total of 208 genes belong to at least two different enriched categories. The colored arrow represents the intensity of the significance for the enriched categories, the darker it is the more significant the category is enriched.

1.2. Proximal cleavage sites are preferentially used in the *rpb1* slow mutant

In *S. cerevisiae*, mutating the transcription termination factor Sen1 in a strain already containing the same slow *rpb1* allele produced shorter non-coding transcripts and lead to a model where the termination window is narrow with earlier termination events (Hazelbaker *et al*., 2013). This same model can be expected in the context of alternative polyadenylation (APA), where the slow mutant would favor transcription termination at the proximal polyadenylation signal (PAS) instead of the distal one.

To verify this assumption, our RNA-seq data was merged with published sequencing data of the 3′ end of RNA poly(A) (Liu *et al*., 2017). The purpose here was, first, to annotate genomic segments strand specific reflecting the usage of multiple PAS for gene expression. To consider a valid APA for our study, we set up a threshold of 50 nucleotides between two signals of APA in the 3'UTR of every annotated gene (coding and non-coding). We ended up with 1723 genes presenting at least two different poly(A) sites in their respective 3'UTR (1538 mRNA, 183 lncRNA, 2snRNA). Secondly, RNA-seq reads counts were performed on each segment allowing us to compare the proportional expression of the segments within the same gene between the WT and the slow mutant to find RNA-seq expression patterns consistent with differential APA usage. Typically, the first segment represents reads from transcription start site (TSS) to the proximal PAS (first PAS), and the second segment represents reads from the proximal PAS to distal PAS (second and more PAS). A ratio for each gene was calculated between the first segment relative to the second one ($\frac{proximal\ segment}{distal\ segment}$) to finally compare those ratios in the slow mutant relative to the WT and ($\frac{\frac{proximal\ segment\ WT}{distal\ segment\ WT}}{\frac{proximal\ segment\ slow}{distal\ segment\ slow}}$) and plot this in a volcano plot (**Figure 8A**). For this analysis, ratios have not been normalized to the length of the segments because here the same segment is studied in two different conditions (WT vs slow) so it reflects the same situation when expression of a gene is studied in two different conditions, one can keep the CPM unit (normalization for sequencing depth) and does not have to normalize for gene length. This resulted in 441 genes in the two biological replicates slow mutants with ratios at least twice smaller (FDR < 0.05; Log2 FC < -1) than the WT ratio, indicating that proximal PAS is privileged for those 441 genes in the slow mutant. The "ratio of ratios" is an estimate of the change in the proportional

usage of the proximal PAS over the distal PAS. A negative Log2 of "ratio of ratios" is indicative that the RNA-seq data is consistent with premature termination as we observe a proportional decrease in RNA-seq coverage after the proximal PAS in the slow mutant. Surprisingly, 75 genes in the slow mutant have their ratio at least twice greater than the WT ratio (FDR < 0.05; Log2 FC > 1), indicating that distal PAS is privileged for those 75 genes in the slow mutant, but will not be further investigated in this work.

Since it appears that proximal PAS are more used than distal ones in the slow mutant genome-wide, we next asked if it was also the case for the non-coding RNA upstream of *tgp1* (*nc-tgp1*). By focusing on the *nc-tgp1* locus, we first confirmed the presence of the previously described PAS1 and PAS2 as well as a PAS1 "bis", very close to the PAS1 but still twice less used than the PAS1 (**Figure 8B**). Then after combining the RNA-seq data, we found that the PAS1 is preferentially chosen in the slow mutants because the reads within the segment between PAS1 bis and PAS2 are relatively twice less abundant than the segment 1 (from TSS to PAS1) in the slow mutants comparatively to the WT.

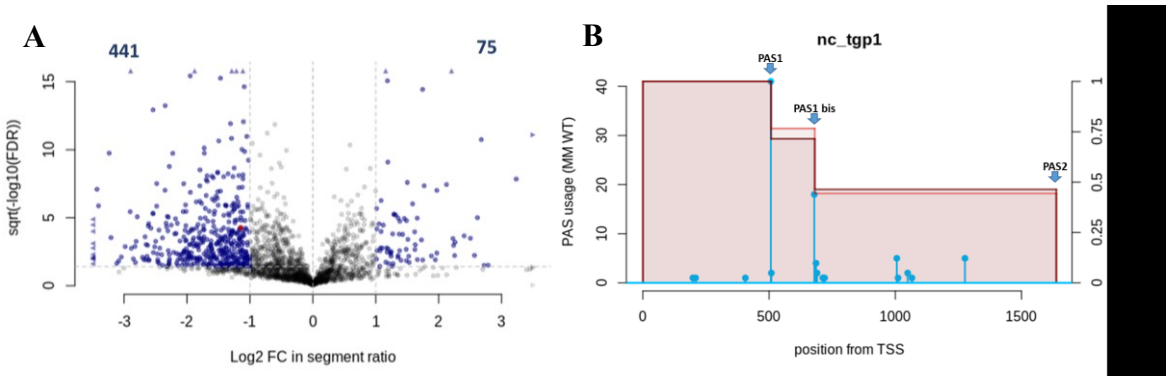

Figure 8. Proximal cleavage sites are preferentially used in the Rpb1 slow mutant.
(**A**) Volcano plot showing differentially PAS usage between the WT and the two biological replicates slow mutants. The blue dots represent genes whose APA is significantly affected (FDR < 0.05) by a slow transcription elongation rate either favoring the proximal PAS (Log2 FC < -1) or distal PAS (Log2 FC > 1). The segment ratio is made from RNA-seq reads mapping at a first segment from the TSS to the first PAS and a second segment from the first PAS to the last one. The ratios are then compared between the WT and the two biological replicates of the slow mutant to differentially analyze proximal or distal PAS usage. (**B**) Graphical representation of merged data between RNA-seq and published 3'Ends of polyA+ RNA sequencing at *nc-tgp1* locus. The vertical blue lines represent the frequency of PAS usage related to the left y-axis. The different PAS are annotated with blue arrows along *nc-tgp1* gene x-axis. The two horizontal red lines represent the RNA-seq reads from the two biological replicates slow mutants. Three segments are calculated, the first one from the TSS to the PAS1, a second one from PAS1 to PAS1 bis and a third one from PAS1 bis to PAS2. All three segments are calculated relatively to the first segment and then differentially analyzed between the WT and slow mutants.

2. Slowdown of transcription elongation rate up-regulates *tgp1* by down-regulating an upstream ncRNA

Genome-wide analyses have revealed that a slow transcription elongation rate gives rise to different up and down-regulated genes relatively to a WT strain, as well as a tendency to process transcription termination at a more proximal polyadenylation signal. In fact, it appears that *tgp1* is significantly affected in both of those analyses in the slow mutants. Indeed, on one hand, it is the most significant up-regulated gene, and on the other hand, alternative polyadenylation seems to occur more often at the proximal PAS (PAS1).

In order to visualize the output of the differential gene expression analysis, a screenshot of the read coverage at the genomic region of *tgp1* was taken to focus on the overexpression of *tgp1* in the slow mutants (**Figure 9A**, red), which actually overshadows completely the read coverage of the WT when both profiles are stacked. Astonishingly, it seems to be the contrary at *nc-tgp1* locus where the read coverage of the WT (**Figure 9A**, blue) is superior compare to the slow mutants.

This observation has been confirmed by reverse transcription followed by polymerase chain reaction (RT-qPCR) using 5 PCR targets in *nc-tgp1* and 3 PCR targets in *tgp1* ORF. There is a 6-fold overexpression of *tgp1* (amplicons 6 to 8) and underexpression of *nc-tgp1* (amplicons 1 to 5) in the slow mutant relative to the WT (**Figure 9B**). From this, one must take into account the overexpression of *tgp1* previously computed through the differential gene expression analysis (**Figure 7A**), and the down-regulation of the non-coding RNA *nc-tgp1* included in the enriched category of "nc-RNA levels" from the list of genes down-regulated (**Figure 7C**).

Since it is known that a deletion of *nc-tgp1* de-represses *tgp1*, we can infer that overexpression of *tgp1* seen in the slow mutant is due to the underexpression of *nc-tgp1* (Ard *et al*., 2014). Then, this underexpression of *nc-tgp1* could be a consequence of the greater use of the PAS1 in the slow mutant, previously computed (**Figure 8B**), although this still needs to be proven from a molecular point of view.

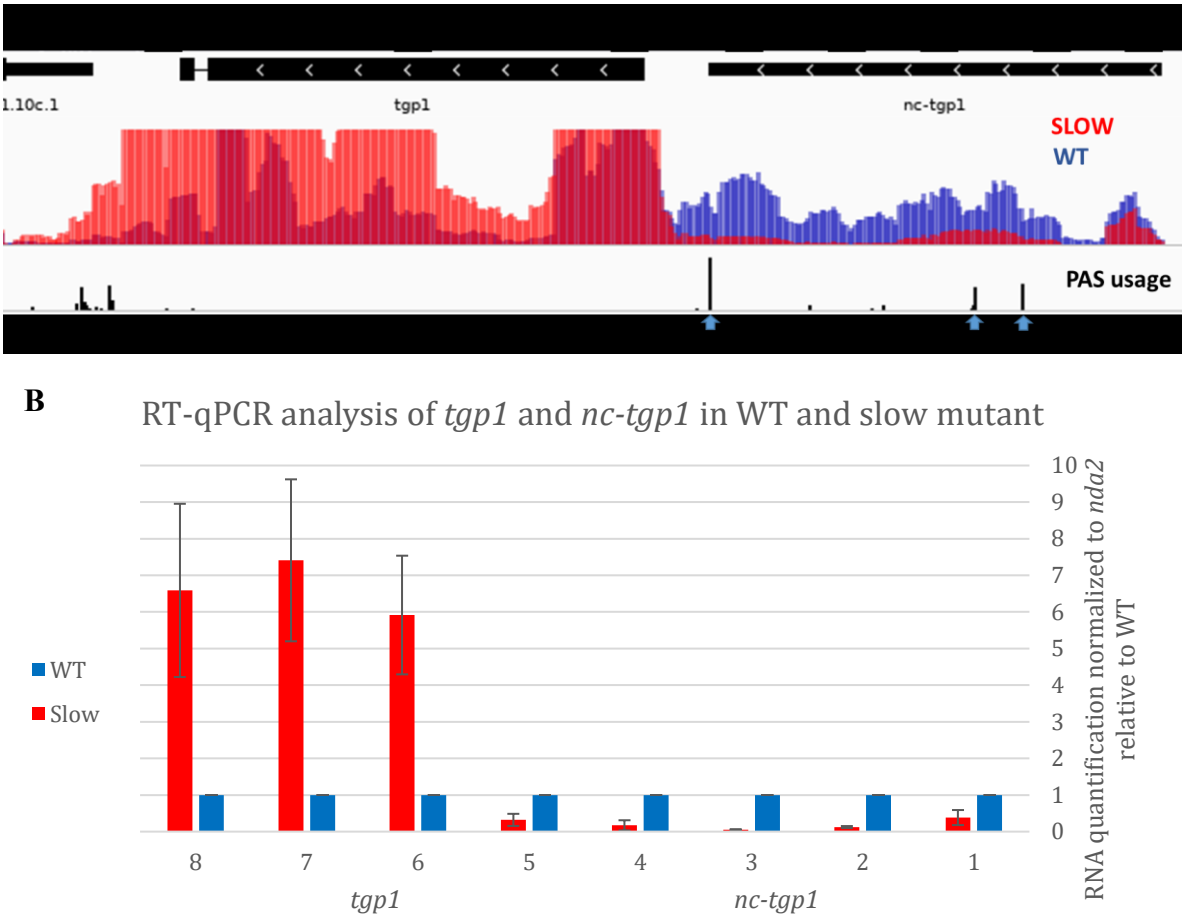

Figure 9. Imbalance of expression at *nc-tgp1* and *tgp1* loci between the WT and the slow mutants.

(**A**) Screenshot of RNA-seq read coverage from IGV browser at *nc-tgp1* and *tgp1* loci with PAS usage from 3'Ends of polyA+ RNA sequencing published data. Black oriented rectangles represent the different annotated ORFs. The mapped reads are represented either in blue for the WT or red for the two biological replicates slow mutants. The PAS usage is represented by black vertical lines and are annotated by blue arrows for *nc-tgp1* locus. (**B**) RT-qPCR analysis of *tgp1* and *nc-tgp1* expression in the slow mutant relative to the WT after normalization to *nda2* (tubulin alpha 1). Error bars represent standard error for 3 independent experiments.

3. The proximal PAS of *nc-tgp1* is preferentially used in the slow mutant

In order to gather mechanistic evidence that a slow transcription elongation rate favors early termination in the *nc-tgp1* locus, different ChIP assays have been carried out using 8 PCR targets at *nc-tgp1* and *tgp1* loci (**Figure 10A**).

First, we looked at how RNAPII density is allocated at those genes with the hypothesis that if there is early termination of transcription, then we would see a quicker decrease of RNAPII density in the 3'end of *nc-tgp1* in the slow mutant.

In the WT strain, maximum RNAPII is reached around PAS1 and then decreases to the basal level for transcription of *tgp1* (**Figure 10B**, black bars). Interestingly, the slow mutant follows the same pattern with an augmentation around PAS1 but 3 times lower than the WT. In addition, RNAPII density in the slow mutant is 3 times higher in *tgp1* ORF (**Figure 10C**), which correlates with its previously validated overexpression (**Figure 9**).These results show that, on one hand, RNAPII density decreases faster in the slow mutant compare to the WT when approaching PAS1, and on the other hand, RNAPII density increases in the slow mutant compared to the WT when *tgp1* is transcribed.

According to what is known about *tgp1* regulation, if transcription termination occurs more frequently at PAS1, then there would be less transcription interference around the *tgp1* promoter. In that case, it could lead to more binding ability for the transcription factor Pho7. Indeed, as expected, after purifying Pho7-TAP and amplifying the regions around *tgp1* promoter, a significant 3-fold enrichment (p-value < 0.01) was observed in the slow mutant compare to the WT at the genomic region where Pho7 is known to bind (**Figure 10D**), with similar expression of tagged protein (**Figure 10E**).

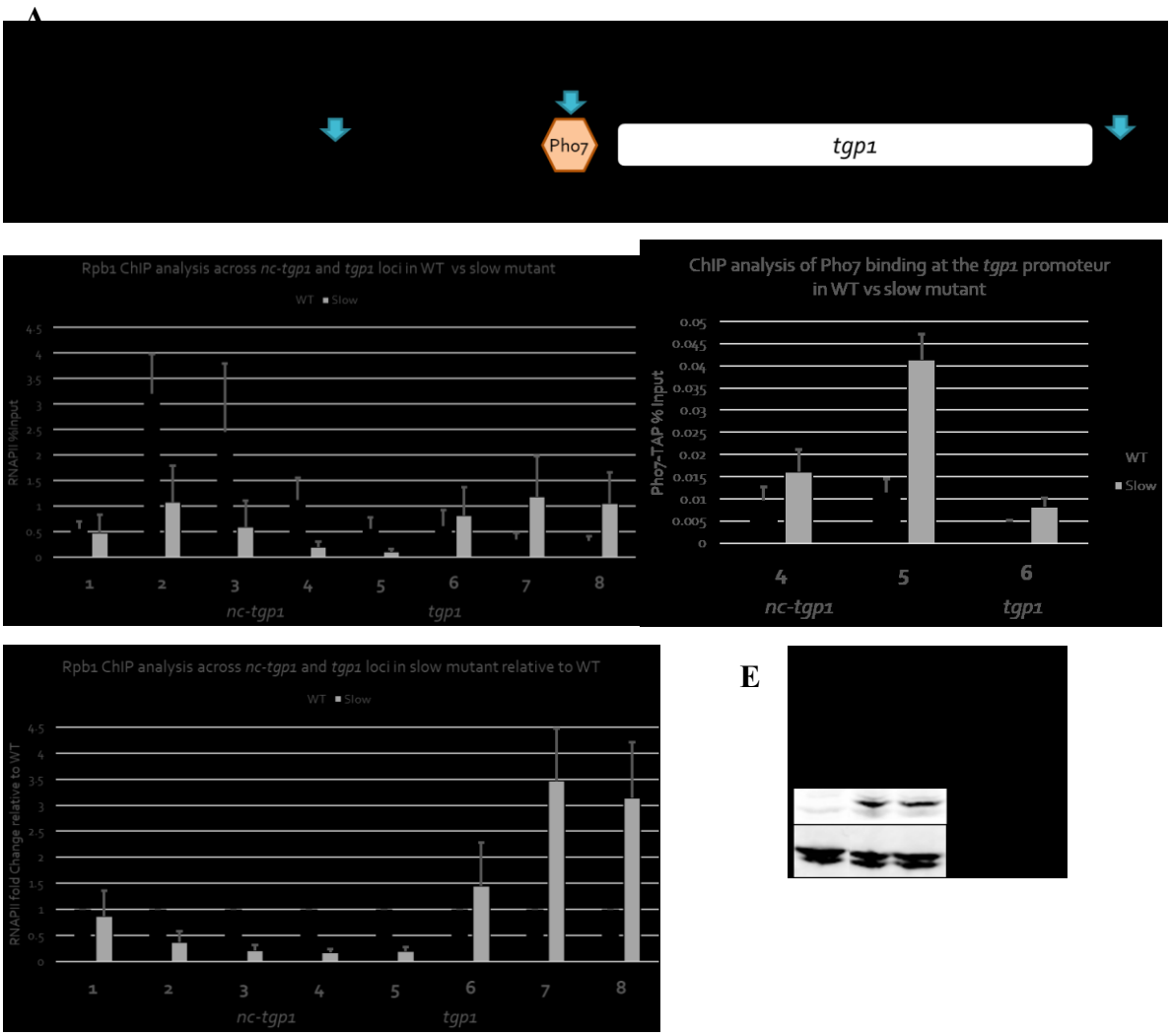

Figure 10. *rpb1* slow allele shows altered RNAP2 density at the tgp1 locus that allow increase Pho7 recruitment.

(**A**) The tandem *nc-tgp1-tgp1* locus is shown with transcription start sites indicated by black arrows indicating the direction of transcription and the *tgp1* ORF represented by a white rectangle. The different PAS are depicted by blue vertical arrows. The Pho7 binding site in the *tgp1* promoter is highlighted by an orange hexagon. The eight PCR amplicons are represented by black horizonal segments numbered from 1 to 8. (**B**)-(**C**) Rpb1 ChIP analysis across *nc-tgp1* and *tgp1* loci in WT (black) vs slow mutant (grey), error bars represent standard error for 10 independent experiments. (**D**) ChIP analysis of Pho7 binding at the *tgp1* promoter in WT (black) vs slow mutant (grey), error bars represent standard error for 3 independent experiments. Student's t-test *p-value < 0.01. (**E**) Western blot analysis of chromosomally-tagged Pho7-TAP in WT and slow mutant expressing cells. A WT no tagged Pho7 was used as a negative control. Tubulin was used as a loading control.

3.1. Altered distribution of transcription termination factors between proximal and distal PAS of nc-tgp1 in *rpb1* slow mutant

Genome-wide analyses have shown global recruitment of mRNA 3′ end processing factors at the end of ncRNA genes (Larochelle *et al*., 2018). Considering the assumption that PAS1 of *nc-tgp1* is preferentially used in the context of a slow transcription elongation rate raised the question as to what the enrichment of those transcription termination factors at the PAS1 in the slow mutant would be compared to the WT. To verify this, we used ChIP-qPCR to examine the binding profile of proteins with conserved roles in mRNA 3′end processing and transcription termination. This analysis included two independent components of the cleavage and polyadenylation factor I (CFI) complex, namely Rna14 and Pcf11, as well as Seb1 because this protein was shown to be important for 3′ end processing of both mRNAs and ncRNAs (Lemay *et al*., 2016).

Consistent with roles in 3′ end processing at mRNA and ncRNA genes, Rna14, Pcf11 and Seb1 all showed strong binding at the PAS1 and PAS2 (**Supplemental Figure 3 and 4**). Since those factors are recruited by RNAPII CTD, it is necessary to normalize their respective profile by RNAPII density. Interestingly, when ChIP assays profiles from independent biological replicates were analyzed in the slow mutant relative to the WT, a noticeable decrease of the density of those factors was discovered near the PAS2 (**Figure 11B**, **11C**, **11D**, PCR target number 6). In contrast, an important increase of the density of those factors was present around the PAS1 (**Figure 11B**, **11C**, **11D**, PCR targets number 1, 2 and 3), even though the Pcf11 binding profile showed the least drastic reallocation between PAS2 and PAS1 (**Figure 11C**). Finally, the levels of Rna14-TAP, Pcf11-TAP and Seb1-HTP, expressed from their respective promoter were similar between the WT and the slow mutant (**Figure 11E**), suggesting that the results observed do not come from an overexpression of tagged proteins.

Based on these results, we conclude that there is an enrichment of transcription termination factors at PAS1 in the slow mutant relative to the WT. But more importantly,

due to the decrease of the density of those factors at PAS2, it suggests a redistribution of those factors from PAS2 toward PAS1 when a slowdown of transcription elongation occurs.

Figure 11. Altered distribution of Rna14, Pcf11 and Seb1 at *nc-tgp1* locus in slow *rbp1* allele.

(**A**) The tandem *nc-tgp1-tgp1* locus is shown with transcription start sites indicated by black arrows indicating the direction of transcription and the *tgp1* ORF represented by a white rectangle. The different PAS are depicted by blue vertical arrows. The eight PCR amplicons are represented by black horizonal segments numbered from 1 to 8. (**B-C**) Average density of respectively Rna14 or Pcf11 normalized to RNAPII using a TAP-tagged version of those factors at *nc-tgp1* and *tgp1* loci in slow mutant relative to a WT strain. (**D**) Same as B and C but using an HTP-tagged version of Seb1. Error bars represent standard error for 3 independent experiments. Non-normalized profiles are available in **Supplemental figure 3** and **Supplemental figure 4.** (**E**) Western blot analyses of chromosomally-tagged Rna14-TAP, Pcf11-TAP and Seb1-HTP in WT and slow mutant expressing cells. WT no tagged Rna14, Pcf11 and Seb1 were used as negative controls. Tubulin was used as loading controls.

3.2. Altered distribution of Ser2 CTD phosphorylation between proximal and distal PAS of nc-tgp1 in *rpb1* slow mutant

Several studies have examined the interplay between the status of CTD phosphorylation and 3′ end processing/transcription termination (Buratowski, 2009; Heidemann *et al*., 2013; Larochelle *et al*., 2018; Lunde *et al*., 2010; Wittmann *et al*., 2017). Since a correlation has been made between genome-wide ChIP-seq profiles of transcription termination factors and Ser2, we were wondering if this residue was also following the same redistribution pattern as observed previously for Rna14, Pcf11 and Seb1 (3.1).

Averaging ChIP assays signal across *nc-tgp1* and *tgp1* loci revealed a Ser2-P pattern similar to the ones for 3'end processing factors (**Supplemental Figure 5B**), as well as after normalizing to RNAPII density because this phosphorylation occurs directly on the C-terminal domain of RNAPII Rpb1 subunit (**Supplemental Figure 5C**). Interestingly, when ChIP assay profiles from independent biological replicates were analyzed in the slow mutant relative to the WT, a noticeable decrease of Ser2-P signal was present near the PAS2 (**Figure 12B**, PCR target number 6). In contrast, an important increase of Ser2-P signal was found around the PAS1 (**Figure 12B**, PCR targets number 1-3). Surprisingly though, similar levels of Ser2-P were assessed by western-blot between a WT strain and a slow mutant (**Figure 12C**), suggesting that it is a local redistribution of Ser2-P from distal to proximal PAS instead of a global increase of Ser2-P in the slow mutant.

Altogether, these results show that there is a relative increased amount of CTD phosphorylated serine2 around the PAS1 of *nc-tgp1* in the slow mutant. In fact, it correlates very well with the relative increased abundancy of 3'end processing factors who would be be most likely to be recruited due to the augmentation of this CTD modification.

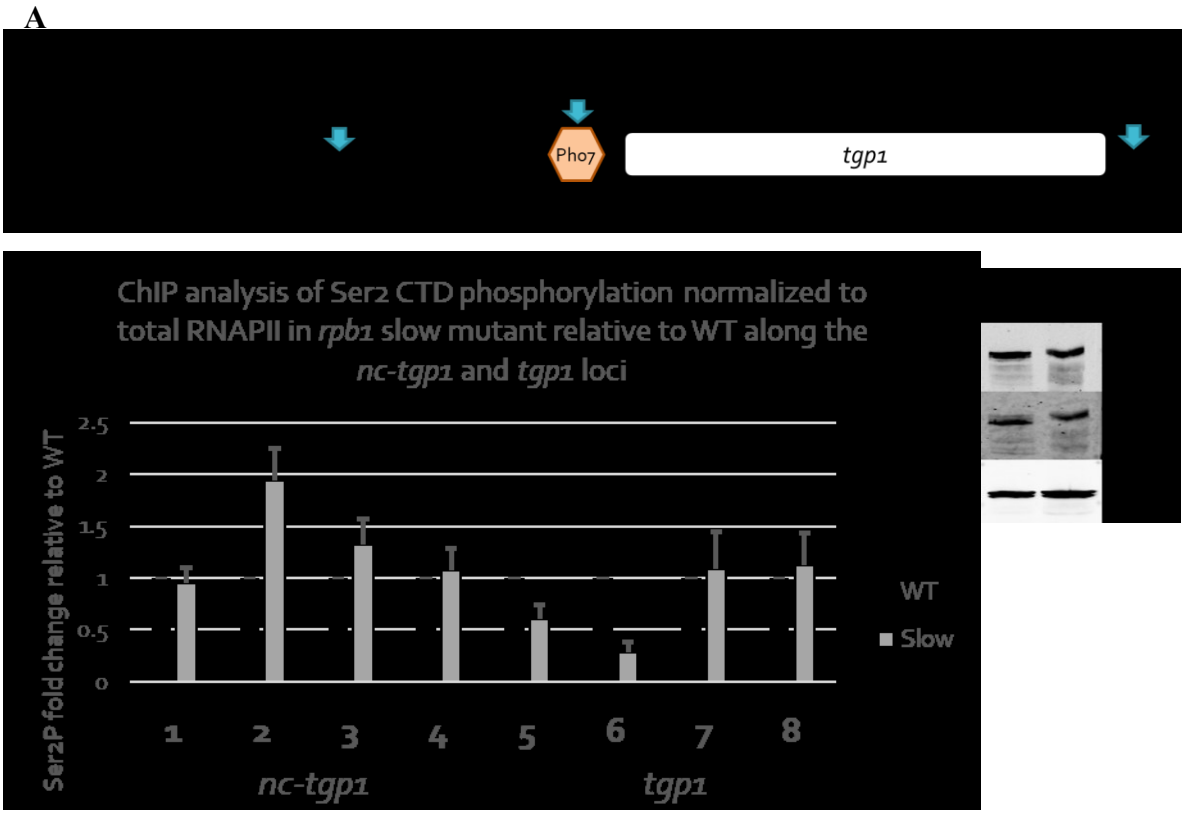

Figure 12. Increased levels of Ser2 CTD phosphorylation at the proximal *nc-tgp1* PAS and concomitant decrease at the distal *nc-tgp1* PAS in the *rpb1* slow mutant.
(**A**) The tandem *nc-tgp1-tgp1* locus is shown with transcription start sites indicated by black arrows indicating the direction of transcription and the *tgp1* ORF represented by a white rectangle. The different PAS are depicted by blue vertical arrows. The eight PCR amplicons are represented by black horizonal segments numbered from 1 to 8. (**B**) Average ChIP assays signal of Ser2 CTD phosphorylation at *nc-tgp1* and *tgp1* loci in slow mutant relative to a WT strain. (**C**) Western blot analysis of total Ser2 CTD phosphorylation in a WT strain and slow mutant.

Discussion

The goal of this study was to investigate the consequences of transcription elongation rate on gene expression in the fission yeast. So far, studies in mammalian cells or in the budding yeast have focused on the impact of transcription elongation rate on splicing or transcription termination and the role of transcription factors on those steps, but it is still unknown how transcription elongation rate mechanistically influences gene expression, and even less in the fission yeast.

We used a direct approach to modify the transcription elongation rate. Thanks to Dr. Julien Berro's team (Yale University), the genome editing CRISPR/Cas9 system in *S. pombe* has been used to generate a Rpb1 mutant strain with a specific and largely studied mutation in the trigger loop (**Figure 1**, N494D) resulting in a RNAPII complex ongoing a slow transcription elongation rate *in vitro* (Kaplan *et al*., 2012 ; Hazelbaker *et al*., 2013 ; Aslanzadeh *et al*., 2018). Using this model, genome-wide gene expression was carried out on the slow mutant by ribo-depleted bulk RNA-seq and differentially compared to a WT strain.

Since transcription is a major step in gene expression, we were not surprised to obtain hundreds of genes significantly differentially expressed between the WT and the Rpb1 slow mutant (**Figure 7A**). In addition, after performing gene set enrichment analysis, the up-regulated genes showed stress response enriched categories (**Figure 7B**), which can explain the slow growth phenotype (**Supplemental Figure 1**) and the increased sensitivity to DNA damage and osmotic stress (**Supplemental Figure 2**).

The most significant up-regulated gene in the slow mutant was *tgp1,* whose product is a transmembrane glycerophosphate transporter. It is activated in response to phosphate starvation with *pho1* and *pho84*. Surprisingly, *pho84* showed similar expression levels between the WT and the slow mutant but more importantly, all the strains have been grown in the same conditions, excluding a phosphate starvation response towards a molecular event related to a slow transcription elongation rate. In fact, *tgp1* is only 6-fold more expressed in the slow mutant compare to the WT (**Supplementary Table 2**), whereas it is overexpressed 30 times more in phosphate lacking media (Ard *et al*., 2014). This 6-fold change has been

confirmed by RT-qPCR where we also discovered an under expression of the upstream long non coding RNA named *nc-tgp1* (**Figure 7B**). This correlates with the non-coding RNAs enriched categories for the down-regulated gene list (**Figure 7C**). This observation validated the hypothesis that *tgp1* is not up-regulated by the lack of phosphate in the media but actually from the down regulation of its cis regulatory lncRNA *nc-tgp1* because it has been demonstrated that deletion of *nc-tgp1* derepresses *tgp1* (Ard *et al*., 2014).

Due to the recent discovery of a proximal polyadenylation signal (PAS) at the *nc-tgp1* locus (Sanchez *et al*., 2018), we next asked if an early alternative polyadenylation event of *nc-tgp1* could be a consequence of a slow transcription elongation rate. Indeed, when combining our RNA-seq data with published 3'READS data (Liu *et al*., 2017), the proximal PAS appeared to be preferentially used genome-wide (**Figure 8A**) as well as at the *nc-tgp1* locus (**Figure 8B,** PAS1).

In order to gather more evidence that the PAS1 (proximal) of *nc-tgp1* is favored over the PAS2 (distal), different ChIP assays were carried out in the slow mutant and the WT. Here we compare the abundance of different targets between the slow mutant and the WT, it is important to normalize the data relative to the WT to really appreciate the differences. First, RNAPII density showed a faster decrease in the slow mutant when approaching the PAS1 (**Figure 10C**). Second, Pho7 binding is 3-fold greater in the slow mutant around *tgp1* promoter (**Figure 10D**). Together, these results confirm the transcriptional interference from the overlap between *nc-tgp1* template and *tgp1* promoter. In other words, a slow transcription elongation rate could favor transcription termination at PAS1 making room for Pho7 to bind at *tgp1* promoter.

In addition, a pattern of redistributed transcription termination factors from PAS2 to PAS1 was observed (**Figure 11**). Since those proteins are indirectly recruited by the RNAPII, it was important to normalize the abundancy of those factors by the density of RNAPII. Furthermore, this result has been correlated with the similar redistribution of CTD phosphorylated serine 2 (**Figure 12**) known to be enriched when the RNA polymerase II is approaching a transcription termination site (Larochelle *et al*., 2018) and acting in the recruitment of 3'end processing factors (Lunde *et al*., 2010; Wittmann *et al*., 2017).

Altogether those results give rise to the following model (**Figure 13**). Based on the study of Dr Ryan Ard (Ard et al., 2014), in phosphate-replete condition transcription of *tgp1* is not desired, so the upstream transcription of *nc-tgp1* continues within *tgp1* gene downstream resulting in transcription interference of *tgp1* in *cis* (**Figure 13A**). In that way, *nc-tgp1* transcription termination either occurs at PAS2 or PAS3 (**Supplementary Figure 4, 5 and Figure 13A)**, both cases leading to the repression of *tgp1*. On one hand, if *nc-tgp1* transcription terminates at PAS2, the transcription termination machinery for *nc-tgp1* would compete with the transcription initiation machinery for *tgp1* by steric hindrance. On the other hand, if *nc-tgp1* transcription readthrough terminates at PAS3 it results in an unstable transcript fusion of *nc-tgp1* and *tgp1* (Sanchez et al., 2018). However, the mechanism of decision making between PAS2 and PAS3 remains unknown.

More recently, the study of Dr Ana Sanchez allowed the discovery of a short form of *nc-tgp1* (Sanchez et al., 2018) related to an APA site upstream of the well-known PAS2 (**Figure 13B**, PAS1). Even though the *cis* and *trans* factors that control *nc-tgp1* transcription are presently unknown, the usage of the N494D slow mutant in my work brought new insights of *tgp1* regulation. The correlation of the relative increased abundancy of Ser2-P with transcription termination factors at PAS1 (**Figure 11 and 12**) as well as the relative decreased density of RNAPII when approaching PAS1 (**Figure 10C**) and the increased binding of Pho7 around *tgp1* promoter (**Figure 10D**) bring the conclusion that a slow transcription elongation rate favors transcription termination at the proximal PAS1. Consequently, this discovery explains why, both RNAPII density at *tgp1* locus (**Figure 10**) and mRNA level are increased for *tgp1* in the slow mutant (**Figure 9**). In other words, the usage of the slow mutant in this study potentially mimic the consequences of phosphate starvation in a WT strain by terminating earlier *nc-tgp1* at PAS1 and allowing the activation of *tgp1* downstream.

Although the function of most lncRNAs is unknown, the number of characterized lncRNAs is growing and many publications suggest that they are important for regulating negatively or positively gene expression in *cis* or in *trans* involved in development, differentiation and human disease (Taft et al., 2010; Wilusz et al., 2009). One of the modes of *cis* regulation by lncRNAs refers to transcription-mediated silencing or transcriptional

interference. It involves the process of transcription itself when the transcription of one gene can repress in *cis* the functional transcription of another gene by influencing enhancer or promoter activity or by blocking RNAPII elongation, splicing or polyadenylation (Palmer et al., 2011; Shearwin et al., 2005). The most common reports of transcriptional interference concern an overlapped promoter, just like our case of *nc-tgp1* and *tgp1*, but studies have focused the molecular mechanisms underlying interference on the promoter state of the gene downstream. They demonstrated the consequences of transcriptional interference from upstream lncRNAs on promoter nucleosome repositioning (Martens et al., 2004) and promoter histone modifications (Houseley et al., 2008; van Werven et al., 2012) from the point of view of RNAPII acting as a carrier of chromatin modifying enzymes. However, based on my findings, I bring a new mechanism of gene regulation through transcription interference involving a slow transcription elongation rate favorizing a proximal transcription termination site on the gene model *tgp1*.

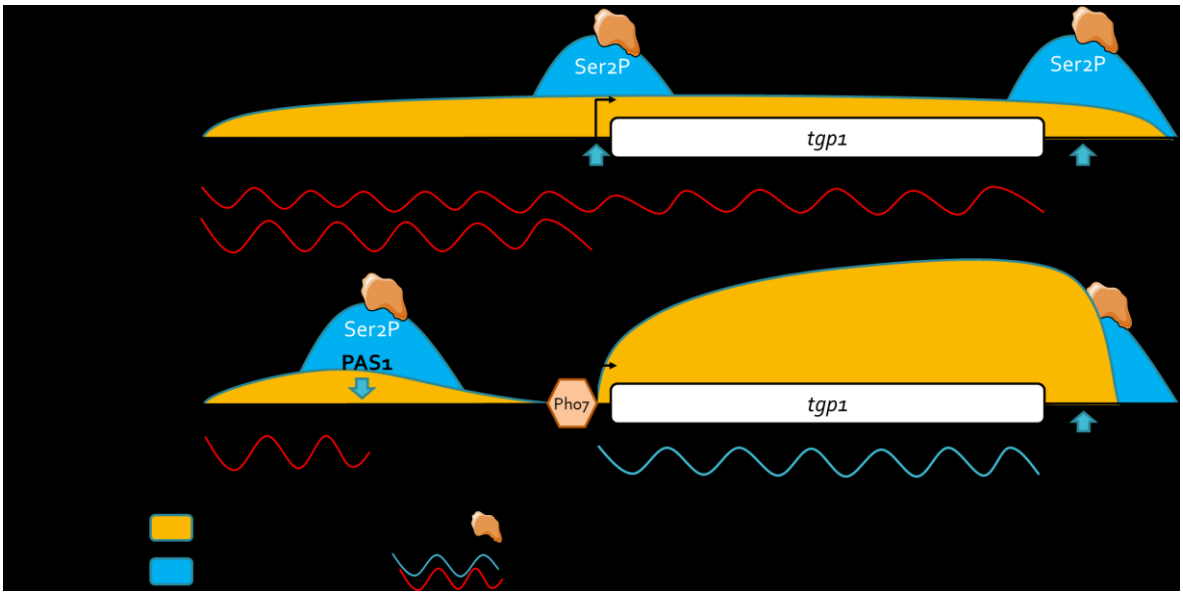

Figure 13. Model of *tgp1* regulation by Rpb1 N494D slow mutant through *nc-tgp1* transcription in phosphate-replete growth.
(**A**) In a WT strain, transcription begins at *nc-tgp1* promoter and either terminates at PAS2 or PAS3 for the readthrough. (**B**) In a slow mutant, transcription begins at *nc-tgp1* promoter and terminates at the APA site PAS1 allowing Pho7 to bind to *tgp1* promoter and induces its transcription.
The transcription by RNAPII is represented in orange. The transcription termination events are represented by the correlation of Ser2-P abundancy in blue with the recruitment of transcription termination factors. The different forms of *nc-tgp1* RNA (Sanchez et al., 2018) are represented in red and *tgp1* RNA in blue.

Conclusion and perspectives

Transcription is a key process for gene expression. By slowing down the transcription elongation rate we significantly changed the gene expression profile of 876 genes in the fission yeast. Then, downstream analyses oriented the study to focus on the *tgp1* gene, coding for a transmembrane glycerophosphate transporter, which was the most significant up-regulated gene in the slow mutant. By combining studies from the literature and ChIP assays we demonstrated that the long non-coding RNA *nc-tgp1*, known to represses *tgp1* in *cis* through transcription interference, is actually being terminated prematurely using the proximal polyadenylation signal (PAS). This early termination event leads to the opportunity of the transcription factor Pho7 to directly bind the chromatin at *tgp1* promoter. Consequently, *tgp1* is over expressed when the amount of phosphate is actually the same between the slow mutant and the WT. In summary, the use of a slow *rpb1* allele in this study allowed the discovery of a new regulatory mechanism for *tgp1* and illustrates the molecular events at this locus in the context of phosphate starvation.

However, some questions remain unanswered. In particular, if *nc-tgp1* is being terminated prematurely in the slow mutant, we would expect an enrichment of this short form of non-coding RNA. We would like to investigate the short form of *nc-tgp1* but studying ncRNAs in yeast is problematic. In yeast, the majority of these ncRNAs, called cryptic unstable transcripts (CUTs) due to their unstable nature, are retained in the nucleus and degraded by the exosome, a major 3′ to 5′ RNA degradation machinery that plays a key role in RNA metabolism, RNA processing and RNA surveillance, and is essential for the viability of eukaryotic cells (Wyers et al., 2005). One of the exosome subunits is Rrp6, which is exclusively associated with the nuclear form of the exosome and is required for the rapid nuclear degradation of CUTs. However, it has been shown that CUTs were stabilized by the deletion of *rrp6* (Wyers *et al*., 2005 ; Davis, Ares, 2006). Furthermore, the nuclear exosome is also involved in the degradation of a group of meiotic mRNAs during vegetative growth. The targeting of these mRNAs to the nuclear exosome requires the RNA-binding protein Mmi1, which recognizes a specific sequence motif (determinant of selective removal or DSR-sequence) on meiotic mRNAs and therefore will indirectly recruit the exosome. In fact,

nc-tgp1 displays a DSR motif within its own locus and becomes detectable in *rrp6*Δ or *mmi1*Δ cells (Sanchez *et al*., 2018).

Moreover, the proximal polyadenylation signal of *nc-tgp1* has been described as a "weak" site due to variation in the consensus sequence (Sanchez *et al*., 2018). Thus, it would be interesting to insert by CRISPR a "strong" polyadenylation signal instead of the weak one in order to potentially rescue the overexpression of *tgp1* observed in the slow mutant.

Finally, some mutations in the trigger loop of Rpb1 have been characterized to accelerate the transcription elongation rate (**Figure 1B**, Kaplan *et al*., 2012). Therefore, if a slow transcription elongation rate shows an overexpression of *tgp1* by favoring the use of the proximal PAS, the experiment described here could be repeated using a fast transcription elongation mutant. Indeed, in phosphate starvation, when the proximal PAS would be preferentially used to express *tgp1*, we could imagine the distal PAS being favored in the fast mutant compare to the WT. Or on the contrary, in phosphate repleted media, a reduction of the use of the proximal PAS in the fast mutant compare to the WT.

Overall, this study only begins to further our understanding of how transcription elongation rate influences gene expression. It is a crucial step in gene expression of every organism and the discoveries related to the consequences on gene expression will be of great value to the scientific community.

List of references

Adelman, K., Lis, J.T., 2012. Promoter-proximal pausing of RNA polymerase II: emerging roles in metazoans. Nat. Rev. Genet. 13, 720–731. https://doi.org/10.1038/nrg3293

Alexander, R.D., Innocente, S.A., Barrass, J.D., Beggs, J.D., 2010. Splicing-Dependent RNA Polymerase Pausing in Yeast. Mol. Cell 40, 582–593. https://doi.org/10.1016/j.molcel.2010.11.005

Allison, L.A., Moyle, M., Shales, M., James Ingles, C., 1985. Extensive homology among the largest subunits of eukaryotic and prokaryotic RNA polymerases. Cell 42, 599–610. https://doi.org/10.1016/0092-8674(85)90117-5

Anders, S., Huber, W., 2010. Differential expression analysis for sequence count data. Genome Biol. 11, R106. https://doi.org/10.1186/gb-2010-11-10-r106

Anders, S., Pyl, P.T., Huber, W., 2015. HTSeq—a Python framework to work with high-throughput sequencing data. Bioinformatics 31, 166–169. https://doi.org/10.1093/bioinformatics/btu638

Aravind, L., Watanabe, H., Lipman, D.J., Koonin, E.V., 2000. Lineage-specific loss and divergence of functionally linked genes in eukaryotes. Proc. Natl. Acad. Sci. U. S. A. 97, 11319–11324. https://doi.org/10.1073/pnas.200346997

Ard, R., Tong, P., Allshire, R.C., 2014. Long non-coding RNA-mediated transcriptional interference of a permease gene confers drug tolerance in fission yeast. Nat. Commun. 5, 5576. https://doi.org/10.1038/ncomms6576

Aslanzadeh, V., Huang, Y., Sanguinetti, G., Beggs, J.D., 2018. Transcription rate strongly affects splicing fidelity and cotranscriptionality in budding yeast. Genome Res. 28, 203–213. https://doi.org/10.1101/gr.225615.117

Azuma, Y., Yamagishi, M., Ueshima, R., Ishihama, A., 1991. Cloning and sequence determination of the *Schizosaccharomyces pombe rpb1* gene encoding the largest subunit of RNA polymerase II. Nucleic Acids Res. 19, 461–468. https://doi.org/10.1093/nar/19.3.461

Baejen, C., Andreani, J., Torkler, P., Battaglia, S., Schwalb, B., Lidschreiber, M., Maier, K.C., Boltendahl, A., Rus, P., Esslinger, S., Söding, J., Cramer, P., 2017. Genome-wide Analysis of RNA Polymerase II Termination at Protein-Coding Genes. Mol. Cell 66, 38-49.e6. https://doi.org/10.1016/j.molcel.2017.02.009

Bähler, J., Wu, J.-Q., Longtine, M.S., Shah, N.G., Iii, A.M., Steever, A.B., Wach, A., Philippsen, P., Pringle, J.R., 1998. Heterologous modules for efficient and versatile PCR-based gene targeting in *Schizosaccharomyces pombe*. Yeast 14, 943–951. https://doi.org/10.1002/(SICI)1097-0061(199807)14:10<943::AID-YEA292>3.0.CO;2-Y

Barabino, S.M.L., Keller, W., 1999. Last but Not Least: Regulated Poly(A) Tail Formation. Cell 99, 9–11. https://doi.org/10.1016/S0092-8674(00)80057-4

Bitton, D.A., Schubert, F., Dey, S., Okoniewski, M., Smith, G.C., Khadayate, S., Pancaldi, V., Wood, V., Bähler, J., 2015. AnGeLi: A Tool for the Analysis of Gene Lists from Fission Yeast. Front. Genet. 6. https://doi.org/10.3389/fgene.2015.00330

Blackwood, E.M., Kadonaga, J.T., 1998. Going the Distance: A Current View of Enhancer Action. Science 281, 60–63. https://doi.org/10.1126/science.281.5373.60

Bolger, A.M., Lohse, M., Usadel, B., 2014. Trimmomatic: a flexible trimmer for Illumina sequence data. Bioinformatics 30, 2114–2120. https://doi.org/10.1093/bioinformatics/btu170

Bortz, P.D.S., Wamhoff, B.R., 2011. Chromatin Immunoprecipitation (ChIP): Revisiting the Efficacy of Sample Preparation, Sonication, Quantification of Sheared DNA, and Analysis via PCR. PLOS ONE 6, e26015. https://doi.org/10.1371/journal.pone.0026015

Buratowski, S., 2009. Progression through the RNA Polymerase II CTD Cycle. Mol. Cell 36, 541–546. https://doi.org/10.1016/j.molcel.2009.10.019

Buratowski, S., 2003. The CTD code. Nat. Struct. Mol. Biol. 10, 679–680. https://doi.org/10.1038/nsb0903-679

Carey, M.F., Peterson, C.L., Smale, S.T., 2009. Chromatin Immunoprecipitation (ChIP). Cold Spring Harb. Protoc. 2009, pdb.prot5279. https://doi.org/10.1101/pdb.prot5279

Carter-O'Connell, I., Peel, M.T., Wykoff, D.D., O'Shea, E.K., 2012. Genome-Wide Characterization of the Phosphate Starvation Response in *Schizosaccharomyces pombe*. BMC Genomics 13, 697. https://doi.org/10.1186/1471-2164-13-697

Casañal, A., Kumar, A., Hill, C.H., Easter, A.D., Emsley, P., Degliesposti, G., Gordiyenko, Y., Santhanam, B., Wolf, J., Wiederhold, K., Dornan, G.L., Skehel, M., Robinson, C.V., Passmore, L.A., 2017. Architecture of eukaryotic mRNA 3′-end processing machinery. Science 358, 1056–1059. https://doi.org/10.1126/science.aao6535

Cho, E.-J., Kobor, M.S., Kim, M., Greenblatt, J., Buratowski, S., 2001. Opposing effects of Ctk1 kinase and Fcp1 phosphatase at Ser 2 of the RNA polymerase II C-terminal domain. Genes Dev. 15, 3319–3329. https://doi.org/10.1101/gad.935901

Conesa, A., Madrigal, P., Tarazona, S., Gomez-Cabrero, D., Cervera, A., McPherson, A., Szcześniak, M.W., Gaffney, D.J., Elo, L.L., Zhang, X., Mortazavi, A., 2016. A survey of best practices for RNA-seq data analysis. Genome Biol. 17, 13. https://doi.org/10.1186/s13059-016-0881-8

Corden, J.L., Cadena, D.L., Ahearn, J.M., Dahmus, M.E., 1985. A unique structure at the carboxyl terminus of the largest subunit of eukaryotic RNA polymerase II. Proc. Natl. Acad. Sci. 82, 7934–7938. https://doi.org/10.1073/pnas.82.23.7934

Coudreuse, D., van Bakel, H., Dewez, M., Soutourina, J., Parnell, T., Vandenhaute, J., Cairns, B., Werner, M., Hermand, D., 2010. A Gene-Specific Requirement of RNA Polymerase II CTD Phosphorylation for Sexual Differentiation in *S. pombe*. Curr. Biol. 20, 1053–1064. https://doi.org/10.1016/j.cub.2010.04.054

Cramer, P., Armache, K.-J., Baumli, S., Benkert, S., Brueckner, F., Buchen, C., Damsma, G.E., Dengl, S., Geiger, S.R., Jasiak, A.J., Jawhari, A., Jennebach, S., Kamenski, T., Kettenberger, H., Kuhn, C.-D., Lehmann, E., Leike, K., Sydow, J.F., Vannini, A., 2008. Structure of Eukaryotic RNA Polymerases. Annu. Rev. Biophys. 37, 337–352. https://doi.org/10.1146/annurev.biophys.37.032807.130008

Dieci, G., Conti, A., Pagano, A., Carnevali, D., 2013. Identification of RNA polymerase III-transcribed genes in eukaryotic genomes. Biochim. Biophys. Acta BBA - Gene Regul. Mech., Transcription by Odd Pols 1829, 296–305. https://doi.org/10.1016/j.bbagrm.2012.09.010

Dieci, G., Fiorino, G., Castelnuovo, M., Teichmann, M., Pagano, A., 2007. The expanding RNA polymerase III transcriptome. Trends Genet. 23, 614–622. https://doi.org/10.1016/j.tig.2007.09.001

Dobin, A., Davis, C.A., Schlesinger, F., Drenkow, J., Zaleski, C., Jha, S., Batut, P., Chaisson, M., Gingeras, T.R., 2013. STAR: ultrafast universal RNA-seq aligner. Bioinformatics 29, 15–21. https://doi.org/10.1093/bioinformatics/bts635

Edwalds-Gilbert, G., Veraldi, K.L., Milcarek, C., 1997. Alternative poly(A) site selection in complex transcription units: means to an end? Nucleic Acids Res. 25, 2547–2561. https://doi.org/10.1093/nar/25.13.2547

Ewing, B., Hillier, L., Wendl, M.C., Green, P., 1998. Base-Calling of Automated Sequencer Traces UsingPhred. I. Accuracy Assessment. Genome Res. 8, 175–185. https://doi.org/10.1101/gr.8.3.175

Fernandez, R., Berro, J., 2016. Use of a fluoride channel as a new selection marker for fission yeast plasmids and application to fast genome editing with CRISPR/Cas9. Yeast 33, 549–557. https://doi.org/10.1002/yea.3178

Fong, N., Brannan, K., Erickson, B., Kim, H., Cortazar, M.A., Sheridan, R.M., Nguyen, T., Karp, S., Bentley, D.L., 2015. Effects of Transcription Elongation Rate and Xrn2 Exonuclease Activity on RNA Polymerase II Termination Suggest Widespread Kinetic Competition. Mol. Cell 60, 256–267. https://doi.org/10.1016/j.molcel.2015.09.026

Glover-Cutter, K., Kim, S., Espinosa, J., Bentley, D.L., 2008. RNA polymerase II pauses and associates with pre-mRNA processing factors at both ends of genes. Nat. Struct. Mol. Biol. 15, 71–78. https://doi.org/10.1038/nsmb1352

Grokhovsky, S.L., 2006. Specificity of DNA cleavage by ultrasound. Mol. Biol. 40, 276–283. https://doi.org/10.1134/S0026893306020142

Grokhovsky, S.L., Il'icheva, I.A., Nechipurenko, D.Y., Golovkin, M.V., Panchenko, L.A., Polozov, R.V., Nechipurenko, Y.D., 2011. Sequence-specific ultrasonic cleavage of DNA. Biophys. J. 100, 117–125. https://doi.org/10.1016/j.bpj.2010.10.052

Gromak, N., West, S., Proudfoot, N.J., 2006. Pause Sites Promote Transcriptional Termination of Mammalian RNA Polymerase II. Mol. Cell. Biol. 26, 3986–3996. https://doi.org/10.1128/MCB.26.10.3986-3996.2006

Grzybowska, E.A., 2012. Human intronless genes: Functional groups, associated diseases, evolution, and mRNA processing in absence of splicing. Biochem. Biophys. Res. Commun. 424, 1–6. https://doi.org/10.1016/j.bbrc.2012.06.092

Hanna-Rose, W., Hansen, U., 1996. Active repression mechanisms of eukaryotic transcription repressors. Trends Genet. 12, 229–234. https://doi.org/10.1016/0168-9525(96)10022-6

Hazelbaker, D.Z., Marquardt, S., Wlotzka, W., Buratowski, S., 2013. Kinetic Competition between RNA Polymerase II and Sen1-Dependent Transcription Termination. Mol. Cell 49, 55–66. https://doi.org/10.1016/j.molcel.2012.10.014

Heckman, D.S., Geiser, D.M., Eidell, B.R., Stauffer, R.L., Kardos, N.L., Hedges, S.B., 2001. Molecular evidence for the early colonization of land by fungi and plants. Science 293, 1129–1133. https://doi.org/10.1126/science.1061457

Heidemann, M., Hintermair, C., Voß, K., Eick, D., 2013. Dynamic phosphorylation patterns of RNA polymerase II CTD during transcription. Biochim. Biophys. Acta BBA - Gene Regul. Mech., RNA polymerase II Transcript Elongation 1829, 55–62. https://doi.org/10.1016/j.bbagrm.2012.08.013

Hoffman, C.S., Wood, V., Fantes, P.A., 2015. An Ancient Yeast for Young Geneticists: A Primer on the *Schizosaccharomyces pombe* Model System. Genetics 201, 403–423. https://doi.org/10.1534/genetics.115.181503

Houseley, J., Rubbi, L., Grunstein, M., Tollervey, D., Vogelauer, M., 2008. A ncRNA Modulates Histone Modification and mRNA Induction in the Yeast GAL Gene Cluster. Mol. Cell 32, 685–695. https://doi.org/10.1016/j.molcel.2008.09.027

Hrdlickova, R., Toloue, M., Tian, B., 2017. RNA-Seq methods for transcriptome analysis. Wiley Interdiscip. Rev. RNA 8, e1364. https://doi.org/10.1002/wrna.1364

Jonkers, I., Kwak, H., Lis, J.T., 2014. Genome-wide dynamics of Pol II elongation and its interplay with promoter proximal pausing, chromatin, and exons. eLife 3. https://doi.org/10.7554/eLife.02407

Jonkers, I., Lis, J.T., 2015. Getting up to speed with transcription elongation by RNA polymerase II. Nat. Rev. Mol. Cell Biol. 16, 167–177. https://doi.org/10.1038/nrm3953

Juven-Gershon, T., Kadonaga, J.T., 2010. Regulation of Gene Expression via the Core Promoter and the Basal Transcriptional Machinery. Dev. Biol. 339, 225–229. https://doi.org/10.1016/j.ydbio.2009.08.009

Kaplan, C.D., 2013. Basic Mechanisms of RNA Polymerase II Activity and Alteration of Gene Expression in *Saccharomyces cerevisiae*. Biochim. Biophys. Acta 1829, 39–54. https://doi.org/10.1016/j.bbagrm.2012.09.007

Kaplan, C.D., Jin, H., Zhang, I.L., Belyanin, A., 2012a. Dissection of Pol II Trigger Loop Function and Pol II Activity–Dependent Control of Start Site Selection In Vivo. PLoS Genet. 8, e1002627. https://doi.org/10.1371/journal.pgen.1002627

Kaplan, C.D., Jin, H., Zhang, I.L., Belyanin, A., 2012b. Dissection of Pol II Trigger Loop Function and Pol II Activity–Dependent Control of Start Site Selection In Vivo. PLoS Genet. 8, e1002627. https://doi.org/10.1371/journal.pgen.1002627

Kaplan, C.D., Larsson, K.-M., Kornberg, R.D., 2008. The RNA Polymerase II Trigger Loop Functions in Substrate Selection and Is Directly Targeted by α-Amanitin. Mol. Cell 30, 547–556. https://doi.org/10.1016/j.molcel.2008.04.023

Kwak, H., Lis, J.T., 2013. Control of Transcriptional Elongation. Annu. Rev. Genet. 47, 483–508. https://doi.org/10.1146/annurev-genet-110711-155440

Larochelle, M., Robert, M.-A., Hébert, J.-N., Liu, X., Matteau, D., Rodrigue, S., Tian, B., Jacques, P.-É., Bachand, F., 2018. Common mechanism of transcription termination at coding and noncoding RNA genes in fission yeast. Nat. Commun. 9, 4364. https://doi.org/10.1038/s41467-018-06546-x

Lemay, J.-F., Marguerat, S., Larochelle, M., Liu, X., Nues, R. van, Hunyadkürti, J., Hoque, M., Tian, B., Granneman, S., Bähler, J., Bachand, F., 2016. The Nrd1-like protein Seb1 coordinates cotranscriptional 3′ end processing and polyadenylation site selection. Genes Dev. 30, 1558–1572. https://doi.org/10.1101/gad.280222.116

Liu, X., Hoque, M., Larochelle, M., Lemay, J.-F., Yurko, N., Manley, J.L., Bachand, F., Tian, B., 2017. Comparative analysis of alternative polyadenylation in *S. cerevisiae* and *S. pombe*. Genome Res. 27, 1685–1695. https://doi.org/10.1101/gr.222331.117

Lopez, P.J., Séraphin, B., 1999. Genomic-scale quantitative analysis of yeast pre-mRNA splicing: Implications for splice-site recognition. RNA 5, 1135–1137.

Lu, F., Portz, B., Gilmour, D.S., 2019. The C-Terminal Domain of RNA Polymerase II Is a Multivalent Targeting Sequence that Supports Drosophila Development with Only Consensus Heptads. Mol. Cell 73, 1232-1242.e4. https://doi.org/10.1016/j.molcel.2019.01.008

Lu, L., Fan, D., Hu, C.-W., Worth, M., Ma, Z.-X., Jiang, J., 2016. Distributive O-GlcNAcylation on the Highly Repetitive C-Terminal Domain of RNA Polymerase II. Biochemistry 55, 1149–1158. https://doi.org/10.1021/acs.biochem.5b01280

Lunde, B.M., Reichow, S.L., Kim, M., Suh, H., Leeper, T.C., Yang, F., Mutschler, H., Buratowski, S., Meinhart, A., Varani, G., 2010. Cooperative interaction of transcription termination factors with the RNA polymerase II C-terminal domain. Nat. Struct. Mol. Biol. 17, 1195–1201. https://doi.org/10.1038/nsmb.1893

Malagon, F., Kireeva, M.L., Shafer, B.K., Lubkowska, L., Kashlev, M., Strathern, J.N., 2006. Mutations in the *Saccharomyces cerevisiae* RPB1 Gene Conferring Hypersensitivity to 6-Azauracil. Genetics 172, 2201–2209. https://doi.org/10.1534/genetics.105.052415

Martens, J.A., Laprade, L., Winston, F., 2004. Intergenic transcription is required to repress the *Saccharomyces cerevisiae* SER3 gene. Nature 429, 571–574. https://doi.org/10.1038/nature02538

Nonet, M., Sweetser, D., Young, R.A., 1987. Functional redundancy and structural polymorphism in the large subunit of RNA polymerase II. Cell 50, 909–915. https://doi.org/10.1016/0092-8674(87)90517-4

O'Neil, D., Glowatz, H., Schlumpberger, M., 2013. Ribosomal RNA Depletion for Efficient Use of RNA-Seq Capacity. Curr. Protoc. Mol. Biol. 103, 4.19.1-4.19.8. https://doi.org/10.1002/0471142727.mb0419s103

Orr-Weaver, T.L., Szostak, J.W., Rothstein, R.J., 1981. Yeast transformation: a model system for the study of recombination. Proc. Natl. Acad. Sci. U. S. A. 78, 6354–6358.

Palmer, A.C., Egan, J.B., Shearwin, K.E., 2011. Transcriptional interference by RNA polymerase pausing and dislodgement of transcription factors. Transcription 2, 9–14. https://doi.org/10.4161/trns.2.1.13511

Proudfoot, N.J., 2016. Transcriptional termination in mammals: Stopping the RNA polymerase II juggernaut. Science 352, aad9926. https://doi.org/10.1126/science.aad9926

Richard, P., Manley, J.L., 2009. Transcription termination by nuclear RNA polymerases. Genes Dev. 23, 1247–1269. https://doi.org/10.1101/gad.1792809

Robertson, G., Hirst, M., Bainbridge, M., Bilenky, M., Zhao, Y., Zeng, T., Euskirchen, G., Bernier, B., Varhol, R., Delaney, A., Thiessen, N., Griffith, O.L., He, A., Marra, M., Snyder, M., Jones, S., 2007. Genome-wide profiles of STAT1 DNA association using chromatin immunoprecipitation and massively parallel sequencing. Nat. Methods 4, 651–657. https://doi.org/10.1038/nmeth1068

Robinson, J.T., Thorvaldsdóttir, H., Winckler, W., Guttman, M., Lander, E.S., Getz, G., Mesirov, J.P., 2011. Integrative Genomics Viewer. Nat. Biotechnol. 29, 24–26. https://doi.org/10.1038/nbt.1754

Rosonina, E., Kaneko, S., Manley, J.L., 2006. Terminating the transcript: breaking up is hard to do. Genes Dev. 20, 1050–1056. https://doi.org/10.1101/gad.1431606

Russell, J., Zomerdijk, J.C.B.M., 2005. RNA-polymerase-I-directed rDNA transcription, life and works. Trends Biochem. Sci. 30, 87–96. https://doi.org/10.1016/j.tibs.2004.12.008

Sanchez, A.M., Shuman, S., Schwer, B., 2018. Poly(A) site choice and Pol2 CTD Serine-5 status govern lncRNA control of phosphate-responsive *tgp1* gene expression in fission yeast. RNA 24, 237–250. https://doi.org/10.1261/rna.063966.117

Schmidt, D., Wilson, M.D., Spyrou, C., Brown, G.D., Hadfield, J., Odom, D.T., 2009. ChIP-seq: Using high-throughput sequencing to discover protein–DNA interactions. Methods, Global approaches to study gene regulation 48, 240–248. https://doi.org/10.1016/j.ymeth.2009.03.001

Schröder, S., Herker, E., Itzen, F., He, D., Thomas, S., Gilchrist, D.A., Kaehlcke, K., Cho, S., Pollard, K.S., Capra, J.A., Schnölzer, M., Cole, P.A., Geyer, M., Bruneau, B.G., Adelman, K., Ott, M., 2013. Acetylation of RNA Polymerase II Regulates Growth-Factor-Induced Gene Transcription in Mammalian Cells. Mol. Cell 52, 314–324. https://doi.org/10.1016/j.molcel.2013.10.009

Schwer, B., Sanchez, A.M., Garg, A., Chatterjee, D., Shuman, S., 2017. Defining the DNA Binding Site Recognized by the Fission Yeast Zn2Cys6 Transcription Factor Pho7 and Its Role in Phosphate Homeostasis. mBio 8, e01218-17. https://doi.org/10.1128/mBio.01218-17

Shearwin, K.E., Callen, B.P., Egan, J.B., 2005. Transcriptional interference – a crash course. Trends Genet. 21, 339–345. https://doi.org/10.1016/j.tig.2005.04.009

Shi, Y., Manley, J.L., 2015. The end of the message: multiple protein–RNA interactions define the mRNA polyadenylation site. Genes Dev. 29, 889–897. https://doi.org/10.1101/gad.261974.115

Sims, R.J., Belotserkovskaya, R., Reinberg, D., 2004. Elongation by RNA polymerase II: the short and long of it. Genes Dev. 18, 2437–2468. https://doi.org/10.1101/gad.1235904

Taft, R.J., Pang, K.C., Mercer, T.R., Dinger, M., Mattick, J.S., 2010. Non-coding RNAs: regulators of disease. J. Pathol. 220, 126–139. https://doi.org/10.1002/path.2638

van Werven, F.J., Neuert, G., Hendrick, N., Lardenois, A., Buratowski, S., van Oudenaarden, A., Primig, M., Amon, A., 2012. Transcription of Two Long Noncoding RNAs Mediates Mating-Type Control of Gametogenesis in Budding Yeast. Cell 150, 1170–1181. https://doi.org/10.1016/j.cell.2012.06.049

Veloso, A., Kirkconnell, K.S., Magnuson, B., Biewen, B., Paulsen, M.T., Wilson, T.E., Ljungman, M., 2014. Rate of elongation by RNA polymerase II is associated with specific gene features and epigenetic modifications. Genome Res. 24, 896–905. https://doi.org/10.1101/gr.171405.113

Voss, K., Forné, I., Descostes, N., Hintermair, C., Schüller, R., Maqbool, M.A., Heidemann, M., Flatley, A., Imhof, A., Gut, M., Gut, I., Kremmer, E., Andrau, J.-C., Eick, D., 2015. Site-specific methylation and acetylation of lysine residues in the C-terminal domain (CTD) of RNA polymerase II. Transcription 6, 91–101. https://doi.org/10.1080/21541264.2015.1114983

Wang, D., Bushnell, D.A., Westover, K.D., Kaplan, C.D., Kornberg, R.D., 2006. Structural Basis of Transcription: Role of the Trigger Loop in Substrate Specificity and Catalysis. Cell 127, 941–954. https://doi.org/10.1016/j.cell.2006.11.023

Wells, J., Farnham, P.J., 2002. Characterizing transcription factor binding sites using formaldehyde crosslinking and immunoprecipitation. Methods 26, 48–56. https://doi.org/10.1016/S1046-2023(02)00007-5

Wilusz, J.E., Sunwoo, H., Spector, D.L., 2009. Long noncoding RNAs: functional surprises from the RNA world. Genes Dev. 23, 1494–1504. https://doi.org/10.1101/gad.1800909

Wittmann, S., Renner, M., Watts, B.R., Adams, O., Huseyin, M., Baejen, C., El Omari, K., Kilchert, C., Heo, D.-H., Kecman, T., Cramer, P., Grimes, J.M., Vasiljeva, L., 2017. The conserved protein Seb1 drives transcription termination by binding RNA

polymerase II and nascent RNA. Nat. Commun. 8, 14861. https://doi.org/10.1038/ncomms14861

Wood, V., 2006. How to get the most from fission yeast genome data: a report from the 2006 European Fission Yeast Meeting computing workshop. Yeast Chichester Engl. 23, 905–912. https://doi.org/10.1002/yea.1419

Wood, V., Gwilliam, R., Rajandream, M.-A., Lyne, M., Lyne, R., Stewart, A., Sgouros, J., Peat, N., Hayles, J., Baker, S., Basham, D., Bowman, S., Brooks, K., Brown, D., Brown, S., Chillingworth, T., Churcher, C., Collins, M., Connor, R., Cronin, A., Davis, P., Feltwell, T., Fraser, A., Gentles, S., Goble, A., Hamlin, N., Harris, D., Hidalgo, J., Hodgson, G., Holroyd, S., Hornsby, T., Howarth, S., Huckle, E.J., Hunt, S., Jagels, K., James, K., Jones, L., Jones, M., Leather, S., McDonald, S., McLean, J., Mooney, P., Moule, S., Mungall, K., Murphy, L., Niblett, D., Odell, C., Oliver, K., O'Neil, S., Pearson, D., Quail, M.A., Rabbinowitsch, E., Rutherford, K., Rutter, S., Saunders, D., Seeger, K., Sharp, S., Skelton, J., Simmonds, M., Squares, R., Squares, S., Stevens, K., Taylor, K., Taylor, R.G., Tivey, A., Walsh, S., Warren, T., Whitehead, S., Woodward, J., Volckaert, G., Aert, R., Robben, J., Grymonprez, B., Weltjens, I., Vanstreels, E., Rieger, M., Schäfer, M., Müller-Auer, S., Gabel, C., Fuchs, M., Düsterhöft, A., Fritzc, C., Holzer, E., Moestl, D., Hilbert, H., Borzym, K., Langer, I., Beck, A., Lehrach, H., Reinhardt, R., Pohl, T.M., Eger, P., Zimmermann, W., Wedler, H., Wambutt, R., Purnelle, B., Goffeau, A., Cadieu, E., Dréano, S., Gloux, S., Lelaure, V., Mottier, S., Galibert, F., Aves, S.J., Xiang, Z., Hunt, C., Moore, K., Hurst, S.M., Lucas, M., Rochet, M., Gaillardin, C., Tallada, V.A., Garzon, A., Thode, G., Daga, R.R., Cruzado, L., Jimenez, J., Sánchez, M., del Rey, F., Benito, J., Domínguez, A., Revuelta, J.L., Moreno, S., Armstrong, J., Forsburg, S.L., Cerutti, L., Lowe, T., McCombie, W.R., Paulsen, I., Potashkin, J., Shpakovski, G.V., Ussery, D., Barrell, B.G., Nurse, P., Cerrutti, L., 2002. The genome sequence of *Schizosaccharomyces pombe*. Nature 415, 871–880. https://doi.org/10.1038/nature724

Wood, V., Harris, M.A., McDowall, M.D., Rutherford, K., Vaughan, B.W., Staines, D.M., Aslett, M., Lock, A., Bähler, J., Kersey, P.J., Oliver, S.G., 2012. PomBase: a comprehensive online resource for fission yeast. Nucleic Acids Res. 40, D695–D699. https://doi.org/10.1093/nar/gkr853

Wyers, F., Rougemaille, M., Badis, G., Rousselle, J.-C., Dufour, M.-E., Boulay, J., Régnault, B., Devaux, F., Namane, A., Séraphin, B., Libri, D., Jacquier, A., 2005. Cryptic Pol II Transcripts Are Degraded by a Nuclear Quality Control Pathway Involving a New Poly(A) Polymerase. Cell 121, 725–737. https://doi.org/10.1016/j.cell.2005.04.030

Yang, C., Stiller, J.W., 2014. Evolutionary diversity and taxon-specific modifications of the RNA polymerase II C-terminal domain. Proc. Natl. Acad. Sci. 111, 5920–5925. https://doi.org/10.1073/pnas.1323616111

Supplementary figures

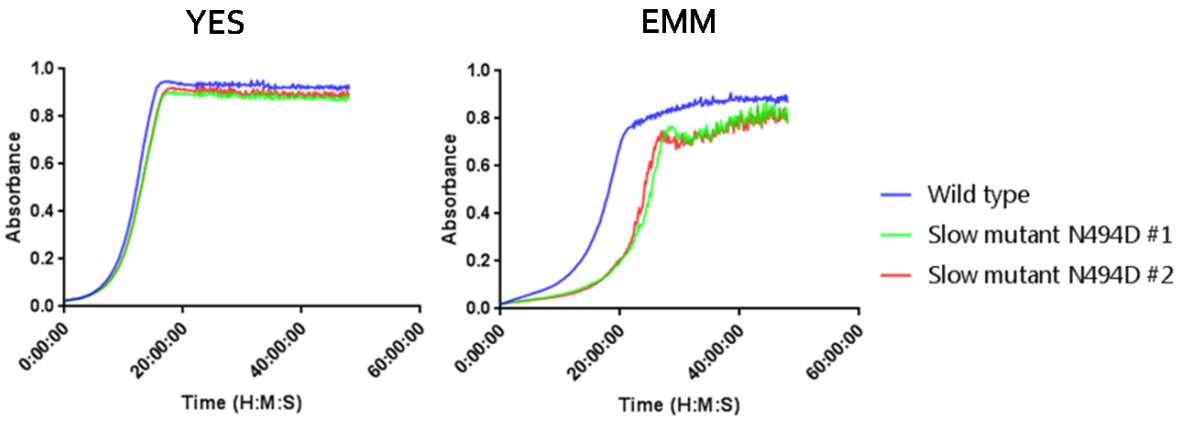

Supplementary Figure 1. Rpb1 slow mutants show reduced growth in minimal media.
Yeast strains were analyzed in liquid rich medium (YES) or synthetic medium (EMM) with OD monitoring in a microplate reader at 30°C. For the slow mutants, two biological replicates harboring the same mutation from the genome edition have been used in this experiment. Similar growth curves were observed in YES whereas the slow mutants showed a slower growth rate in EMM. Those observations have shown reproducibility for two liquid growth assay experiments. Values represent the mean of three technical replicates.

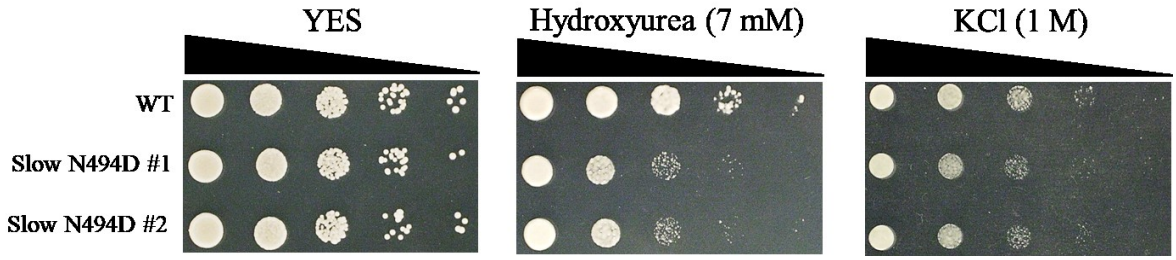

Supplementary Figure 2. Sensibility of WT and slow mutant strains to DNA damage and osmotic stress.
Ten-fold serial dilutions of wild-type (FBY2323) and slow mutants (FBY2324 and FBY2325). Cells were spotted on rich media (YES) with or without hydroxyurea or KCl at indicated concentrations.

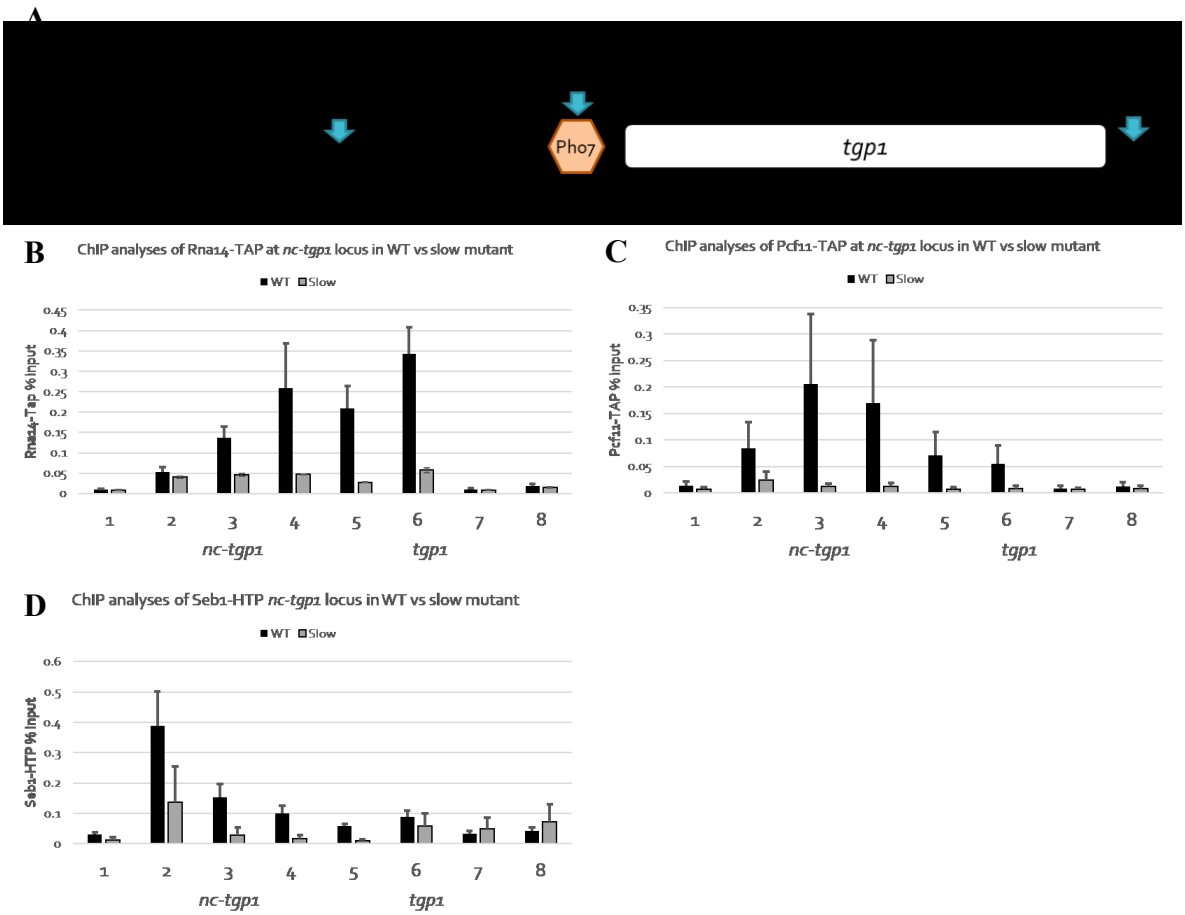

Supplementary Figure 3. Consistent binding profiles of 3'end processing factors at PAS1 and PAS2.

(**A**) The tandem *nc-tgp1-tgp1* locus is shown with transcription start sites indicated by black arrows indicating the direction of transcription and the *tgp1* ORF represented by a white rectangle. The different PAS are depicted by blue vertical arrows. The eight PCR amplicons are represented by black horizonal segments numbered from 1 to 8. (**B-C**) Average ChIP assays profile using a TAP-tagged version of respectively Rna14 or Pcf11 in a WT strain and slow mutant. (**D**) Average ChIP assays profile using an HTP-tagged version of Seb1 in a WT strain and slow mutant. Error bars represent standard error for 3 independent experiments.

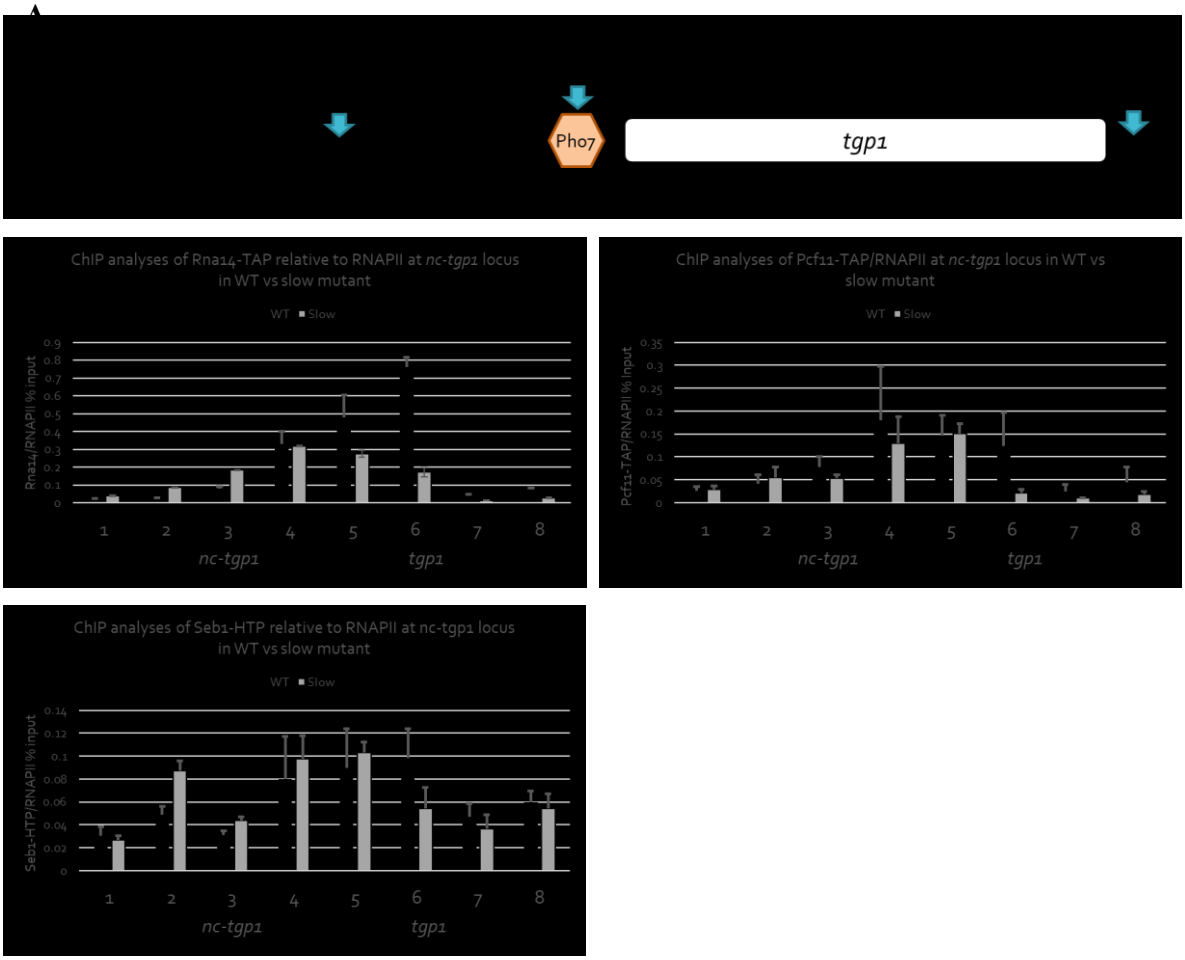

Supplementary Figure 4. Binding profiles of Rna14, Pcf11 and Seb1 normalized by RNAPII show a maximum binding around PAS2.

(**A**) The tandem *nc-tgp1-tgp1* locus is shown with transcription start sites indicated by black arrows indicating the direction of transcription and the *tgp1* ORF represented by a white rectangle. The different PAS are depicted by blue vertical arrows. The eight PCR amplicons are represented by black horizonal segments numbered from 1 to 8. (**B-C**) Average density of respectively Rna14 or Pcf11 relative to RNAPII using a TAP-tagged version of those factors in a WT strain and slow mutant. (**D**) Same as B and C but using an HTP-tagged version of Seb1. Error bars represent standard error for 3 independent experiments.

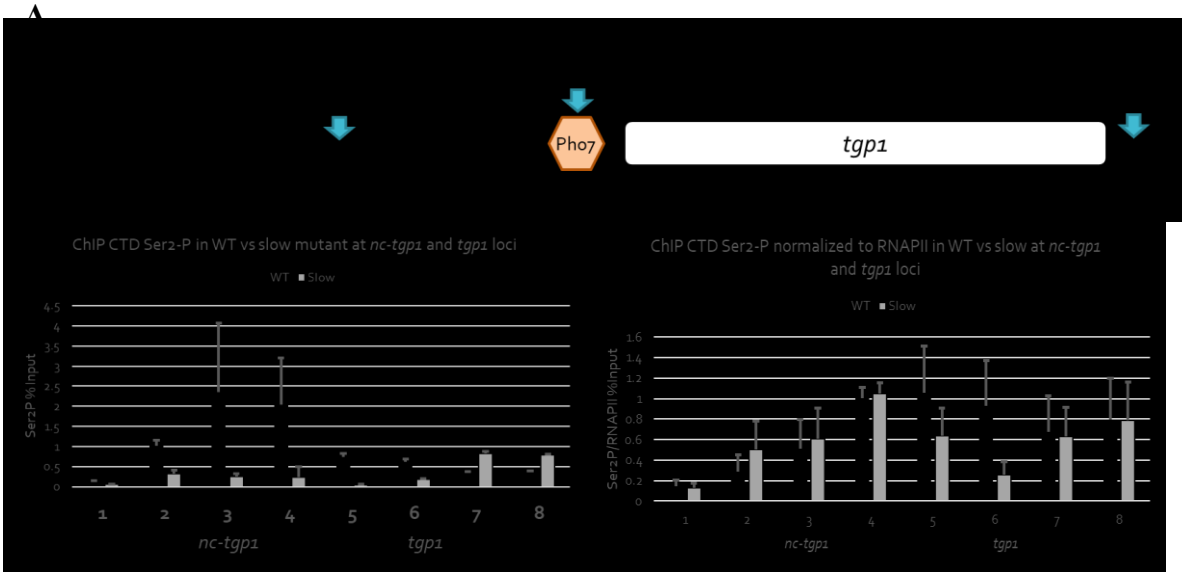

Supplementary Figure 5. RNAPII Ser2 CTD phosphorylation colocalize with 3′ end processing factors at *nc-tgp1* locus.

(**A**) The tandem *nc-tgp1-tgp1* locus is shown with transcription start sites indicated by black arrows indicating the direction of transcription and the *tgp1* ORF represented by a white rectangle. The different PAS are depicted by blue vertical arrows. The eight PCR amplicons are represented by black horizonal segments numbered from 1 to 8. (**B**) Average ChIP assays profile Ser2-P at *nc-tgp1* and *tgp1* loci in a WT strain and slow mutant. (**C**) Average ChIP assays profile Ser2-P normalized to RNAPII density at nc-tgp1 and tgp1 loci in a WT strain and slow mutant. Error bars represent standard error for 3 independent experiments.

Supplementary tables

Supplementary Table 1. List of *S. pombe* strains used in this study

Name	Genotype	Reference
FBY2323	h- ade6-M216 leu1-32 ura4-D18 his3-D1 fex1Δ fex2Δ	(Fernandez and Berro, 2016)
FBY2324	h- ade6-M216 leu1-32 ura4-D18 his3-D1 fex1Δ fex2Δ rpb1 (N494D)	(Fernandez and Berro, 2016)
FBY2325	h- ade6-M216 leu1-32 ura4-D18 his3-D1 fex1Δ fex2Δ rpb1 (N494D)	(Fernandez and Berro, 2016)
FBY2538	h- ade6-M216 leu1-32 ura4-D18 his3-D1 fex1Δ fex2Δ Seb1-HTP::kanMX6	This study
FBY2541	h- ade6-M216 leu1-32 ura4-D18 his3-D1 fex1Δ fex2Δ rpb1 (N494D) Seb1-HTP::kanMX6	This study
FBY2542	h- ade6-M216 leu1-32 ura4-D18 his3-D1 fex1Δ fex2Δ Pho7-TAP::natMX6	This study
FBY2545	h- ade6-M216 leu1-32 ura4-D18 his3-D1 fex1Δ fex2Δ rpb1 (N494D) Pho7-TAP::natMX6	This study
FBY2549	h- ade6-M216 leu1-32 ura4-D18 his3-D1 fex1Δ fex2Δ Rna14-TAP::natMX6	This study
FBY2551	h- ade6-M216 leu1-32 ura4-D18 his3-D1 fex1Δ fex2Δ rpb1 (N494D) Rna14-TAP::natMX6	This study
FBY2556	h- ade6-M216 leu1-32 ura4-D18 his3-D1 fex1Δ fex2Δ Pcf11-TAP::natMX6	This study
FBY2557	h- ade6-M216 leu1-32 ura4-D18 his3-D1 fex1Δ fex2Δ rpb1 (N494D) Pcf11-TAP::natMX6	This study

Supplementary Table 2. List of 382 up-regulated genes in the slow mutants

gene_symbol	Log2_FC	deseq.adj.pvalue	WT.norm	Slow1.norm	Slow2.norm
tgp1	2.498	2.3E-23	3321	18315	19211
mfm3	2.704	2.9E-15	99	627	659
mag2	2.663	2.2E-14	93	635	545
SPBCPT2R1.07c	2.173	2.2E-14	414	1995	1741
mug14	1.78	2.6E-14	642	2223	2188
fkh1	1.517	2.2E-11	4107	11950	11557
bit2	2.154	1.2E-10	139	638	601
SPAPB15E9.02c	1.429	6.8E-10	858	2283	2336
SPAC6G10.06	2.529	1.5E-09	100	627	523
SPAC1002.01	1.542	2.6E-09	520	1581	1449
eic2	1.538	0.000000003	521	1563	1466
mfm1	2.869	5.3E-09	1553	10177	12527
gpd3	1.974	0.000000027	2915	10509	12398
SPMITTRNAALA.01	1.995	0.000000059	115	431	484

SPAC3G9.11c	1.224	0.000000077	1088	2420	2663
mam2	1.098	0.00000025	2849	6409	5788
swi5	1.075	0.00000027	2072	4255	4472
SPAC26A3.14c	1.485	0.00000031	5469	14212	16403
SPMITTRNAILE.01	1.816	0.00000036	138	504	469
isp6	1.237	0.00000044	5987	15018	13203
ste6	1.1	0.00000049	3341	7338	6989
tum1	1.25	0.00000057	753	1781	1799
SPMITTRNATYR.01	1.645	0.00000063	206	632	654
SPBP8B7.32	1.086	0.00000085	3461	7420	7275
SPNCRNA.1348	2.229	0.000001	47	229	214
map1	1.023	0.0000011	1988	3913	4166
gal10	1.231	0.0000015	683	1662	1545
srp7	1.776	0.0000017	13571	44034	48921
cox6	1.358	0.0000019	9526	23791	25050
SPBC1685.12c	1.197	0.000002	767	1731	1784
SPNCRNA.134	1.27	0.0000032	533	1319	1253
SPAC186.05c	2.287	0.0000042	76	333	411
SPBPB21E7.04c	1.918	0.0000044	74	294	265
SPNCRNA.679	1.31	0.0000067	439	1017	1160
ypt1	1.135	0.0000067	7309	16536	15578
SPCC1442.14c	1.033	0.0000074	1201	2426	2489
spo13	1.636	0.0000096	142	414	472
SPAPJ695.02	2.849	0.000012	13	95	92
SPNCRNA.920	1.484	0.000012	312	801	942
SPAC31G5.21	0.981	0.000012	1426	2692	2938
arc5	0.949	0.000014	1625	3055	3220
SPBPB2B2.05	1.126	0.000015	732	1579	1618
atf1	0.994	0.000015	4538	9029	9054
apc13	1.347	0.000016	307	812	751

SPAC9E9.02	1.321	0.000016	352	947	812
SPACUNK4.16c	1.439	0.000019	13326	35930	36311
snx3	1.073	0.000029	2943	6610	5774
mug143	1.407	0.000042	370	1065	900
mug190	0.997	0.000059	4935	9218	10477
usp109	0.883	0.000059	2975	5361	5613
rgs1	0.876	0.000062	2927	5300	5445
sdh2	1.122	0.000063	9618	20007	21853
SPBC29A3.03c	0.881	0.000063	1647	3052	3014
SPNCRNA.1114	1.422	0.000078	184	475	512
SPNCRNA.1697	1.091	0.00008	592	1324	1198
cid2	0.888	0.000085	1414	2764	2469
SPAC17C9.11c	0.889	0.000092	3670	6576	7021
apc15	1.021	0.000094	797	1599	1635
syf2	0.853	0.000096	1861	3262	3460
snR94	1.306	0.000099	3673	9839	8322
SPATRNAPRO.02	2.429	0.00012	17	95	91
cta3	2.22	0.00014	745	3048	3900
bis1	0.95	0.00016	1013	1871	2043
SPAC4D7.02c	0.893	0.00016	1215	2366	2148
lsm6	0.864	0.00018	4135	7514	7535
opi10	1.153	0.00019	406	877	929
lsd90	0.993	0.00019	776	1531	1558
ste11	0.897	0.00022	6396	12479	11338
mug191	0.811	0.00022	2484	4108	4611
cox13	1.032	0.00025	9977	19589	21227
SPNCRNA.1294	1.147	0.00026	374	830	826
ste4	0.83	0.00029	3753	6535	6807
SPAC144.16	0.801	0.00032	1851	3138	3315
ret3	1.098	0.00042	12456	25370	27949

SPAC17A5.19	1.081	0.00042	451	925	982
aif1	0.777	0.00044	2129	3511	3788
SPAC17G6.07c	0.871	0.00046	3562	6098	6929
SPNCRNA.713	0.96	0.00057	708	1342	1411
snoR02	1.373	0.00059	680	1598	1925
mug2	0.928	0.00059	814	1512	1584
SPNCRNA.1648	0.773	0.00059	1744	3041	2919
SPNCRNA.388	0.776	0.00061	1818	3001	3225
erp5	0.789	0.00065	3531	5751	6454
SPBC27B12.14	0.755	0.00066	1814	3239	2881
SPNCRNA.1159	1.28	0.00068	175	424	424
ppk31	0.918	0.00071	813	1489	1583
acp1	0.799	0.00073	4444	7569	7900
SPNCRNA.728	0.879	0.00076	955	1733	1779
Tf2-6	1.099	0.00078	333	735	692
ntp1	0.896	0.00078	8431	15203	16185
SPATRNAVAL.04	2.787	0.00085	8	53	52
SPBC36.02c	1.105	0.00087	1659	3282	3857
SPAC22F8.05	0.806	0.00088	4997	8246	9228
SPBTRNATRP.02	3.432	0.001	4	40	55
atp15	1.265	0.001	1876	4100	4918
mbx2	0.746	0.001	1830	3037	3101
gcg1-antisense-2	1.293	0.0011	151	348	393
SPCC1919.07	1.357	0.0012	1171	2712	3290
nxt2	0.738	0.0012	1954	3101	3416
mug16	0.965	0.0013	534	1069	1016
SPNCRNA.304	0.807	0.0013	1158	2062	1991
alp31	0.745	0.0013	1760	2824	3078
SPAC222.18	0.738	0.0013	1637	2840	2621
idh1	0.796	0.0014	6467	11168	11291

SPBPB2B2.16c	2.138	0.0015	41	204	155
SPBTRNALEU.05	2.319	0.0016	13	68	61
SPCC306.08c	0.751	0.0017	4108	6521	7312
spn6	0.976	0.0018	481	920	971
SPNCRNA.901	1.321	0.002	116	268	311
SPNCRNA.111	1.003	0.002	13772	26279	28920
mrp10	0.902	0.002	2549	4420	5109
SPNCRNA.905	0.798	0.002	1223	2269	1982
SPAC343.04c	0.783	0.002	6217	10135	11264
rum1	0.701	0.002	3077	5035	4966
SPBC18H10.05	0.742	0.0021	1550	2438	2749
SPAC607.08c	0.728	0.0022	2288	3560	4021
SPNCRNA.875	0.684	0.0022	2295	3715	3659
sft1	0.868	0.0023	711	1327	1269
SPNCRNA.855	2.084	0.0024	17	82	64
arp2	0.906	0.0024	11573	21002	22359
SPBTRNAPRO.04	3.222	0.0025	8	59	84
SPAC1F12.10c	0.889	0.0025	1617	2777	3212
lsm3	0.764	0.0025	4557	7244	8237
SPNCRNA.774	1.338	0.0026	99	237	261
pnn1	0.717	0.0026	1619	2592	2730
SPAC222.17	0.695	0.0026	1843	2965	3001
gal7	0.684	0.0027	1919	3119	3047
SPNCRNA.794	1.157	0.0028	178	400	393
SPNCRNA.1169	1.141	0.0028	192	418	428
SPAC17G6.03	0.685	0.0028	3474	5680	5488
dsc3	0.686	0.0029	3776	6315	5836
ste7	1.017	0.0031	1567	2910	3435
SPCC320.04c	0.746	0.0031	6775	11568	11152
SPAC27F1.10	1.566	0.0032	48	129	158

shg1	0.692	0.0032	1655	2737	2612
SPBPB2B2.11	1.104	0.0033	211	448	459
SPAC4G8.03c	0.702	0.0033	1664	2598	2816
SPNCRNA.1454	1.119	0.0035	190	425	398
SPCC1739.08c	0.994	0.0037	306	653	567
SPBC1683.12	0.726	0.0037	1399	2200	2429
SPAC19A8.07c	0.675	0.0037	3293	5057	5459
SPNCRNA.569	1.2	0.0038	621	1291	1564
SPNCRNA.1391	0.897	0.0039	605	1215	1037
thp1	0.72	0.0039	3292	5081	5770
mad2	0.658	0.0039	2007	3228	3107
dph4	0.647	0.0039	2424	3861	3731
spk1	0.65	0.0041	3371	5589	4991
SPAC19G12.09	0.649	0.0041	2860	4521	4446
SPBC1604.16c	0.855	0.0043	618	1119	1115
cid13	0.637	0.0043	2301	3733	3422
mhf1	0.839	0.0046	672	1158	1249
SPCC794.15	0.689	0.0046	1519	2452	2447
SPAC3F10.12c	0.654	0.0046	3081	4716	4981
bet5	0.786	0.0047	871	1471	1535
kms1	0.662	0.0047	1851	2881	2979
aca1	0.641	0.0047	3119	4990	4736
Tf2-4	3.051	0.005	246	2445	1637
SPNCRNA.1067	1.309	0.005	85	207	212
SPAC186.04c	2.895	0.0051	14	86	123
atp20	0.752	0.0051	7981	12617	14259
SPBC119.03	0.674	0.0051	1666	2567	2750
SPNCRNA.989	1.243	0.0052	104	243	249
tam9	0.733	0.0052	1058	1865	1649
oma1	0.708	0.0052	1371	2114	2369

SPAC11D3.04c	0.698	0.0052	1386	2226	2273
SPAC15A10.07	0.694	0.0052	2642	4007	4547
SPAC12G12.11c	0.664	0.0052	3756	5696	6208
SPAC13F5.07c	1.14	0.0057	153	311	364
SPAC977.13c	1.454	0.0059	51	142	140
SPAC1B3.20	0.893	0.0059	450	829	841
pvg2	0.616	0.0059	2619	4194	3829
SPRRNA.52	1.827	0.006	316	967	1276
SPBPB2B2.06c	0.83	0.006	12623	23320	21565
SPMITTRNAMET.02	1.339	0.0062	71	178	179
SPNCRNA.1553	1.218	0.0063	105	244	244
spc24	0.665	0.0063	4835	7681	7656
SPBC1683.01	0.66	0.0063	4227	7104	6248
SPNCRNA.220	1.944	0.0065	17	67	66
mfm2	0.902	0.0065	5916	11981	10132
SPCTRNALYS.12	2.893	0.0066	4	30	35
SPNCRNA.648	1.608	0.0066	84	223	287
SPNCRNA.519	1.028	0.0066	214	452	421
SPNCRNA.1565	0.914	0.0066	385	710	744
SPBC15D4.08c	0.897	0.0068	425	759	824
spc19	0.745	0.007	897	1537	1470
mei2	0.976	0.0072	17194	31196	36431
SPBC4B4.12c	0.649	0.0072	1601	2543	2477
SPNCRNA.1473	0.924	0.0073	346	648	664
stc1	0.836	0.0074	581	966	1110
SPNCRNA.1666	1.183	0.0076	110	250	251
cmc4	0.772	0.0076	724	1301	1171
isd11	0.618	0.0076	2649	3857	4275
SPAC664.13	0.846	0.0077	497	914	872
rsm27	0.612	0.008	3363	5242	5035

SPCTRNAGLN.06	2.853	0.0081	4	29	35
ats1	0.669	0.0081	5969	9242	9733
gos1	1.172	0.0082	1848	3742	4588
SPNCRNA.1046	1.071	0.0087	170	330	386
ght3	1.447	0.0088	179	548	428
SPCC1259.16	0.725	0.0089	1348	2075	2382
btn1	0.925	0.0094	320	570	646
oct1	0.606	0.0095	3326	5014	5115
SPAC29E6.09	0.686	0.0097	1217	1870	2048
pet117	0.698	0.0099	1134	1739	1942
mug35	1.114	0.01	1944	4645	3772
SPNCRNA.623	1.079	0.01	635	1212	1472
SPNCRNA.909	1.027	0.01	187	370	394
SPNCRNA.1350	0.965	0.01	243	471	478
SPSNORNA.54	0.642	0.01	1582	2324	2617
SPBC26H8.12	0.588	0.01	3095	4789	4515
SPATRNAVAL.02	3.017	0.011	3	25	29
SPNCRNA.1691	1.157	0.011	105	231	237
SPNCRNA.993	1.103	0.011	133	270	301
SPNCRNA.536	0.999	0.011	212	389	460
SPAC105.02c	0.829	0.011	9405	15389	18021
tam7	0.73	0.011	804	1398	1269
SPNCRNA.841	0.647	0.011	1430	2156	2323
orc6	0.645	0.011	1477	2219	2403
SPNCRNA.976	1.049	0.012	149	323	293
SPBTRNAPRO.07	1.899	0.013	30	96	129
SPNCRNA.621	1.111	0.013	543	1054	1293
mrpl28	1	0.013	5682	10294	12429
SPNCRNA.1617	0.986	0.013	193	384	379
rpl4102	0.932	0.013	3681	6403	7648

wtf17	0.873	0.013	446	750	886
Tf2-10	0.852	0.013	365	679	639
atp16	0.71	0.013	7899	13872	11968
SPBC530.07c	0.663	0.013	7984	12516	12769
new13	0.653	0.013	1259	1963	1996
SPAC186.06	2.258	0.014	16	64	90
SPNCRNA.1035	1.386	0.014	319	732	936
SPAC513.02	1.018	0.014	161	332	319
mrps16	0.958	0.014	2101	3708	4457
SPAC56F8.13	0.842	0.014	394	687	727
SPBC19G7.19	0.599	0.014	1594	2535	2293
rlp1	0.575	0.014	3653	5649	5236
ini1	0.84	0.015	770	1264	1492
SPNCRNA.499	0.818	0.015	2199	4204	3548
mim1	0.779	0.015	2486	3934	4596
SPCC16A11.15c	0.746	0.015	618	1082	989
SPNCRNA.1495	1.157	0.016	119	237	294
pol4	0.848	0.016	332	635	559
SPNCRNA.1518	0.7	0.016	1214	1832	2114
rec11	0.675	0.016	961	1569	1500
SPAC1687.21	0.617	0.016	6974	11095	10294
SPCC794.04c	0.587	0.016	1692	2603	2480
inv1	1.371	0.017	560	1634	1262
atp18	1.34	0.017	1172	2606	3333
fbp1	0.911	0.017	222	455	379
SPMIT.03	0.786	0.017	15485	27549	25858
hht2	0.662	0.017	9472	15338	14629
ins1	0.56	0.017	2152	3151	3196
coq7	0.553	0.017	3265	5031	4547
SPBC216.03	0.545	0.017	2309	3567	3170

SPNCRNA.1385	1.233	0.018	67	141	177
SPNCRNA.1477	0.828	0.018	355	642	620
ptc1	0.821	0.018	2778	4500	5321
SPNCRNA.1214	0.746	0.018	563	991	897
mot2	0.696	0.018	8875	13336	15413
SPAC6G9.16c	0.675	0.018	900	1425	1450
SPCC330.03c	0.646	0.018	1146	1713	1874
SPNCRNA.1011	0.616	0.018	1256	2016	1832
SPNCRNA.1279	0.573	0.018	1956	2790	3030
SPAC17C9.14	0.553	0.018	3261	4892	4674
SPNCRNA.1614	1.202	0.019	67	161	150
SPBC83.13	0.753	0.019	14847	25939	24120
erp2	0.609	0.019	6426	9465	10140
ubp8	0.552	0.019	2537	3625	3814
SPMIT.02	1.215	0.02	31748	75188	72254
ecl3	1.176	0.02	1368	3451	2728
SPCC663.18	0.563	0.02	3814	5510	5757
SPAC23C4.04c	0.983	0.021	563	1004	1223
ykt6	0.638	0.021	8297	12060	13760
SPBC12C2.04	0.612	0.021	3831	5468	6240
SPBC609.01	0.546	0.021	2065	3085	2944
SPNCRNA.1556	1.118	0.022	85	191	176
SPNCRNA.626	1.078	0.022	525	990	1226
SPNCRNA.1472	0.993	0.022	149	281	312
SPBC25B2.10	0.859	0.022	2287	3780	4516
gdh2	0.819	0.022	18456	34882	30226
SPAC6C3.05	0.782	0.022	466	741	860
fsv1	0.773	0.022	1061	1966	1660
SPNCRNA.1496	0.765	0.022	449	795	729
dak1	0.621	0.022	7549	10939	12288

sgt1	0.552	0.022	2026	2878	3061
slm1	0.547	0.022	3395	4850	5071
ace2	0.86	0.023	1055	1744	2086
bet1	0.738	0.023	537	906	886
mug37	0.671	0.023	890	1523	1309
mug185	0.543	0.023	2025	2954	2948
SPCTRNAALA.12	2.944	0.024	8	46	71
SPAC16C9.01c	0.88	0.025	1787	2988	3591
dli1	0.855	0.025	259	470	467
SPNCRNA.607	0.806	0.025	314	591	506
SPBC651.02	0.605	0.025	1134	1832	1615
SPACUNK4.15	0.657	0.026	843	1328	1329
SPAPB17E12.09	1.314	0.027	41	108	94
SPCC63.05	0.838	0.027	3432	5589	6684
meu25	0.798	0.027	336	589	580
spt2	0.639	0.027	4274	6186	7129
SPAC824.07	0.578	0.027	1395	2124	2041
mcp5	0.569	0.027	1411	2213	1972
SPNCRNA.1346	1.281	0.028	44	115	98
SPAP27G11.16	1.005	0.028	118	238	235
SPNCRNA.1589	0.813	0.028	314	535	568
SPAC12G12.17	0.682	0.028	728	1098	1240
meu23	0.625	0.028	1248	2065	1783
SPBC21B10.02	0.576	0.028	1323	2064	1882
SPAC23D3.17	1.467	0.029	1474	3505	4647
SPNCRNA.923	1.374	0.029	223	501	655
mug20	1.25	0.029	92	247	191
SPBC19C7.04c	1.15	0.029	1901	4731	3708
SPNCRNA.1489	0.708	0.029	575	925	954
mug15	1.432	0.03	365	850	1121

SPAC11D3.19	1.391	0.03	277	829	625
SPNCRNA.687	0.899	0.03	172	348	294
cds1	0.516	0.03	3079	4353	4454
SPBC2G2.17c	1.243	0.031	236	629	485
eta2	1.188	0.032	800	1603	2043
rec27	0.961	0.032	136	253	277
img2	0.727	0.032	2158	3284	3862
fum1	0.569	0.032	6899	9984	10486
SPNCRNA.810	1.171	0.033	59	127	138
SPCTRNAASN.05	1.557	0.034	21	56	71
SPAC27E2.14	0.883	0.034	451	752	911
hop1	0.856	0.034	213	387	385
SPNCRNA.870	0.661	0.034	2154	3675	3136
ubx2	0.524	0.034	1969	2752	2912
spo12	0.573	0.035	1249	1887	1831
SPBC428.10	0.52	0.035	3664	5033	5476
SPBC11C11.01	0.508	0.035	3177	4416	4622
SPNCRNA.1635	0.836	0.036	246	410	470
SPNCRNA.788	0.8	0.036	297	564	468
rpl4101	0.683	0.036	6505	9629	11262
dak2	1.77	0.037	288	1151	813
mug147	1.528	0.037	1059	2598	3510
SPNCRNA.1383	0.968	0.037	123	226	256
rga3	0.676	0.037	13432	19919	23012
isa1	0.603	0.037	6358	10376	8944
SPNCRNA.560	0.926	0.038	137	275	246
SPNCRNA.698	0.782	0.038	286	507	476
nas6	0.536	0.038	1716	2371	2606
rpl3703	0.906	0.039	24785	42638	50245
ade6	0.594	0.039	10539	16476	15330

SPRRNA.53	1.4	0.04	29	66	87
SPNCRNA.498	1.275	0.04	135	284	370
spd2	1.018	0.041	26465	47648	59553
SPCTRNAILE.09	2.166	0.042	6	27	32
SPCC338.18	1.091	0.042	70	140	157
tim11	0.638	0.042	8632	12416	14445
hcn1	0.58	0.042	1041	1575	1537
fra2	0.568	0.042	1104	1753	1519
Tf2-12	1.067	0.043	73	152	153
whi5	0.676	0.043	575	880	958
mug133	0.727	0.044	365	618	591
rpl35a	0.587	0.044	975	1471	1459
spd1	0.568	0.044	2087	3315	2869
pre3	0.557	0.044	7794	10914	12015
grx4	0.536	0.044	6418	9047	9560
rpn7	0.535	0.044	7147	10517	10195
SPCC1827.05c	0.565	0.045	8373	11681	13095
SPNCRNA.986	0.563	0.045	1090	1672	1549
prf1	0.56	0.045	7975	11048	12475
nse2	0.525	0.045	1564	2245	2256
hcs1	0.522	0.045	6477	9513	9086
mrp7	0.504	0.045	2027	2731	3018
sno12	0.971	0.046	99	204	182
SPNCRNA.1396	0.868	0.046	158	301	277
lsm8	0.612	0.046	808	1221	1250
ppk33	0.545	0.046	1279	1898	1834
SPAC1002.20	2.03	0.047	8	31	31
gmf1	0.807	0.047	1196	2298	1887
SPNCRNA.1048	0.998	0.048	606	1075	1346
mug136	0.697	0.048	444	703	738

SPCTRNASER.13	2.245	0.049	5	25	27
snoR69	1.041	0.049	78	144	178
SPBC28E12.02	0.911	0.049	130	237	251
SPNCRNA.1630	0.715	0.049	377	612	626
SPNCRNA.572	0.88	0.05	145	271	261
SPNCRNA.1613	0.811	0.05	206	369	352
SPBC23G7.06c	0.799	0.05	6029	9506	11479
SPAC24H6.08	0.584	0.051	945	1370	1465

Supplementary Table 3. List of 494 down-regulated genes in the slow mutants

gene_symbol	Log2_FC	deseq.adj.pvalue	WT.norm	Slow1.norm	Slow2.norm
SPBC660.05	-2.777	1.7E-46	4117	633	567
urg2	-2.248	1.4E-24	2416	516	501
urg1	-1.893	6.3E-22	3526	955	944
str1	-1.611	4.4E-20	6639	2074	2273
rpl2701	-1.591	3.5E-19	7025	2359	2305
SPAC2H10.01	-2.518	5.9E-19	884	152	157
SPCP20C8.02c	-2.742	2.6E-18	609	97	84
SPCC16C4.21	-1.838	2.7E-17	2484	759	630
SPAC8E11.10	-1.456	8.4E-16	7078	2662	2497
SPAC24H6.10c	-1.506	2.9E-15	7391	2898	2304
rps801	-1.97	3.2E-15	43857	11494	10895
mcp7	-1.374	2.2E-14	5668	2213	2161
ptr2	-1.374	5.8E-13	4045	1679	1439
aat1	-1.303	5.8E-13	6801	2631	2881
SPBC1683.05	-1.282	1.5E-12	6336	2555	2657
SPBPB8B6.05c	-1.522	1.9E-12	2483	896	833
SPAC8C9.05	-1.284	8.5E-12	7925	3377	3131
SPAC1039.02	-1.236	9.2E-12	5464	2255	2386
pyp2	-1.547	3.6E-11	1818	611	634
SPNCRNA.1235	-1.401	8.1E-11	2478	926	950
SPAC4G9.22	-1.218	8E-10	3706	1740	1445
rps2601	-1.554	9.2E-10	38979	12129	14427
SPCC1884.01-antisense-1	-1.287	3.8E-09	2447	1003	1003
rpl702	-1.345	4.8E-09	23479	10132	8358
SPCP20C8.03	-3.207	6.4E-09	110	14	9
SPNCRNA.1696	-1.341	0.000000015	1834	731	717
rpl1601	-1.134	0.000000016	9395	4539	4020

mfs2	-1.449	0.00000004	1314	545	416
put4	-1.395	0.000000044	1339	474	545
pac2	-1.065	0.000000044	7103	3540	3250
SPAC3G6.05	-1.136	0.000000046	2992	1348	1375
SPBC1271.04c	-1.012	0.000000093	5775	2796	2933
hem2	-1.086	0.00000013	11441	5395	5380
frp1	-1.658	0.00000017	547	153	194
SPCC320.08	-1.01	0.00000017	6906	3314	3545
pus1	-0.981	0.00000023	5122	2517	2673
SPNCRNA.1649	-1.97	0.00000027	268	54	82
byr3	-1.084	0.00000027	13459	6413	6280
SPBC646.07c	-1.007	0.00000027	4196	2205	1968
SPAC1B3.04c	-1.246	0.00000037	1638	688	693
sdh4	-1.034	0.00000039	10387	4916	5233
alo1	-0.975	0.00000044	4205	2110	2169
SPAC1039.01	-1.322	0.00000047	1221	466	511
SPBC18H10.20c	-1.153	0.00000068	22887	9867	10713
SPCC584.16c	-1.504	0.00000069	685	237	246
SPNCRNA.877	-2.556	0.00000072	119	19	22
pgt1	-0.993	0.0000009	9053	4477	4622
SPAC29E6.07	-1.563	0.000001	545	178	191
SPAC977.12	-0.998	0.000001	3386	1751	1638
urg3	-0.931	0.0000011	5504	2795	2981
SPBC1271.10c	-1.058	0.0000014	2538	1219	1220
rar1	-1.059	0.0000015	16101	7986	7468
rrn3	-1.001	0.0000015	9951	5227	4716
dsd1	-0.948	0.0000018	7355	3844	3779
rpb6	-0.943	0.0000021	3913	2134	1935
vht1	-1.261	0.0000023	34519	15434	13378
SPNCRNA.655	-1.169	0.0000029	1506	650	689

SPAC1565.05	-0.914	0.0000029	5811	3147	3022
cdb4	-0.945	0.0000044	9851	4926	5311
atx1	-0.894	0.0000044	4361	2336	2359
cbf12	-0.903	0.0000048	6146	3385	3187
thi9	-1.162	0.0000066	30549	13476	13834
pog1	-0.873	0.0000067	5975	3082	3442
SPCC1795.12c	-0.933	0.0000068	9843	5060	5250
dea2	-1.033	0.000011	2032	1008	978
SPNCRNA.885	-1.249	0.000012	946	417	378
SPAC2C4.05	-1.148	0.000012	5022	2548	1981
SPCC584.13	-1.113	0.000012	1451	655	686
rpc34	-0.967	0.000012	2533	1289	1303
SPAC694.04c	-0.881	0.000012	6621	3708	3482
SPNCRNA.1531	-0.864	0.000014	4489	2619	2311
SPNCRNA.1432	-1.606	0.000015	308	92	111
SPBC365.16	-0.869	0.000015	7431	3911	4229
SPAC869.02c	-1.166	0.000016	1216	578	506
SPAC2E1P3.05c	-1.12	0.000016	1353	611	635
SPAC1B3.13	-0.876	0.000016	7358	4086	3932
sec2302	-0.854	0.000017	4216	2400	2263
ade9	-0.882	0.000018	8126	4460	4361
rlp24	-0.828	0.000024	5715	3102	3337
eft202	-1.065	0.00003	16141	8617	6815
SPCC1529.01	-0.823	0.00003	4986	2816	2822
dph6	-0.829	0.000036	4380	2590	2341
SPAC105.03c	-0.828	0.000036	5651	3293	3072
laf2	-1.108	0.000041	1869	975	758
SPBC115.03	-0.961	0.000046	1987	985	1057
SPNCRNA.142	-1.791	0.000047	183	54	51
gcg1	-0.895	0.000056	2619	1416	1400

fra1	-0.802	0.000059	5077	2940	2886
new8	-1.23	0.000066	685	295	289
rpl802	-0.835	0.000066	8191	4603	4580
fmn1	-0.818	0.000069	6358	3814	3397
asa1	-0.865	0.00008	2975	1771	1495
SPBC4F6.13c	-0.85	0.00008	10105	5695	5517
lag1	-0.782	0.000088	5109	2937	3007
tif11	-0.881	0.000091	14112	7781	7547
swp1	-0.796	0.000094	5161	3190	2753
SPCC126.01c	-0.788	0.000094	5417	3206	3068
hht1	-0.828	0.000097	10461	5530	6255
SPNCRNA.460	-4.574	0.00011	26	0	2
lsm2	-0.99	0.00011	1583	837	757
SPBC30B4.09	-2.004	0.00012	1575	528	258
SPAC1A6.10	-0.808	0.00012	6869	4198	3649
rps602	-0.814	0.00013	9699	5237	5797
pdx1	-0.825	0.00014	9512	5523	5215
SPCC14G10.02	-0.786	0.00015	6606	3947	3716
adg1	-1.197	0.00018	1834	673	927
SPAC637.09	-0.764	0.00018	5954	3510	3501
SPNCRNA.1626	-0.828	0.00019	13094	7071	7682
SPCC1450.03	-0.746	0.0002	4727	2750	2888
lys7	-1.102	0.00021	900	459	380
SPAC1687.07	-1.054	0.00021	996	465	494
SPBC713.04c	-0.799	0.00021	9389	5386	5405
SPCC18.17c	-0.776	0.00021	3441	2023	1996
isp7	-0.763	0.00021	4353	2734	2393
SPAC11D3.11c	-0.936	0.00023	1506	731	845
SPBC839.03c	-0.891	0.00023	1931	1035	1048
mrpl7	-0.799	0.00023	3003	1759	1692

SPBC21C3.19	-0.771	0.00023	3362	1952	1988
SPAC18B11.06	-0.763	0.00023	3261	1794	2049
pho4	-1.136	0.00026	45113	20518	20525
git3	-0.741	0.00026	4114	2450	2473
SPBP4H10.14c	-0.799	0.00029	2837	1660	1601
prs5	-0.871	0.00031	2147	1273	1074
rds1	-0.861	0.00035	2082	1182	1111
ubp12	-0.776	0.00035	9290	5380	5469
erg31	-0.746	0.00036	3866	2436	2174
ser2	-0.732	0.00036	3830	2272	2340
rhp42	-0.803	0.00039	2568	1463	1482
set10	-0.725	0.00044	5273	3268	3111
SPBC3H7.05c	-0.75	0.00051	9299	5212	5845
SPNCRNA.1297	-1.193	0.00054	450	181	212
vma7	-0.758	0.00059	8669	5324	4930
obr1	-0.711	0.00059	4281	2397	2837
SPBC1652.02	-0.72	0.00061	7341	4167	4750
SPBC215.11c	-0.94	0.00062	1325	742	640
SPAC823.09c	-0.897	0.00062	1525	840	797
SPBC776.08c	-0.738	0.00066	7655	4705	4476
SPAC26A3.17c	-0.769	0.00067	10939	6644	6196
mug64	-0.733	0.00069	8764	5005	5545
mpc2	-0.702	0.00071	4986	3132	2998
SPBC409.08	-0.705	0.00072	5531	3455	3330
sal3	-0.819	0.00073	19645	9994	12277
SPAC11D3.14c	-0.776	0.00073	2504	1462	1464
SPNCRNA.1644	-0.748	0.00074	2754	1586	1694
gmh6	-0.732	0.00077	7199	4608	4061
has1	-0.742	0.0008	10467	6066	6448
SPCC188.10c	-1.005	0.00082	863	439	420

avt5	-0.971	0.00082	1081	603	500
SPAC29A4.03c	-0.77	0.00087	11658	7371	6302
SPBC244.02c	-0.701	0.00094	3671	2313	2204
SPBC23G7.13c	-0.909	0.001	1162	584	654
srb11	-0.943	0.0011	986	489	537
SPNCRNA.863	-0.7	0.0011	6770	4238	4094
agn2	-0.866	0.0012	1425	789	775
SPAC1B2.03c	-0.702	0.0012	6753	4334	3968
new25	-0.834	0.0013	1549	851	887
SPBC29A3.11c	-0.737	0.0013	2662	1620	1573
rpc19	-0.723	0.0013	2697	1582	1685
trl1	-0.68	0.0013	6119	3825	3812
ght8	-0.886	0.0014	27833	15152	14971
laf1	-0.825	0.0014	1776	1087	917
qcr7	-0.774	0.0014	15667	9459	8860
rps902	-0.668	0.0014	4456	2840	2769
sgp1	-0.74	0.0016	2563	1608	1461
rga5	-0.729	0.0017	2694	1729	1520
gln1	-0.704	0.0017	8666	5399	5242
SPBC1683.04	-0.703	0.0017	2713	1576	1758
cat1	-0.655	0.0018	4857	3096	3075
SPNCRNA.329	-2.135	0.002	56	9	17
SPNCRNA.1690	-0.815	0.002	1580	927	869
SPBC17D1.01	-0.743	0.002	14188	8752	8207
rpl101	-0.782	0.0022	5503	3517	2882
rps001	-0.785	0.0023	20915	11797	12483
SPCC737.05	-0.776	0.0023	2214	1419	1164
SPAC23G3.05c	-0.686	0.0023	2695	1571	1779
ppk32	-0.668	0.0023	3311	2120	2048
hsk1	-0.632	0.0023	3768	2239	2624

SPAC637.08	-0.74	0.0024	3323	2174	1803
SPAC30D11.11	-0.671	0.0024	7035	4570	4269
SPAC11D3.02c	-0.663	0.0024	6613	4285	4066
SPAC16C9.02c	-0.657	0.0024	5916	3881	3624
las1	-0.655	0.0025	3284	2053	2117
rpl1602	-1.246	0.0026	80807	34934	33223
rrp46	-1.096	0.0027	9775	5294	3852
rps402	-0.761	0.0027	19758	11084	12240
klf1	-0.706	0.0027	2633	1719	1508
SPAC7D4.03c	-0.652	0.0027	5141	3523	3020
SPNCRNA.1055	-1.55	0.0028	112	31	46
SPBC29A3.06	-0.663	0.0028	8647	5214	5712
SPAC2C4.12c	-0.65	0.0028	3885	2642	2310
SPBC2A9.06c	-0.642	0.0028	3578	2285	2302
prl53	-2.727	0.0029	32	6	3
SPBC887.17	-0.792	0.0029	23719	13043	14360
scp1	-0.689	0.0029	10177	6582	6039
nic1	-0.65	0.0029	3662	2470	2195
mis16	-0.636	0.0029	4259	2836	2644
SPAC688.16	-0.79	0.003	1542	911	871
mmi1	-0.637	0.003	6103	3862	3987
gut2	-0.746	0.0032	2064	1340	1121
SPNCRNA.604	-1.871	0.0033	70	22	16
mdm10	-0.925	0.0033	732	377	394
krp1	-0.655	0.0033	7432	4806	4633
txl1	-0.634	0.0033	4089	2784	2484
SPBC359.01	-0.87	0.0035	954	518	526
SPAC821.05	-0.678	0.0035	9752	6412	5778
mdl1	-0.652	0.0036	7116	4738	4321
ptf1	-0.616	0.0036	3830	2432	2565

SPNCRNA.1435	-0.928	0.0037	661	327	368
SPAC222.08c	-0.66	0.0037	8357	5418	5159
rpc40	-0.612	0.0038	5309	3359	3588
SPNCRNA.218	-1.589	0.0039	95	24	39
SPNCRNA.1308	-1.581	0.0039	96	24	40
SPBPB7E8.01	-0.758	0.0039	20613	12334	12050
imt1	-0.748	0.0039	1731	1059	1002
rpl402	-0.775	0.004	24316	13421	14995
fip1	-0.704	0.004	2053	1218	1304
rpl1902	-1.279	0.0041	98097	36001	44872
SPBC15C4.04c	-0.705	0.0041	11472	7685	6389
SPBP16F5.06	-0.615	0.0041	4529	3047	2865
SPAC1093.05	-0.65	0.0042	10080	6159	6687
SPNCRNA.1087	-0.915	0.0046	672	352	361
rpl301	-0.869	0.0046	32919	19757	16279
SPBC1711.15c	-0.74	0.0046	1580	903	990
idi1	-0.614	0.0046	6529	4092	4439
mug73	-1.394	0.0048	136	50	53
vba2	-0.596	0.0048	3938	2503	2708
tom40	-0.609	0.005	6770	4208	4667
SPCC18.05c	-0.585	0.005	4239	2623	3031
SPNCRNA.1444	-1.429	0.0051	131	56	40
SPAC212.12	-1.375	0.0051	692	329	204
trm11	-0.613	0.0051	3409	2241	2217
SPBC1683.03c	-0.629	0.0052	2859	1798	1900
mot1	-0.721	0.0055	19087	11671	11483
dis3	-0.669	0.0055	13172	8369	8194
SPAC890.04c	-0.615	0.0056	7175	4608	4764
fio1	-0.603	0.0056	6775	4241	4681
ura3	-0.653	0.0057	12824	7786	8529

SPAC513.07	-0.597	0.0057	4784	3232	3093
SPBC530.15c	-0.585	0.0058	4490	2923	3063
moc3	-0.658	0.0062	2395	1543	1491
SPBC691.04	-0.591	0.0062	6082	3871	4204
per1	-0.611	0.0063	3037	1958	2020
ssr2	-0.59	0.0063	4598	3116	2994
SPAC959.06c	-0.991	0.0064	411	197	217
rcd1	-0.655	0.0064	2447	1602	1507
plg7	-0.64	0.0064	2395	1451	1625
SPBC4.02c	-0.615	0.0065	7289	4887	4630
SPCC18.02	-0.606	0.0065	3053	1964	2050
cis4	-0.586	0.0065	4838	3242	3205
rnp24	-0.578	0.0065	5290	3379	3709
tim50	-0.574	0.0065	4316	2764	3035
pfl7	-1.474	0.0066	103	34	40
jmj4	-0.714	0.0066	1764	1142	1009
SPCC1682.08c	-0.604	0.0066	3210	2128	2095
SPAC1399.04c	-0.818	0.0068	952	551	528
rib4	-0.739	0.0068	1352	775	846
hhf3	-0.586	0.0069	6254	3981	4354
mug111	-0.639	0.0072	2360	1466	1565
SPAC3H1.06c	-0.582	0.0072	4054	2755	2663
mal1	-0.681	0.0073	1836	1112	1180
mcl1	-0.587	0.0073	3723	2542	2413
SPNCRNA.1097	-0.832	0.0074	870	509	468
SPBC1347.13c	-0.802	0.0076	960	549	553
snd1	-0.577	0.0077	5228	3511	3497
sum3	-0.872	0.008	40380	21971	22164
urb2	-0.619	0.008	10632	6781	7061
rps1701	-0.78	0.0081	1414	726	922

nem1	-0.691	0.0081	1807	1172	1065
SPAC2F3.11	-0.571	0.0083	4279	2918	2842
SPBC3B8.08	-0.646	0.0084	2136	1322	1408
arx1	-0.603	0.0084	3092	2137	1934
fur4	-0.673	0.0085	2457	1684	1396
ire1	-0.589	0.0086	3311	2269	2134
SPBC15C4.02	-0.578	0.0089	5593	3837	3658
SPNCRNA.1318	-0.722	0.009	1276	719	829
vrs2	-0.579	0.0091	4391	3163	2713
SPCC613.01	-0.662	0.0092	2139	1451	1252
spb70	-0.572	0.0098	3452	2332	2312
bgl2	-0.76	0.01	1002	557	627
SPNCRNA.762	-0.746	0.01	1120	652	684
isp4	-0.659	0.01	1831	1128	1191
gpd2	-0.637	0.01	15798	9591	10722
SPAC23H4.15	-0.618	0.01	12087	7769	7984
dbp7	-0.595	0.01	2732	1780	1838
SPBC3H7.02	-0.593	0.01	9899	6173	6952
utp15	-0.569	0.01	6224	4118	4274
SPAC1071.03c	-0.565	0.01	5171	3580	3409
snR93	-1.475	0.011	88	31	32
ght5	-0.721	0.011	24975	15028	15278
SPBC17A3.02	-0.677	0.011	1579	960	1016
rrs1	-0.677	0.011	1568	942	1020
taf6	-0.588	0.011	9516	6150	6509
skb15	-0.569	0.011	3281	2246	2178
SPBC30D10.07c	-0.568	0.011	6358	4235	4342
ckb2	-0.55	0.011	3891	2574	2742
snR88	-2.178	0.012	33	5	10
SPNCRNA.119	-1.329	0.012	121	55	41

SPNCRNA.710	-0.963	0.012	347	171	185
SPAC806.11	-0.961	0.012	395	223	182
SPBC15D4.13c	-0.949	0.012	397	216	196
rps1902	-0.72	0.012	5165	3465	2803
SPCC126.12	-0.627	0.012	2152	1408	1379
SPCC736.03c	-0.561	0.012	3608	2557	2332
SPAC9G1.05	-0.558	0.012	6880	4400	4945
SPCC11E10.07c	-0.554	0.012	6040	3993	4233
SPCC320.03	-0.539	0.012	4669	3044	3384
SPNCRNA.664	-1.298	0.013	125	58	43
SPBC2G5.04c	-0.59	0.013	2780	1927	1765
ppc1	-0.577	0.013	3017	2117	1925
SPCC1259.08	-0.577	0.013	8889	5809	6109
hmg1	-0.569	0.013	7668	5107	5232
SPNCRNA.564	-1.61	0.014	61	14	26
SPNCRNA.771	-0.722	0.014	1042	597	666
SPAC2F3.05c	-0.705	0.014	1228	740	766
utp10	-0.694	0.014	23085	14558	13986
prs1	-0.605	0.014	12127	8157	7794
SPAC4G8.07c	-0.585	0.014	2491	1619	1703
SPBC1703.03c	-0.571	0.014	8333	5568	5652
sof1	-0.553	0.014	5588	3914	3701
SPNCRNA.1599	-0.814	0.015	988	487	638
SPNCRNA.1417	-0.759	0.015	912	557	520
SPAC23H4.16c	-0.648	0.015	1717	1134	1057
rrp12	-0.632	0.015	18278	11078	12509
imt3	-0.608	0.015	2233	1506	1423
tea3	-0.595	0.015	9818	7001	5999
SPCC18B5.08c	-0.579	0.015	2590	1726	1742
los1	-0.569	0.015	8253	5624	5504

cig1	-0.562	0.015	3602	2635	2243
trm112	-0.557	0.015	3045	2087	2053
SPAC823.08c	-0.546	0.015	3367	2314	2297
efc25	-0.536	0.015	4482	3120	3060
lys4	-1.006	0.016	15458	8989	6407
SPCC1884.01	-0.932	0.016	335	168	184
SPAC664.12c	-0.62	0.016	1783	1113	1207
hta1	-0.581	0.016	9960	6911	6403
ely5	-0.572	0.016	2624	1764	1766
SPBC1718.04	-0.56	0.016	3264	2367	2061
SPCPB16A4.05c	-0.546	0.016	3708	2730	2347
mse1	-0.541	0.016	3971	2863	2595
mug184	-0.537	0.016	4472	3223	2941
fma1	-0.532	0.016	5155	3553	3576
atg16	-0.817	0.017	647	404	330
rep1	-0.749	0.017	867	530	502
cpc2	-0.674	0.017	22895	14397	14312
SPNCRNA.1319	-0.67	0.017	1208	690	829
btb2	-0.643	0.017	1780	1239	1040
orc5	-0.613	0.017	2032	1364	1292
SPCC1259.02c	-0.594	0.017	13157	8818	8617
SPBC3H7.11	-0.575	0.017	2582	1771	1696
SPBC215.01	-0.575	0.017	8499	6084	5329
SPCC553.12c	-0.571	0.017	2657	1844	1733
SPAC1751.04	-0.57	0.017	2741	1914	1776
SPAC1039.06	-0.561	0.017	2924	2063	1899
msa1	-0.556	0.017	2820	1902	1936
erg2	-0.553	0.017	3156	2260	2042
SPAC1399.02	-0.552	0.017	2666	1711	1926
ddb1	-0.551	0.017	7446	5100	5064

gpi7	-0.533	0.017	4390	3169	2898
SPCC18.13	-0.518	0.017	3502	2267	2625
SPNCRNA.1333	-2.252	0.018	28	5	7
SPCC16A11.01	-0.734	0.018	6562	4390	3499
aim22	-0.648	0.018	1541	1010	955
erg12	-0.631	0.018	1871	1317	1097
SPAC29A4.13	-0.603	0.018	2142	1483	1336
SPAC11D3.08c	-0.583	0.018	2300	1561	1508
SPBC56F2.08c	-0.581	0.018	12244	8207	8165
SPAC1786.02	-0.556	0.018	9733	6342	6899
SPNCRNA.438	-0.728	0.019	1016	675	551
SPAC17A2.02c	-0.561	0.019	10385	6906	7172
SPBC1A4.09	-0.56	0.019	8305	5919	5348
SPCC613.07	-0.543	0.019	2886	1962	2001
nrd1	-0.541	0.019	3075	2166	2059
SPAC1B2.06	-0.928	0.02	304	156	163
ppr6	-0.643	0.02	1555	1053	937
arg5	-0.597	0.02	15214	10158	9961
SPAC22E12.01	-0.591	0.02	1953	1238	1357
rps901	-0.561	0.02	10126	6938	6787
gpt2	-0.523	0.02	3583	2567	2418
SPBC16E9.10c	-0.502	0.02	4541	3031	3384
SPAC589.05c	-0.654	0.021	1356	870	854
set13	-0.608	0.021	1820	1227	1160
dbp2	-0.591	0.021	16995	10440	12130
SPAC12G12.09	-0.53	0.021	3194	2251	2171
cdc45	-0.524	0.021	6229	4315	4349
erd2	-0.52	0.021	3809	2766	2547
tom20	-0.746	0.022	14056	7318	9450
SPBC18H10.18c	-0.695	0.022	1153	781	642

SPCC777.17c	-0.642	0.022	1306	800	874
eng1	-0.635	0.022	12286	7089	8731
rng3	-0.601	0.022	1889	1278	1211
rps802	-0.579	0.022	13984	9396	9330
grc3	-0.513	0.022	4844	3502	3283
SPBC1604.06c	-0.508	0.022	3534	2423	2548
nxt1	-0.683	0.023	1148	765	664
kap114	-0.513	0.023	5540	3915	3850
SPCC191.05c	-0.754	0.024	670	401	394
rpa2	-0.586	0.024	15750	10460	10521
rpb8	-0.548	0.024	5881	4355	3690
trp3	-0.511	0.024	5687	3996	3988
SPAC144.12	-0.502	0.024	5664	3862	4136
SPNCRNA.431	-0.974	0.025	226	111	119
SPNCRNA.1358	-0.828	0.025	1732	1110	841
glt1	-0.78	0.025	42108	24134	24898
mmd1	-0.565	0.026	1980	1280	1397
esf1	-0.54	0.026	10960	7279	7800
SPAC24H6.11c	-0.521	0.026	6247	4578	4127
lsb5	-0.505	0.026	4073	3020	2717
rpl44	-0.599	0.027	17085	11761	10795
SPCC584.01c	-0.579	0.027	16250	10666	11094
SPBC17D1.05	-0.571	0.027	14094	9769	9211
erg28	-0.56	0.027	12991	8906	8718
tim44	-0.556	0.027	12448	8512	8425
utp25	-0.531	0.027	6345	4744	4034
cog3	-0.512	0.027	3666	2770	2370
SPMITTRNACYS.01	-3.169	0.028	14	1	2
tam6	-1.224	0.028	110	58	36
SPAC17G6.11c	-0.543	0.028	8656	6424	5460

res1	-0.523	0.028	2861	2048	1932
rax2	-0.518	0.028	7024	5055	4753
SPCC4G3.17	-0.513	0.028	5566	4203	3596
SPAC6F6.13c	-0.796	0.029	7349	3628	4841
rps101	-0.738	0.029	38868	21957	24658
gpi14	-0.662	0.029	4122	2881	2329
SPAC31A2.10	-0.561	0.029	2252	1623	1428
SPNCRNA.1458	-1.009	0.03	202	118	82
rps3	-0.825	0.03	53075	28102	31812
pyp3	-0.682	0.03	959	625	570
SPBC418.02	-0.55	0.03	2179	1499	1477
etp1	-0.525	0.03	9003	6305	6205
skb1	-0.514	0.03	7841	5479	5502
rps1501	-0.508	0.03	6152	4522	4132
SPAC18B11.11	-0.505	0.03	3583	2701	2346
SPAC343.13	-0.693	0.031	879	572	515
hem15	-0.645	0.031	1189	799	721
ubc14	-0.632	0.031	1393	987	810
SPAC823.07	-0.623	0.031	1466	1039	862
lcf2	-0.635	0.032	24863	15935	16077
moe1	-0.531	0.032	11037	7634	7640
mdm28	-0.526	0.032	10456	7258	7268
mrp17	-0.521	0.032	2535	1764	1768
rps401	-0.894	0.033	63663	35781	32725
SPNCRNA.1092	-0.893	0.034	237	108	147
cwf24	-0.559	0.034	1780	1160	1257
SPBP22H7.02c	-0.51	0.034	7720	5557	5283
mpg1	-0.51	0.034	8338	5846	5866
SPAC2C4.06c	-0.506	0.034	2639	1805	1913
SPNCRNA.197	-1.565	0.035	47	14	18

abh1	-0.513	0.035	2814	2076	1866
SPNCRNA.1298	-1.328	0.036	73	31	26
fub2	-0.864	0.036	5325	3372	2480
SPBC4B4.04	-0.52	0.036	10602	7426	7362
SPCC70.03c	-0.51	0.036	8277	5943	5680
meu34	-0.503	0.037	2914	2154	1958
SPNCRNA.861	-0.879	0.038	279	162	141
sen2	-0.609	0.038	1400	999	836
SPAC890.05	-0.593	0.038	9109	5411	6665
SPNCRNA.1352	-0.813	0.039	412	267	202
SPCC757.05c	-0.57	0.039	1697	1191	1095
cif1	-0.532	0.039	2096	1318	1583
uvi15	-0.505	0.039	7553	5635	5008
SPBC1683.06c	-0.713	0.04	624	391	370
ter1	-0.653	0.04	3060	2158	1732
otu1	-0.519	0.04	2263	1582	1576
SPAC328.09	-0.534	0.041	2746	2059	1731
SPAPB24D3.06c	-0.534	0.041	1927	1300	1361
SPAP11E10.01	-0.517	0.041	2313	1640	1591
new12	-0.962	0.042	179	74	110
SPCC4B3.02c	-0.669	0.042	891	611	509
dbp3	-0.573	0.042	14630	8837	10832
SPAC11D3.06	-0.572	0.042	1389	884	984
arg3	-0.562	0.042	6068	4490	3732
SPAC25B8.06c	-0.535	0.042	2205	1635	1407
SPBC776.06c	-0.502	0.042	2649	1936	1802
rrg9	-0.964	0.043	560	339	235
imt2	-0.762	0.043	441	263	257
tsc2	-0.505	0.043	10005	7176	6926
SPNCRNA.423	-1.105	0.044	116	61	46

SPCC569.03	-0.608	0.044	1027	624	724
rpl1502	-0.592	0.044	22947	15133	15309
git5	-0.585	0.044	1378	944	893
abc2	-0.54	0.044	16589	11106	11719
yrs1	-0.515	0.044	11712	8384	8011
SPNCRNA.911	-1.12	0.045	100	41	51
SPAC8E11.01c	-0.575	0.045	1416	962	939
rpl502	-0.503	0.045	12959	8559	9729
mfs1	-0.7	0.046	5013	2682	3492
elf1	-0.553	0.046	17242	12123	11377
SPNCRNA.1602	-0.629	0.047	1034	717	620
SPBP23A10.06	-0.591	0.047	1321	936	818
ibp1	-0.568	0.047	1625	1199	992
cti1	-0.518	0.047	2278	1702	1479
clr2	-0.514	0.047	2089	1448	1477
SPNCRNA.1207	-2.139	0.049	21	5	5
meu29	-0.559	0.049	1476	1004	1000
rpl2101	-0.546	0.049	1753	1265	1136
SPNCRNA.953	-0.539	0.049	1673	1149	1155

Supplementary Table 4. Gene list analysis of the 382 up-regulated genes in the slow mutant

Category_Name	GeneSet_Name	over_represented under_represented	List_Frequency	Background_Frequency	Corrected_pvalue
GO Biological Process	pheromone-dependent signal transduction involved in conjugation with cellular fusion	Enriched	2.094240838 (8/382)	0.271234832 (19/7005)	0.00121184
GO Biological Process	signal transduction involved in conjugation with cellular fusion	Enriched	2.094240838 (8/382)	0.299785867 (21/7005)	0.00245112
GO Biological Process	response to pheromone	Enriched	2.356020942 (9/382)	0.428265525 (30/7005)	0.00498635
GO Biological Process	cellular response to pheromone	Enriched	2.356020942 (9/382)	0.428265525 (30/7005)	0.00498635
GO Biological Process	G-protein coupled receptor signaling pathway	Enriched	2.094240838 (8/382)	0.356887937 (25/7005)	0.00725759
Gene Expression	Reproduction module	Enriched	14.65968586 (56/382)	4.225553176 (296/7005)	9.74595E-14
Gene Expression	Core Environmental Stress Response induced	Enriched	19.89528796 (76/382)	7.723054961 (541/7005)	4.90506E-12
Gene Expression	Oxidative Stess Cluster 4	Enriched	16.4921466 (63/382)	5.91006424 (414/7005)	3.01199E-11
Gene Expression	Stress module	Enriched	8.90052356 (34/382)	1.941470378 (136/7005)	3.01199E-11
Gene Expression	Nitrogen depletion total meiotic genes	Enriched	10.47120419 (40/382)	3.01213419 (211/7005)	2.04581E-09
Gene Expression	Nitrogen depletion continuous meiotic genes	Enriched	5.497382199 (21/382)	0.985010707 (69/7005)	4.12461E-08
Gene Expression	Meiosis sporulation module	Enriched	10.73298429 (41/382)	3.882940757 (272/7005)	1.25823E-06
Gene Expression	Nitrogen depletion delayed meiotic genes	Enriched	3.664921466 (14/382)	0.542469665 (38/7005)	3.27646E-06
Gene Expression	Early meiotic genes	Enriched	5.759162304 (22/382)	1.399000714 (98/7005)	5.47663E-06
Gene Expression	Induced rnc1 mutant	Enriched	4.45026178 (17/382)	1.099214847 (77/7005)	0.000315512
Gene Expression	Ste11 targets	Enriched	3.926701571 (15/382)	0.885082084 (62/7005)	0.000356055
Gene Expression	Induced pan3 mutant	Enriched	2.617801047 (10/382)	0.428265525 (30/7005)	0.000951126
Gene Expression	Induced Dbr1 deletion	Enriched	10.47120419 (40/382)	4.925053533 (345/7005)	0.00154587
Gene Expression	Caffeine and Rapamycin induced	Enriched	9.42408377 (36/382)	4.339757316 (304/7005)	0.00245112
Gene Expression	Induced mug187 mutant	Enriched	3.403141361 (13/382)	0.827980014 (58/7005)	0.00297469
Gene Expression	Sty1 but not Atf1 activated genes	Enriched	2.617801047 (10/382)	0.499643112 (35/7005)	0.00302965

Gene Expression	Respiration module	Enriched	2.879581152 (11/382)	0.670949322 (47/7005)	0.00708287
Phenotypes (FYPO)	inviable cell	Underrepresented	12.30366492 (47/382)	22.21270521 (1556/7005)	0.000290173
Phenotypes (FYPO)	abnormal cellular component organization during vegetative growth	Underrepresented	4.97382199 (19/382)	12.54817987 (879/7005)	0.000336326
Phenotypes (FYPO)	inviable cell population	Underrepresented	11.78010471 (45/382)	21.4703783 (1504/7005)	0.000337576
Phenotypes (FYPO)	inviable vegetative cell population	Underrepresented	11.78010471 (45/382)	21.27052106 (1490/7005)	0.000402918
Phenotypes (FYPO)	abnormal cellular physical quality phenotype during vegetative growth	Underrepresented	17.80104712 (68/382)	28.17987152 (1974/7005)	0.000819663
Phenotypes (FYPO)	inviable vegetative cell	Underrepresented	10.9947644 (42/382)	19.85724483 (1391/7005)	0.000980878
Phenotypes (FYPO)	abnormal cellular physical quality phenotype	Underrepresented	24.86910995 (95/382)	35.63169165 (2496/7005)	0.00157609
Phenotypes (FYPO)	abnormal vegetative cell morphology	Underrepresented	9.162303665 (35/382)	17.0592434 (1195/7005)	0.00275584
Phenotypes (FYPO)	abnormal subcellular component during vegetative growth	Underrepresented	5.759162304 (22/382)	12.54817987 (879/7005)	0.00297469
Phenotypes (FYPO)	abnormal cell morphology	Underrepresented	15.70680628 (60/382)	24.62526767 (1725/7005)	0.00466407
Phenotypes (FYPO)	abnormal microtubule cytoskeleton organization	Underrepresented	0.785340314 (3/382)	4.568165596 (320/7005)	0.00559735
Phenotypes (FYPO)	microtubule cytoskeleton organization phenotype	Underrepresented	0.785340314 (3/382)	4.568165596 (320/7005)	0.00559735
Phenotypes (FYPO)	inviable after spore germination	Underrepresented	5.497382199 (21/382)	11.77730193 (825/7005)	0.00620368
Phenotypes (FYPO)	abnormal microtubule cytoskeleton organization during vegetative growth	Underrepresented	0.785340314 (3/382)	4.468236974 (313/7005)	0.00725759
Phenotypes (FYPO)	abnormal regulation of conjugation	Enriched	2.356020942 (9/382)	0.471092077 (33/7005)	0.00889607
Phenotypes (FYPO)	abnormal response to pheromone	Enriched	2.356020942 (9/382)	0.471092077 (33/7005)	0.00889607
Phenotypes (FYPO)	abnormal transcriptional response to pheromone	Enriched	2.094240838 (8/382)	0.371163455 (26/7005)	0.00893103
Phenotypes (FYPO)	abnormal vegetative cell shape	Underrepresented	8.376963351 (32/382)	15.28907923 (1071/7005)	0.00962284
Protein Features	Number of amino acids	Lower	318.0326087	472.655967078189	2.26504E-15
Protein Features	Molecular weight (kDa)	Lower	36.01722319	53.3015431975308	2.39132E-15
Protein Features	Protein Half Life (minutes)	Lower	649.02	819.946483398785	0.00157609
Protein Features	Homo sapiens orthologs	Underrepresented	39.790575916230 4 (152/382)	50.321199143469 (3525/7005)	0.00559735
Protein Features	Lysine	Higher	0.074423535	0.067540460267044	0.00868688
Transcript Features	Ribosomal density (rb/kb)	Higher	7.229120718	4.38104237408602	2.26504E-15

Transcript Features	mRNA level (WT)	Lower	2096.798866	2838.62971574337	7.41018E-08
Transcript Features	Annotated transcript length	Lower	1516.701571	1879.33519553073	8.94839E-07
Transcript Features	Relative Pol II occupancy	Lower	1.068941176	1.35469424460432	0.00820736

Supplementary Table 5. Gene list analysis of the 494 down-regulated genes in the slow mutant

Category_Name	GeneSet_Name	over_represented under_represented	List_Frequency	Background Frequency	Corrected_pvalue
GO Biological Process	ribosome biogenesis	Enriched	15.1821862348178 (75/494)	5.4389721627409 (381/7005)	3.74905E-14
GO Biological Process	ribonucleoprotein complex biogenesis	Enriched	15.587044534413 (77/494)	6.5524625267666 (459/7005)	1.10439E-10
GO Biological Process	ncRNA metabolic process	Enriched	13.5627530364372 (67/494)	5.72448251249108 (401/7005)	5.10987E-09
GO Biological Process	rRNA processing	Enriched	9.31174089068826 (46/494)	3.32619557458958 (233/7005)	3.09853E-08
GO Biological Process	biological process	Enriched	87.246963562753 (431/494)	75.8315488936474 (5312/7005)	3.32409E-08
GO Biological Process	transmembrane transport	Enriched	11.336032388664 (56/494)	4.53961456102784 (318/7005)	4.18638E-08
GO Biological Process	rRNA metabolic process	Enriched	9.31174089068826 (46/494)	3.42612419700214 (240/7005)	7.51368E-08
GO Biological Process	ncRNA processing	Enriched	11.1336032388664 (55/494)	4.85367594575303 (340/7005)	8.91026E-07
GO Biological Process	nitrogen compound transport	Enriched	6.47773279352227 (32/494)	2.12705210563883 (149/7005)	2.19708E-06
GO Biological Process	cellular process	Enriched	72.6720647773279 (359/494)	62.2698072805139 (4362/7005)	9.33389E-05
GO Biological Process	anion transmembrane transport	Enriched	4.04858299595142 (20/494)	1.25624553890079 (88/7005)	0.000340978
GO Biological Process	amino acid transport	Enriched	2.42914979757085 (12/494)	0.499643112062812 (35/7005)	0.000389761
GO Biological Process	anion transport	Enriched	4.8582995951417 (24/494)	1.74161313347609 (122/7005)	0.000489245
GO Biological Process	amino acid transmembrane transport	Enriched	2.22672064777328 (11/494)	0.442541042112777 (31/7005)	0.000635175
GO Biological Process	organelle fission	Underrepresented	1.61943319838057 (8/494)	5.7530335474661 (403/7005)	0.000663542
GO Biological Process	import into cell	Enriched	2.22672064777328 (11/494)	0.456816559600286 (32/7005)	0.000840391
GO Biological Process	import across plasma membrane	Enriched	2.22672064777328 (11/494)	0.456816559600286 (32/7005)	0.000840391
GO Biological Process	nuclear division	Underrepresented	1.61943319838057 (8/494)	5.65310492505353 (396/7005)	0.000856425
GO Biological Process	L-amino acid transport	Enriched	1.61943319838057 (8/494)	0.242683797287652 (17/7005)	0.00102357
GO Biological Process	ribosomal small subunit biogenesis	Enriched	4.25101214574899 (21/494)	1.48465381870093 (104/7005)	0.00111245

GO Biological Process	L-arginine import	Enriched	1.21457489878543 (6/494)	0.142755174875089 (10/7005)	0.00226528
GO Biological Process	arginine import	Enriched	1.21457489878543 (6/494)	0.142755174875089 (10/7005)	0.00226528
GO Biological Process	L-arginine transport	Enriched	1.21457489878543 (6/494)	0.142755174875089 (10/7005)	0.00226528
GO Biological Process	L-arginine transmembrane transport	Enriched	1.21457489878543 (6/494)	0.142755174875089 (10/7005)	0.00226528
GO Biological Process	arginine transmembrane transport	Enriched	1.21457489878543 (6/494)	0.142755174875089 (10/7005)	0.00226528
GO Biological Process	organic acid transport	Enriched	2.63157894736842 (13/494)	0.699500356887937 (49/7005)	0.00255245
GO Biological Process	carboxylic acid transport	Enriched	2.63157894736842 (13/494)	0.699500356887937 (49/7005)	0.00255245
GO Biological Process	organic acid transmembrane transport	Enriched	2.42914979757085 (12/494)	0.613847251962884 (43/7005)	0.00299364
GO Biological Process	ion transmembrane transport	Enriched	5.66801619433198 (28/494)	2.48394004282655 (174/7005)	0.00340289
GO Biological Process	maturation of SSU-rRNA	Enriched	3.4412955465587 (17/494)	1.14204139900071 (80/7005)	0.00341893
GO Biological Process	L-alpha-amino acid transmembrane transport	Enriched	1.417004048583 (7/494)	0.214132762312634 (15/7005)	0.00344205
GO Biological Process	nitrogen compound metabolic process	Enriched	35.2226720647773 (174/494)	27.1092077087794 (1899/7005)	0.00406228
GO Biological Process	arginine transport	Enriched	1.21457489878543 (6/494)	0.157030692362598 (11/7005)	0.00406228
GO Biological Process	lysine import	Enriched	1.21457489878543 (6/494)	0.157030692362598 (11/7005)	0.00406228
GO Biological Process	L-lysine import	Enriched	1.21457489878543 (6/494)	0.157030692362598 (11/7005)	0.00406228
GO Biological Process	organic anion transport	Enriched	3.4412955465587 (17/494)	1.17059243397573 (82/7005)	0.00436282
GO Biological Process	maturation of SSU-rRNA from tricistronic rRNA transcript (SSU-rRNA, 5.8S rRNA, LSU-rRNA)	Enriched	2.63157894736842 (13/494)	0.756602426837973 (53/7005)	0.00547693
GO Biological Process	ion transport	Enriched	6.47773279352227 (32/494)	3.14061384725196 (220/7005)	0.00715253
GO Biological Process	L-amino acid import	Enriched	1.21457489878543 (6/494)	0.171306209850107 (12/7005)	0.00716438

GO Biological Process	L-lysine transmembrane transport	Enriched	1.21457489878543 (6/494)	0.171306209850107 (12/7005)	0.00716438
GO Biological Process	L-lysine import across plasma membrane	Enriched	1.01214574898785 (5/494)	0.114204139900071 (8/7005)	0.00728083
GO Biological Process	L-lysine import into cell	Enriched	1.01214574898785 (5/494)	0.114204139900071 (8/7005)	0.00728083
GO Biological Process	cell division	Underrepresented	0.809716599190283 (4/494)	3.61170592433976 (253/7005)	0.00772314
GO Biological Process	organic cyclic compound metabolic process	Enriched	32.5910931174089 (161/494)	25.0678087080657 (1756/7005)	0.00895515
GO Biological Process	single-organism organelle organization	Underrepresented	7.69230769230769 (38/494)	13.1334760885082 (920/7005)	0.00895515
GO Biological Process	sphingolipid biosynthetic process	Enriched	1.61943319838057 (8/494)	0.328336902212705 (23/7005)	0.00946184
GO Biological Process	organonitrogen compound metabolic process	Enriched	12.1457489878543 (60/494)	7.43754461099215 (521/7005)	0.00978697
Gene Expression	Caffeine and Rapamycin repressed	Enriched	19.0283400809717 (94/494)	4.46823697359029 (313/7005)	8.44625E-33
Gene Expression	Core Environmental Stress Response repressed	Enriched	21.8623481781377 (108/494)	6.26695217701642 (439/7005)	5.65706E-30
Gene Expression	Induced pat1.114 mutant	Enriched	14.3724696356275 (71/494)	5.39614561027837 (378/7005)	2.99277E-12
Gene Expression	Ribosomal protein module 2	Enriched	10.3238866396761 (51/494)	3.82583868665239 (268/7005)	1.18206E-08
Gene Expression	Oxidative Stess Cluster 6	Enriched	7.48987854251012 (37/494)	2.5553176302641 (179/7005)	4.8973E-07
Gene Expression	Oxidative Stess Cluster 10	Enriched	3.84615384615385 (19/494)	0.870806566738044 (61/7005)	4.3927E-06
Gene Expression	htb1 brl1 brl2 set1 mutant repressed	Enriched	6.07287449392713 (30/494)	1.97002141327623 (138/7005)	4.44699E-06
Gene Expression	Ribosomal protein module Homol D E	Enriched	7.69230769230769 (38/494)	3.16916488222698 (222/7005)	5.67231E-05
Gene Expression	Cell cycle periodically expressed	Enriched	13.3603238866397 (66/494)	7.10920770877944 (498/7005)	7.61041E-05
Gene Expression	Repressed Dbr1 deletion	Enriched	7.48987854251012 (37/494)	3.32619557458958 (233/7005)	0.000397722
Gene Expression	Amino acid metabolism module	Enriched	5.26315789473684 (26/494)	1.95574589578872 (137/7005)	0.000397722
Gene Expression	Oxidative Stess Cluster 9	Enriched	5.46558704453441 (27/494)	2.11277658815132 (148/7005)	0.000530375
Gene Expression	Cell Cycle Cluster 4	Enriched	5.66801619433198 (28/494)	2.26980728051392 (159/7005)	0.00068364

Gene Expression	Oxidative Stess Cluster 11	Enriched	4.65587044534413 (23/494)	1.67023554603854 (117/7005)	0.000721882
Gene Expression	Induced SPAC17H9 04c mutant	Enriched	3.84615384615385 (19/494)	1.27052105638829 (89/7005)	0.00126594
Gene Expression	Repressed spt6 mutant	Enriched	1.82186234817814 (9/494)	0.385438972162741 (27/7005)	0.0057658
Phenotypes (FYPO)	cell phenotype	Enriched	86.8421052631579 (429/494)	70.5353319057816 (4941/7005)	2.70753E-15
Phenotypes (FYPO)	cell population viability	Enriched	87.0445344129555 (430/494)	70.6780870806567 (4951/7005)	2.70753E-15
Phenotypes (FYPO)	phenotype	Enriched	87.246963562753 (431/494)	71.0920770877944 (4980/7005)	3.2652E-15
Phenotypes (FYPO)	cell population phenotype	Enriched	87.0445344129555 (430/494)	70.8636688079943 (4964/7005)	3.28059E-15
Phenotypes (FYPO)	cellular physical quality phenotype	Enriched	86.2348178137652 (426/494)	70.0071377587438 (4904/7005)	5.58698E-15
Phenotypes (FYPO)	vegetative cell phenotype	Enriched	85.0202429149798 (420/494)	68.8222698072805 (4821/7005)	1.46432E-14
Phenotypes (FYPO)	cellular physical quality phenotype during vegetative growth	Enriched	84.6153846153846 (418/494)	68.3654532476802 (4789/7005)	1.46432E-14
Phenotypes (FYPO)	cell viability	Enriched	85.2226720647773 (421/494)	69.5074946466809 (4869/7005)	7.15274E-14
Phenotypes (FYPO)	viable vegetative cell with normal cell morphology	Enriched	56.6801619433198 (280/494)	44.4396859386153 (3113/7005)	4.12552E-06
Phenotypes (FYPO)	normal cell morphology	Enriched	63.3603238866397 (313/494)	51.8058529621699 (3629/7005)	2.05356E-05
Phenotypes (FYPO)	normal vegetative cell morphology	Enriched	63.3603238866397 (313/494)	51.7487508922198 (3625/7005)	2.05356E-05
Phenotypes (FYPO)	normal phenotype	Enriched	68.2186234817814 (337/494)	57.3590292648108 (4018/7005)	6.37781E-05
Phenotypes (FYPO)	viable vegetative cell population	Enriched	67.4089068825911 (333/494)	56.6595289079229 (3969/7005)	8.19659E-05
Phenotypes (FYPO)	viable vegetative cell	Enriched	63.3603238866397 (313/494)	52.6338329764454 (3687/7005)	0.000121541
Phenotypes (FYPO)	viable cell population	Enriched	67.4089068825911 (333/494)	56.859386152748 (3983/7005)	0.000122133
Phenotypes (FYPO)	viable cell	Enriched	63.3603238866397 (313/494)	52.6909350463954 (3691/7005)	0.000144201
Phenotypes (FYPO)	normal vegetative phenotype	Enriched	65.7894736842105 (325/494)	55.260528194147 (3871/7005)	0.000162494
Phenotypes (FYPO)	inviable after spore germination, without cell division	Enriched	12.3481781376518 (61/494)	7.15203426124197 (501/7005)	0.00210857

Phenotypes (FYPO)	inviable after spore germination, without cell division, with abnormal germ tube morphology	Enriched	5.26315789473684 (26/494)	2.21270521056388 (155/7005)	0.00384578
Phenotypes (FYPO)	abnormal phenotype	Enriched	64.7773279352227 (320/494)	56.4596716630978 (3955/7005)	0.00946184
Protein Domains (Pfam)	Amino acid permease	Enriched	1.01214574898785 (5/494)	0.114204139900071 (8/7005)	0.00728083
Protein Domains (Pfam)	Major Facilitator Superfamily	Enriched	2.42914979757085 (12/494)	0.685224839400428 (48/7005)	0.00787962
Protein Features	Glutamic acid	Lower	0.0565112896113241	0.0660338227478138	8.25525E-11
Protein Features	Valine	Higher	0.066415046214053	0.0602659980510806	1.17199E-09
Protein Features	S.cerevisiae orthologs	Enriched	70.2429149797571 (347/494)	55.7744468236974 (3907/7005)	4.42542E-09
Protein Features	Asparagine	Lower	0.0458489224721031	0.0510031960168226	1.61689E-07
Protein Features	Nitrogen content	Lower	1.3483399811237	1.36731438301884	3.34215E-07
Protein Features	Glycine	Higher	0.0569013300924529	0.0503929881606619	1.04756E-06
Protein Features	Lysine	Lower	0.0620996791448227	0.0684520802522902	5.48698E-06
Protein Features	Glutamine	Lower	0.0347078197667617	0.0385671177208081	3.57811E-05
Protein Features	Alanine	Higher	0.0676338570719653	0.0629322969189161	7.91722E-05
Protein Features	Homo sapiens orthologs	Enriched	61.1336032388664 (302/494)	50.321199143469 (3525/7005)	0.000121861
Protein Features	Tryptophan	Higher	0.0130727202665548	0.011038781899495	0.000231345
Protein Features	Protein Half Life (minutes)	Higher	956.527450980392	798.070886075947	0.000500445
Transcript Features	protein coding	Enriched	88.663967611336 (438/494)	73.3190578158458 (5136/7005)	8.22262E-15
Transcript Features	mRNA copies per proliferating cell	Lower	9.81348472505092	141.164213135048	2.73756E-12
Transcript Features	mRNA level	Higher	3527.5093578199	2732.02169582478	1.27145E-09
Transcript Features	ncRNA level	Underrepresented	10.3238866396761 (51/494)	21.8843683083512 (1533/7005)	2.51098E-09
Transcript Features	Top 20% shortest transcripts	Underrepresented	9.7165991902834 (48/494)	20 (1401/7005)	7.39741E-08
Transcript Features	Top 10% shortest transcripts	Underrepresented	3.4412955465587 (17/494)	9.99286224125625 (700/7005)	5.43852E-06
Transcript Features	Annotated transcript length	Higher	2033.53036437247	1846.36046690217	2.53312E-05